The Long-term Impact of Land Use Land Cover Change on Urban Climate: Evidence from the Phoenix Metropolitan Area, Arizona

by

Chuyuan Wang

A Dissertation Presented in Partial Fulfillment
of the Requirements for the Degree
Doctor of Philosophy

Approved July 2018 by the
Graduate Supervisory Committee:

Soe W. Myint, Chair
Anthony J. Brazel
Zhihua Wang
David M. Hondula

ARIZONA STATE UNIVERSITY

August 2018

ABSTRACT

This dissertation research studies long-term spatio-temporal patterns of surface urban heat island (SUHI) intensity, urban evapotranspiration (ET), and urban outdoor water use (OWU) using Phoenix metropolitan area (PMA), Arizona as the case study. This dissertation is composed of three chapters. The first chapter evaluates the SUHI intensity for PMA using Moderate Resolution Imaging Spectroradiometer (MODIS) land surface temperature (LST) product and a time-series trend analysis to discover areas that experienced significant changes of SUHI intensity between 2000 and 2017. The heating and cooling effects of different urban land use land cover (LULC) types was also examined using classified Landsat satellite images. The second chapter is focused on urban ET and the impacts of urban LULC change on ET. An empirical model of urban ET for PMA was built using flux tower data and MODIS land products using multivariate regression analysis. A time-series trend analysis was then performed to discover areas in PMA that experienced significant changes of ET between 2001 and 2015. The impact of urban LULC change on ET was examined using classified LULC maps. The third chapter models urban OWU in PMA using a surface energy balance model named METRIC (Mapping Evapotranspiration at high spatial Resolution with Internalized Calibration) and time-series Landsat Thematic Mapper 5 imagery for 2010. The relationship between urban LULC types and OWU was examined with the use of very high-resolution land cover classification data generated from the National Agriculture Imagery Program (NAIP) imagery and regression analysis. Socio-demographic variables were selected from census data at the census track level and analyzed against OWU to study their relationship using correlation analysis. This dissertation makes significant contributions and expands the knowledge of long-term urban

climate dynamics for PMA and the influence of urban expansion and LULC change on regional climate. Research findings and results can be used to provide constructive suggestions to urban planners, decision-makers, and city managers to formulate new policies and regulations when planning new constructions for the purpose of sustainable development for a desert city.

DEDICATION

This dissertation is dedicated to my brilliant and supportive wife, Zhouzhou He, to my always encouraging, ever faithful parents, Kehui Li (mother) and Yinsheng Wang (father), and to my beloved grandfather in heaven, Shiping Li.

ACKNOWLEDGEMENT

This dissertation is based upon work supported and funded by the National Science Foundation (grant number: BCS-1026865) and Central Arizona Phoenix Long-Term Ecological Research (CAP-LTER) program at Arizona State University. The first and second chapters are also supported by a National Aeronautics and Space Administration (NASA) funded project (NASA award number: NNX12AM88G) titled ‘‘Understanding Impacts of Desert Urbanization on Climate and Surrounding Environments to Foster Sustainable Cities Using Remote Sensing and Numerical Modeling”. The third chapter is also supported by an National Oceanic and Atmospheric Administration (NOAA) funded project (NOAA award number: NA12OAR4310100) titled “Evaluation of Drought Risks and its Impact on Agricultural Land and Water Use to Support Adaptive Decision-making”.

The author would also like to acknowledge and sincerely thank his graduate supervisory committee members that include Dr. Soe W. Myint (Chair), Dr. Anthony J. Brazel, Dr. Zhihua Wang, and Dr. David M. Hondula and my fellow colleagues for their assistance in providing solid guidance and constructive suggestions for the development of this dissertation.

TABLE OF CONTENTS

LIST OF TABLES

Table Page

LIST OF FIGURES

INTRODUCTION AND LITERATURE REVIEW

URBAN HEAT ISLAND AND LAND USE LAND COVER CHANGE

Conversions from natural terrain and agricultural land to built-up environment has taken place ubiquitously worldwide at an alarming rate to meet the ever-increasing demand of rapid urban population growth (Seto et al., 2011). Urban growth is among the most rapid, dramatic, and irreversible forms of human modification of the environment (Buyantuyev and Wu, 2010; Dietzel et al., 2005). Associated with the use of construction and building materials, urbanization modifies surface energy balance and hydrological cycle, leading to significant impacts on local and regional hydroclimate (Owen et al., 1998; Kondoh and Nishiyama 2000; Zhang et al., 2009; Georgescu et al., 2012; Wang et al., 2013).

One of the significant environmental consequences of urban expansion is the elevated temperature in densely-built urban areas in comparison to the surrounding rural areas, or more commonly referred to as the urban heat island (UHI) effect (Voogt and Oke, 2003). The UHI has important and widespread implications for urban ecosystems, energy use, and life quality of urban residents. The UHI effect has been linked, among many adverse environmental impacts, with increased energy consumption and water use; compromised human health and comfort; and downgraded air quality. In addition, excessive urban warming, particularly at nighttime, can increase the duration and magnitude of heat waves, causing higher risk of mortality and other heat-related health problems (Clarke, 1972; Whitman et al., 1997). Since its first discovery in 1818, the UHI effect has been a primary focus in climatology and urban ecology (Arnfield, 2003; Howard, 1833), and there is an ever-increasing number of studies focusing on various aspects of the UHI, including its formation, development, as well as mitigation strategies (Jauregui, 1997; Oke, 1982; Oke, 2002; Onishi et al., 2010; Rizwan et al., 2008).

The UHI effect has been extensively studied for the Phoenix metropolitan area (PMA) in the State of Arizona, United States. For example, the UHI spatial and temporal properties for the summer between 1949 and 1985 were investigated using air temperature data collected from local weather stations (Brazel et al., 2007; Balling and Brazil, 1987a). It was found that summer temperatures were the highest in central Phoenix and were rising most rapidly in the downtown area, while temperatures were decreasing outside of the city (Balling and Brazil, 1987a). Urban development and expansion, especially housing development, was the primary contributor of the Phoenix UHI effect from 1990 to 2004 (Brazel et al., 2007; Lee et al., 2012). The usage of air temperature data collected from a limited amount of local weather stations in these studies, however, has restrictions because these data are not continuous. Therefore, the spatial temperature trends for the entire metropolitan area cannot be adequately quantified in this case. For this reason, some scientists have turned to the use of remotely-sensed data for UHI analysis. The surface urban heat island (SUHI) effect is observed by using remotely-sensed thermal infrared data, such as Landsat and ASTER satellite thermal infrared data, which allow the retrieval of land surface temperature (LST) (Yuan and Bauer, 2007; Chen et al., 2006; Kato and Yamaguchi, 2005; Nichol et al., 2009; Liu and Zhang, 2011). The relationship between detailed land use land cover (LULC) types and LST derived from ASTER imagery was studied by Myint et al. (2013). It has been discovered that dark impervious surfaces, rather than buildings in the city, are primarily responsible for extreme heat in Phoenix (Myint et al., 2013). This finding has also been confirmed by Imhoff et al. (2010). Zheng et al. (2014) examined the effects of spatial configuration of paved surfaces on LST in Phoenix urban area using local Moran's I and suggested that aggregate warming effects were mainly contributed by clustered paved surfaces. On the other hand, it has been found that increasing irrigated landscape can lower nighttime temperatures (Gober et al., 2009), which can be a possible UHI mitigation strategy to prevent daytime heat storage and help lower LST. This strategy, however, requires a significant amount of water that is very scarce in a desert city. Using cool and reflective materials has become an effective strategy to mitigate the UHI effect in the urban built environment (Rossi et al., 2014; Santamouris et al., 2001; Uemoto et al., 2010; Jo et al., 2010). However, it is recommended that this strategy needs to be determined on a city-by-city basis because the mitigation potential of those materials depends on different urban environmental factors (Yang et al., 2015).

Although metropolitan Phoenix's UHI effect has been well studied, much of the literature neglects the area's long-term spatio-temporal pattern of SUHI intensity and its relationship with LULC change. It is necessary to identify regions that are being increasingly heated and cooled in order to further understand how LULC change influences the SUHI effect.

URBAN EVAPOTRANSPIRATION AND LAND USE LAND COVER CHANGE

Urbanization also has significant impact on evapotranspiration (ET). ET is an essential component of water and energy budgets of urban areas, yet it is still highly uncertain (Pittenger and Shaw, 2007, 2010; Pataki et al., 2011a; Shields and Tague, 2012;

Sun et al., 2012; Nouri et al., 2013b). Heterogeneous urban land cover is a patchwork of vegetation and built structures, which results in complex patterns of ET (Grimmond et al., 1996; Grimmond and Oke, 1999; Offerle et al., 2006; Anderson and Vivoni, 2016). In addition, there is a paucity of in situ measurements of ET in virtually all types of urban land cover (Boegh et al., 2009; Hart et al., 2009; Pittenger and Shaw, 2010; Pataki et al., 2011b; Nouri et al., 2013b). In dry regions, urban ET may be much larger than the surrounding natural ecosystem and therefore plays a significant role in local hydrologic fluxes (Grimmond and Oke, 1999). Measuring and modeling ET is therefore particularly challenging in urban regions with diverse and nonnative plant composition (Pataki et al., 2011b; Peters et al., 2011).

ET is one of the major components of the hydrologic cycle, but the impacts of urbanization on ET vary largely with local climatic conditions. Liu et al. (2010) studied the relationship between different LULC types and urban ET for a semi-arid city in Oklahoma, USA, and found that different LULC types have different ET rates in the urban area with the lowest ET found in highly developed areas. They also argued that the conversion from natural vegetated landscape and waterbody to built-up environment could significantly lower ET (Liu et al., 2010). On the other hand, Balling and Brazel (1987b) studied ET rates using Phoenix, Arizona, USA as the study area, and found that rapid urbanization had caused a significant increase of ET level under a subtropical desert climate.

In many circumstances, urban ET exceeds precipitation and is mainly sustained by the use of external water (Grimmond and Oke 1999), and urban vegetation receives a substantial amount of water from anthropogenic irrigation, especially in arid and semiarid areas (Gober et al., 2009; Johnson and Belitz, 2012). A previous study reported that irrigation of private gardens consumes about 16–34% of the total urban water supplied, let alone the water used for irrigating large open space such as public parks and golf courses (Mitchell, Mein, and McMahon 2001). Field experiments also found that potential ET rate of irrigated urban lawn was about 1.3 times greater than that from a rural pasture (Oke, 1979). This phenomenon is especially significant to desert cities because irrigated urban vegetation patches can help the city stay cooler than the surrounding dry desert region, which is known as the urban oasis effect (Oke 1979; Yang et al., 2015b).

Although the impacts of LULC change on urban ET rate have long been a focal research area, most studies made use of temporally discrete ET data collected from local weather stations or flux towers, which only provide information for a limited spatial coverage surrounding the station. Predicting and mapping ET for the spatial continuum of the entire urban area remain challenging. A number of numerical methods have been developed for estimating urban ET during the past decade, which can be broadly categorized into two groups. The first group uses urban land surface models where ET is calculated using a bulk transfer formula (Best et al., 2011; Niu et al., 2011). This group of models is able to solve ET physically with a reasonable accuracy. However, it requires accurate estimates of input parameters related to urban geometry and thermal properties, which are not readily available from field collections and are very difficult to acquire. The second group is the empirical models that are developed from regression analysis using in situ ET measurements (Granger and Hedstrom 2011; Morton 1983). Compared to the urban land surface models, empirical models are more site-specific, which may not be applicable to areas with different geographical and meteorological conditions. On the other hand, empirical models require significantly less input data and are usually more accurate at the local scale, as information of physical processes is implicitly contained in the measurements.

Many remote-sensing based models have been developed and widely used to model and map ET at both regional and global scales, such as SEBAL (Bastiaanssen et al., 1998, 2005), METRIC (Allen et al., 2007a), ReSET (Elhaddad and Garcia 2008), and ALARM (Suleiman and Crago 2002) to name a few. All these models quantify the surface energy balance using remotely sensed thermal data as an input that are associated with evaporation and transpiration processes to provide predicted ET maps. However, all these models also require the input of meteorological data to some degree, such as wind speed, humidity, solar radiation, and air temperature, which are very difficult to collect simultaneously with the acquisition of satellite images. Furthermore, meteorological data are usually collected from a limited number of local weather stations. An extrapolation technique is, therefore, required to predict and map ET for a larger geographic area which is sometimes not accurate for locations that are far away from weather stations. Some other studies developed models to estimate urban ET using remotely sensed data through vegetation indices, such as the normalized difference vegetation index (NDVI) (Nouri et al., 2013a; Johnson and Belitz 2012). These models may be effectively applicable to a city with relatively high vegetation cover, but is not applicable to the PMA due to its unique desert environment.

One of the most widely used satellite remotely sensed dataset is the moderate-resolution imaging spectroradiometer (MODIS) data that provides daily observations for the entire surface of the Earth. Many MODIS land products have been produced at various spatial and temporal resolutions to meet different scientific demands. One of the most popular products is the MODIS global terrestrial ET product (MOD16) that provides regional and global observations for surface water and energy balances and soil moisture status (Mu et al., 2007; Mu, Zhao, and Running 2013). The predicted ET data from this product, however, are not available for urban areas because the model was not specifically developed for the urban land cover type. In addition, this dataset only covers the time period from 2000 to 2010 at 1 km spatial resolution. The short temporal coverage and relatively coarse spatial resolution make it unsatisfactory for urban ET studies. Therefore, a specific model is needed to predict urban ET using remotely sensed data at a finer spatial resolution for a longer temporal coverage in order to study spatial and temporal changes of urban ET.

URBAN OUTDOOR WATER USE AND LAND USE LAND COVER CHANGE

The annual precipitation of the PMA was only 157 mm in 2016, which is far less than the national average of 805 mm (NOAA, 2016). Phoenix water supply mainly comes from rivers and vast underground aquifers (Guhathakurta and Gober, 2007). Although water is naturally scarce in the desert, Phoenix ranks among the highest in the U.S. cities in water demand and water use. Many previous studies were focused on the residential sector of urban water use because it accounts for approximately 67% of the total urban water supply (Guhathakurta and Gober, 2007; Balling and Gober, 2007), and the rest is mainly shared by municipal, agricultural, industrial, and landscaping irrigation. Balling and Gober (2007) investigated how residential water use in Phoenix was influenced by climate variables. Guhathakurta and Gober (2007) examined the urban heat island (UHI) effects on single-family residences' water use. Guhathakurta and Gober (2010) studied the feedback relationships between residential water use and vegetation intensity, diurnal temperature variation, and characteristics of the built environment. Wentz and Gober (2007) investigated the determinants of single-family water use in Phoenix using municipal water records and census data. Previous research did not pay specific attention to the urban total outdoor water use (OWU) other than residential water use in Phoenix. Kaplan *et al.,* (2014) used modeled evapotranspiration (ET) data as a proxy to total OWU to compared seasonal OWU between a dry and a wet year, and to compared OWU among different urban LULC types. The above studies have made great contributions to our current understandings of urban water use in Phoenix. The literature, however, neglected the spatio-temporal pattern of urban OWU and the determinant factors of urban OWU in terms of LULC types, built environment, vegetation species, and socio-demographic variables.

With an ever-increasing population and improved economic conditions, water scarcity is becoming a global reality, especially in arid regions. Total water withdrawals in the U.S. peaked in 1980 and have remained relatively steady since (U.S. Geological Survey, 2014). While withdrawals for public water supply have increased due to population growth, per capita water use has declined (Coomes, 2010).

An American family on average can use 400 gallons of water per day, and about 30 percent of that is devoted to outdoor uses. More than half of that OWU is for watering lawns and gardens. Nationwide, landscape irrigation is estimated to account for almost one-third of all residential water use, totaling more than 7 billion gallons per day.

Water use varies greatly depending on geographic location and season, largely as a result of differences in climate. Water withdrawals for irrigation and landscaping are highest in the drier regions of the West and Southwest, where population growth is often greatest. Water resource is the key of sustainability to a desert city like Phoenix. Although water is naturally scarce in the desert, Phoenix ranks among the highest in the U.S. cities in terms of water use and water demand. Although many studies have examined residential water use in PMA, no research has ever paid attention to the total OWU. The relationship between urban OWU and LULC types, built environment, and socio-demographic variables in PMA remain unknown.

RESEARCH OBJECTIVES AND DISSERTATION STRUCTURE

This dissertation is designed to fill gaps in literature regarding spatio-temporal dynamics of SUHI intensity, urban ET and OWU and their relationships with LULC types using the PMA as the study area. The overarching goal of this dissertation is to study the effects of urbanization on urban climate and the spatio-temporal dynamics of urban climate in terms the UHI effect, urban ET, and water use, using PMA as the study area. In more detail, this dissertation is going to:

1) provide an extensive review for the existing literature and scientific approaches on urban climate studies;

2) develop new modeling approaches to quantify the spatio-temporal dynamics of the SUHI intensity and urban ET for the PMA and to examine the relationship with urban LULC types;

3) model urban OWU using remotely sensed data and weather data, and examine the relationship between OWU and urban land use types for the PMA.

This dissertation is going to be composed of three main chapters, each of which seeks to answer one of the following questions and to address the hypotheses:

Question 1: What is the spatio-temporal pattern of the SUHI intensity in the PMA between 2000 and 2017? What is the impact of LULC change on the SUHI intensity?

Hypothesis 1: The increasing SUHI intensity trend should be observed in newly urbanized areas, rather than existing developed areas. Increasing area of buildings and impervious surfaces should have a heating effect, while increasing green spaces should perform a cooling effect for the urban environment.

Question 2: What is the empirical relationship between in situ ET measurements and remotely sensed data? What is the spatio-temporal pattern of the urban ET for the PMA? What is the relationship between LULC change and urban ET change?

Hypothesis 2: Urban ET is hypothesized to have a statistically significant relationship with surface albedo, green space area, and land surface temperature. Areas of low vegetation cover but high impervious surface cover should have low ET values. Areas of high vegetation cover but low impervious surface cover should have high ET values. Increasing ET trend should be observed in the areas with increasing green space, while decreasing ET trend should be found in newly urbanized area with little vegetation cover.

Question 3: What is the spatial pattern of urban OWU in the PMA in summer and winter, respectively? What is the relationship between urban land use and OWU? What are the socio-demographic factors that influence urban OWU?

Hypothesis 3: OWU in the PMA should be higher in the areas of higher vegetation cover, but lower in the areas of lower vegetation cover; higher in the summer, but lower in the winter. The ranking of OWU for different urban land uses in the PMA is hypothesized as: parks > mesic residential > oasis residential > xeric residential > industrial > business/commercial. The socio-demographic variables that have potential impact on the urban OWU are mean lot size, median housing value, median household income, education level, and age.

This dissertation will encompass an introductory chapter, three chapters of peer-reviewed manuscripts, and a concluding chapter. The three manuscripts are:

Chapter 1: Spatio-temporal Modeling of the Urban Heat Island in the Phoenix Metropolitan Area: Land Use Change Implications

This study examines the spatial and temporal patterns of the surface urban heat island (SUHI) intensity in the PMA and the relationship with land use land cover (LULC) change between 2000 and 2014. The objective is to identify specific regions in Phoenix that have been increasingly heated and cooled to further understand how LULC change influences the SUHI intensity.

Chapter 2: Empirical Modelling and Spatio-temporal Patterns of Urban Evapotranspiration for the Phoenix Metropolitan Area, Arizona

In this study an empirical model for predicting urban ET is examined for the PMA using *in-situ* ET measurements from a local flux tower and remotely-sensed MODIS land products. Annual ET maps of Phoenix are then created for the period from 2001 to 2017 using the empirical model developed. A time-series trend analysis is finally performed using predicted ET maps to discover the spatio-temporal patterns of ET changes during the study period.

Chapter 3: Predicting and Understanding Urban Outdoor Water Use in a Desert City — A Case Study of Phoenix, Arizona

This research is first going to predict Phoenix urban OWU and to examine its spatio-temporal pattern for 2010 using modeled evapotranspiration data from Landsat images and precipitation data from weather stations based on the water balance equation. The relationship between urban OWU and different LULC types will then be explored using a high-resolution classified LULC thematic map. Socio-demographic determinants that potentially influence urban OWU are going to be investigated using statistical analyses based on census data and social survey data.

Research findings and results from this dissertation will reveal the critical interactions between urbanization and the climate at the municipal scale. A comprehensive understanding of this nexus will offer insights on effective urban ecosystem services, smart city growth, and sustainable resource management.

CHAPTER 1

SPATIO-TEMPORAL MODELING OF THE URBAN HEAT ISLAND IN THE PHOENIX METROPOLITAN AREA: LAND USE CHANGE IMPLICATIONS

INTRODUCTION

The greater Phoenix metropolitan area (PMA) in the State of Arizona, United State has a subtropical desert climate that makes it one of the warmest cities in the United States. It also has one of the most significant urban climate effects in the world (Hanson et al., 1999). Despite the excessive heat in the summer, Phoenix ranks among the fastest growing cities in the United States. The increasing population has resulted in rapid urban expansion in the past few decades. Concomitant with this rapid rate of urbanization, the urban heat island (UHI) phenomenon has been exacerbated. UHI has been linked, among many adverse environmental impacts, with increased energy consumption (Akbari et al., 2001; Kolokotroni et al., 2012) and water use (Guhathakurta and Gober, 2007; Brazel et al., 2007); compromised human health and comfort (Taha et al., 2004); and downgraded air quality (Taha et al., 1994; Filleul et al., 2006). These issues have not only become increasingly prominent in Phoenix.

The UHI effect has been extensively studied for the Phoenix metropolitan area. For example, the UHI spatial and temporal properties for the summer between 1949 and 1985 were investigated using air temperature data collected from local weather stations (Balling and Brazel, 1987; Brazel et al., 2007). It was found that summer temperatures were the highest in central Phoenix and were rising most rapidly in the downtown area, while temperatures were decreasing outside of the city (Balling and Brazel, 1987). Urban development and expansion, especially housing development, was the primary contributor of the Phoenix UHI effect from 1990 to 2004 (Brazel et al., 2007; Lee et al., 2012). The usage of air temperature data collected from a limited amount of local weather stations in these studies, however, has restrictions because these data are not continuous. Therefore, the spatial temperature trends for the entire metropolitan area cannot be adequately quantified in this case. For this reason, some scientists have turned to the use of remotely sensed data for UHI analysis. The surface urban heat island (SUHI) effect is observed by using remotely sensed thermal infrared data, such as Landsat and ASTER satellite thermal infrared data, which allow the retrieval of land surface temperature (LST) (Kato and Yamaguchi, 2005; Chen et al., 2006; Yuan and Bauer, 2007; Nichol et al., 2009; Liu and Zhang, 2011). The relationship between detailed land use land cover (LULC) types and LST derived from ASTER imagery was studied by Myint et al. (2013). It has been discovered that dark impervious surfaces, rather than buildings in the city, are primarily responsible for extreme heat in Phoenix (Myint et al., 2013). This finding has also been confirmed by Imhoff et al. (2010). Zheng et al. (2014) examined the effects of spatial configuration of paved surfaces on LST in Phoenix urban area using local Moran's *I* and suggested that aggregate warming effects were mainly contributed by clustered paved surfaces. On the other hand, it has been found that increasing irrigated landscape can lower nighttime temperatures (Gober et al., 2009), which can be a possible UHI mitigation strategy to prevent daytime heat storage and help lower LST. This strategy, however, requires a significant amount of water that is very scarce in a desert city. Using cool and reflective materials has become an effective strategy to mitigate the UHI effect in the urban built environment (Jo et al., 2010; Santamouris et al., 2011; Uemoto et al., 2010; Rossi et al., 2014). However, it is recommended that this strategy needs to be determined on a city-by-city basis because the mitigation potential of those materials depends on different urban environmental factors (Yang et al., 2015).

Although metropolitan Phoenix's UHI effect has been well studied, much of the literature neglects the area's long-term spatio-temporal pattern of SUHI intensity and its relationship with LULC change. It is necessary to identify regions that are being increasingly heated and cooled in order to further understand how LULC change influences the SUHI effect. The main objective of this study is to examine which areas of the Phoenix metropolitan area have experienced statistically significant LST increases and decreases compared to surrounding non-urbanized areas for both daytime and nighttime. In addition, this research explores the relationship between LULC change and urban LST variations in Phoenix.

STUDY AREA

The Phoenix metropolitan area is located in central Arizona, USA, and is the sixth largest U.S. city, with an estimated population of 4.4 million (U.S. Census Bureau, 2016), encompassing a total area of approximately 2,800 km^2 (Figure 1). It is located in the northeast part of the Sonoran Desert and receives an average annual precipitation of 204 mm (8.03 in.) (U.S. Climate Data, 2016). The daily high temperature exceeds 37.8 °C (100 °F) for an average of 110 days every year, which normally occurs from late May until early September. The highest temperature can reach more than 43.3 °C (110 °F) for an annual average of 18 days. The study area has diverse LULC types, including commercial, industrial, and residential areas; undisturbed desert; agriculture; grassland; and water bodies.

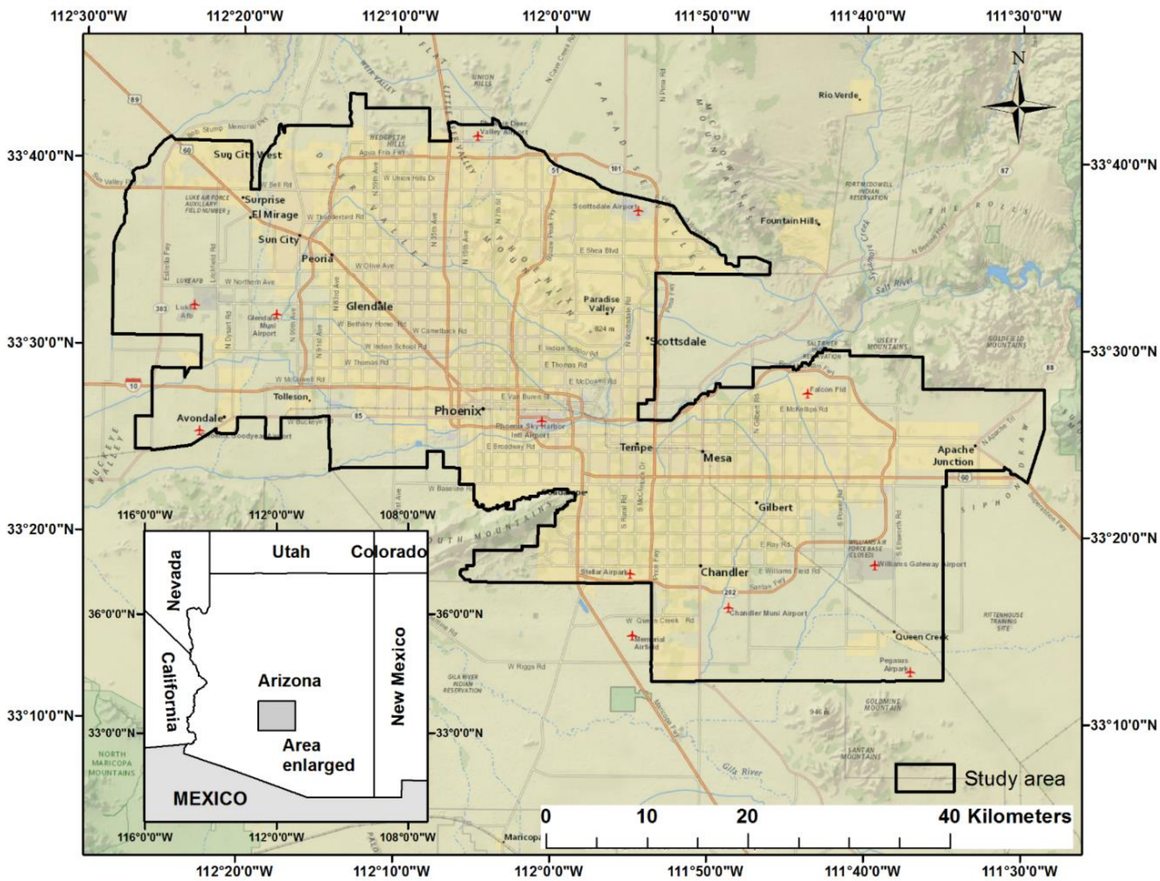

Figure 1.1 Map of study area: Phoenix metropolitan area.

DATA AND METHODS

DATA

Satellite remote sensing offers a great opportunity to acquire continuous LST data without direct physical contact with the surface, with sufficient spatial resolution to distinguish between urban and surrounding rural areas. The MODerate-resolution Imaging Spectroradiometer (MODIS) global LST product is one of the most widely used remotely sensed LST dataset for SUHI studies (Tran et al., 2006; Cheval and Dumitrescu, 2009; Rajasekar and Weng, 2009; Imhoff et al., 2010; Tomlinson et al., 2010; Schwarz et al., 2011; Peng et al., 2012). This study uses MODIS LST 8-day composite imagery (MOD11A2) from 2000 to 2017 for both daytime and nighttime. Although the spatial resolution of MODIS LST imagery (1,000 m) is slightly coarse, a total number of 2,766 pixels are evaluated for the entire Phoenix metropolitan area that gives a relatively large sample size. For this study, we restrict the analysis to June as Phoenix has relatively hot, dry, clear, and calm weather conditions for most of the month. It is, therefore, considered an ideal time period for urban LST evaluations (Brazel et al., 2000; Brazel et al., 2007). Four MODIS LST June images are available — June 1, June 9, June 17, and June 25 — during the selected time frame except for 2001, which has only two images available — June 1 and June 9. Hence, a total of 58 pairs of daytime and nighttime LST images are collected for the entire study period.

LULC maps of 2000 and 2017 are used to study the relationship between LULC change and urban LST variations. One is generated using a Landsat 5 Thematic Mapper (TM) image acquired on June 14, 2000 (Figure 2a), and the other is generated using a Landsat 8 Operational Land Imager (OLI) image from June 13, 2017 (Figure 2c). Both images have 30 m spatial resolution and have been classified into six major LULC classes that include water, impervious surface, vegetation, urban/residential area, open soil, and fallow cropland (Figures 2b and 2d) using the Iterative Self-Organizing Data Analysis (ISODATA) unsupervised classification algorithm. The “impervious surface” class refers to asphalt and pavements such as parking lots, roads, and highways, whereas the “urban/residential” class represents built-up areas such as large commercial buildings and houses. A minimum of 50 sample points per LULC class were generated using a stratified random sampling approach for the classification accuracy assessment. The assessment was done using Google Earth with the help of local area knowledge. The producer’s accuracy, user’s accuracy, overall accuracy, and Kappa coefficient are calculated from the error matrix and reported in Table 1. The overall accuracy of image classification exceeds 85% for both LULC maps (Table 1).

MODIS LST IMAGE PROCESSING AND DATA ANALYSIS

SUHI is normally defined as the LST difference between urban and its surrounding suburban background (Oke, 1995; Steward and Oke, 2012), denoted by $\Delta T_{\text{u-r}}$ in the subsequent context. Using this definition, a 10-20 km buffer region is first created for the non-urbanized areas surrounding the Phoenix metropolitan boundary in ArcMap software. This buffer is selected because there is no converted natural landscape in this region. In order to avoid confusion and for a fair comparison, mountainous regions and large water bodies within the buffer are manually removed, and only areas that have an elevation that falls within 2 standard deviations from the mean elevation of the city are retained.

The metropolitan and rural buffer pixels are extracted from the MODIS LST images and pixel values are converted to LST in degrees Celsius (°C) for both daytime and nighttime images. The mean metropolitan and buffer LST images are then calculated by averaging four June LST images for every year (two images for 2001), resulting in 15 daytime and 15 nighttime mean LST images. Finally, the mean LST is calculated for the entire buffer region for every year and subtracted from each Phoenix metropolitan pixel to generate LST difference maps. These maps are named Level-1 products. The pixel values, $\Delta T_{\text{u-r}}$, now represent LST differences between the metropolitan and non-urbanized buffer area.

Using the year sequence of 2000 to 2017 as the independent variable and $\Delta T_{\text{u-r}}$ as the dependent variable, a time-series trend analysis is then performed using ordinary least square (OLS) regression on every single pixel to examine if $\Delta T_{\text{u-r}}$ has significantly changed during the study period. Since this study is designed to examine pixels that have experienced statistically significant changes in $\Delta T_{\text{u-r}}$, the regression results that have a *p*-value less than 0.05 are retained for all Level-1 products. This procedure generates a *p*-value map, an *R*-squared value map, and a regression slope coefficient map for both daytime and nighttime. These maps are named Level-2 products. The detailed LST image processing and data analysis workflow is shown in Figure 3.

LULC CHANGE ANALYSIS

This step analyzes LULC change in the Phoenix metropolitan area and its relationship with $\Delta T_{\text{u-r}}$ variations between 2000 and 2017. All the pixels in Level-2 products that have experienced statistically significant increases and decreases in $\Delta T_{\text{u-r}}$ are separated for both daytime and nighttime images. The separated pixels (1,000 m resolution) are used to mask 2000 and 2017 Phoenix LULC maps (30 m resolution) respectively, resulting in eight LULC maps (30 m resolution) for the specific areas of daytime increasing $\Delta T_{u\text{-}r}$; daytime decreasing $\Delta T_{u\text{-}r}$; nighttime increasing $\Delta T_{u\text{-}r}$; and nighttime decreasing $\Delta T_{u\text{-}r}$ for 2000 and 2017 respectively.

The total area of each LULC class from all the maps generated above are then calculated and compared between 2000 and 2017. The area percentage difference of each LULC class within the same 1,000 m Level-2 product pixel is also calculated. The area percentage difference is positive if there is an area increase, and negative if the area percentage decreases. For example, in 2000 there was 30% urban/residential area, 40% open soil, 20% vegetation, and 10% impervious surface within one particular 1,000 m Level-2 product pixel. The area percentages became 60% urban/residential area, 10% open soil, 10% vegetation, and 20% impervious surface in 2017. The area percentage differences are +30%, -30%, -10%, and +10% for urban/residential area, open soil, vegetation, and impervious surface respectively within that particular Level-2 product pixel. For the analysis of the impact of LULC change on LST variation, the LULC area percentage difference values (*x*-variable) are then analyzed against the regression slope coefficient values from Level-2 products (*y*-variable) using Pearson's correlation analysis. The correlation coefficients (*r*) and *p*-values are reported.

RESULTS

REGRESSION RESULTS

The regression results (Figures 4-6) show that the Phoenix metropolitan area has experienced very significant $\Delta T_{u\text{-}r}$ changes between 2000 and 2017 for both daytime and nighttime. For the slope coefficients we neglect all the slope values between ± 0.143 °C/year. A slope value between ± 0.143 °C/year approximately represents a mean $\Delta T_{u\text{-}r}$ change of less than 2°C between 2000 and 2017, which is negligible for SUHI intensity studies. The red pixels have positive slope coefficients representing the areas with increasingly higher LST than the surrounding non-urbanized areas, while the areas that have negative slope coefficients (blue pixels) represent an increasingly lower LST than the non-urbanized areas during the study period (Figure 4). The greater the absolute value of the slope coefficient is, the higher the $\Delta T_{u\text{-}r}$ change will be.

These results indicate that most significant changes of SUHI intensity have taken place on outskirts of the city with no significant changes observed in existing developed urban areas. The areas being continuously cooled during the daytime are all located on the city outskirts and the total area is approximately 47 km^2. The largest drop of $\Delta T_{u\text{-}r}$ is approximately 4 °C from 2000 to 2017. Most increasing daytime $\Delta T_{u\text{-}r}$ areas are found in the southeastern (e.g. southeast Chandler) and western (e.g. west Phoenix) parts of the metropolitan Phoenix that encompass a total area of 176 km^2, which is almost three times larger than the areas being cooled. $\Delta T_{u\text{-}r}$ has increased significantly from 2000 to 2017 during the daytime, ranging from 2 °C to 7.35 °C with the highest increase of $\Delta T_{u\text{-}r}$ found in the western part of Phoenix.

The nighttime images demonstrate a similar spatial distribution pattern, but no significantly decreasing trend was found for nighttime $\Delta T_{u\text{-}r}$. In fact, all pixels in the nighttime images show a very significant increase of $\Delta T_{u\text{-}r}$ encompassing a total area of 410 km^2, which is more than twice as large as the daytime areas. The highest $\Delta T_{u\text{-}r}$ increase at night was 5.35 °C and can be observed mostly in the southeastern part of the Phoenix metropolitan area (e.g. southeast Chandler and south Gilbert).

The R-squared (Figure 5) and p-value (Figure 6) images show that the regions that have experienced the highest significant changes of $\Delta T_{\text{u-r}}$ for the daytime are in the southeast (e.g. southeast Chandler and south Gilbert), west (e.g. west Phoenix), and northwest (e.g. west Surprise and southwest El Mirage). At night, the southeastern (e.g. southeast Chandler and south Gilbert) and western (e.g. west Phoenix and north Goodyear) parts of the metropolitan area have the highest R^2 values (Figure 5) and all pixels are significant at the 0.01 level (Figure 6). The nighttime $\Delta T_{\text{u-r}}$ changes are found to be much more significant and the relationships are much stronger than the daytime $\Delta T_{\text{u-r}}$.

LULC CHANGE ANALYSIS RESULTS

The total area of LULC types for those regions that have experienced significant $\Delta T_{\text{u-r}}$ changes for 2000 and 2017 are shown in Figure 7. Note that the urban/residential and impervious surface areas increase dramatically in each scenario, while the areas of water, fallow cropland, and open soil decrease. For the daytime increasing $\Delta T_{\text{u-r}}$ regions (Figure 7a), the urban/residential area has increased more than fourfold from 10.58 km^2 to 45.57 km^2, and the impervious surface area has almost tripled from 14.9 km^2 to 41.63 km^2. The decrease of vegetation area from 86.03 km^2 to 40.85 km^2 is the most notable among all the other LULC types. The same LULC change pattern was also found for the regions where $\Delta T_{\text{u-r}}$ has increased at night (Figure 7b). In this case, the total area of the urban/residential class has increased from 35.33 km^2 to 134.52 km^2 and impervious surface area has increased from 35.96 km^2 to 89.97 km^2, while all the other LULC types, including vegetation, have decreased. This suggests that urbanization is the major LULC change characteristic between 2000 and 2017 for those regions that have experienced increasing $\Delta T_{u\text{-}r}$. Figure 7c shows LULC areas for the regions where daytime $\Delta T_{u\text{-}r}$ has significantly decreased. While both the urban/residential and impervious surface areas for these regions increased, vegetation also increased from 10.48 km^2 to 16.1 km^2. This suggests that vegetation increase can help lower daytime urban surface temperature.

The correlation analysis results (Table 2) further explain how LULC changes influence $\Delta T_{u\text{-}r}$ variation and which LULC change has the most significant effect on the variability of the SUHI intensity. Both open soil and impervious surface areas have significant positive correlations ($p < 0.05$) with the regression slope coefficient for both daytime and nighttime, indicating a heating effect contributed to the UHI effect. The correlation between open soil areas and slope coefficient is much weaker for the nighttime scenario ($r = 0.1237$, $p < 0.05$) than the daytime ($r = 0.4287$, $p < 0.01$), while urban/residential areas tend to have a stronger heating effect at night ($r = 0.3009$, $p < 0.01$). Vegetation cover has highly significant negative correlation with the slope coefficient for both daytime ($r = -0.6087$, $p < 0.01$) and nighttime ($r = -0.4157$, $p < 0.01$), which means that the vegetation has a strong cooling effect that can mitigate the UHI effect in Phoenix. In addition, fallow cropland is also found to have a potential cooling effect at night, but the correlation is relatively weak although it is still highly significant ($r = -0.1463$, $p < 0.01$).

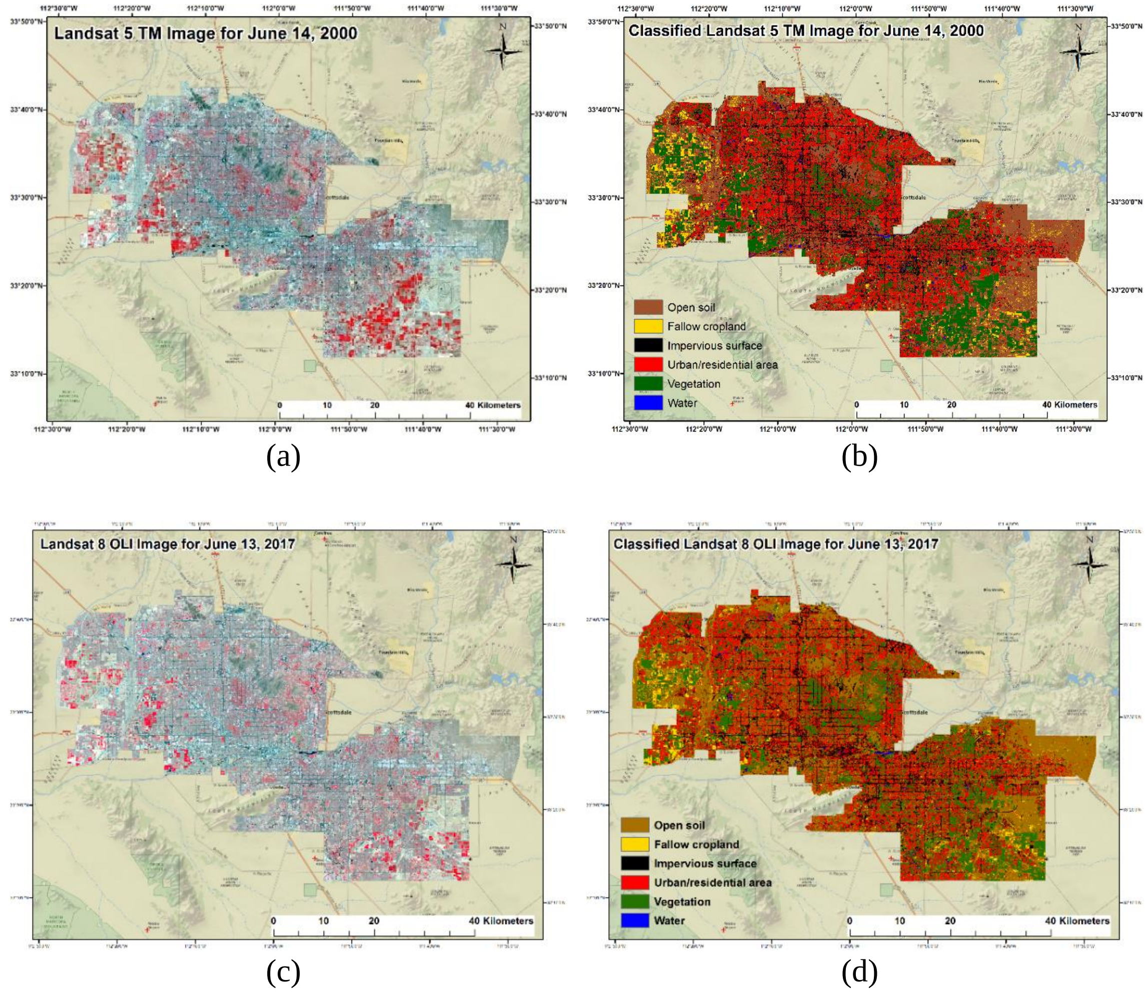

Figure 1.2 Landsat color infrared (CIR) imagery (a and c) and classified LULC maps (b and d) for the Phoenix metropolitan area. The six LULC classes include open soil, fallow cropland, impervious surface, urban/residential area, vegetation, and water.

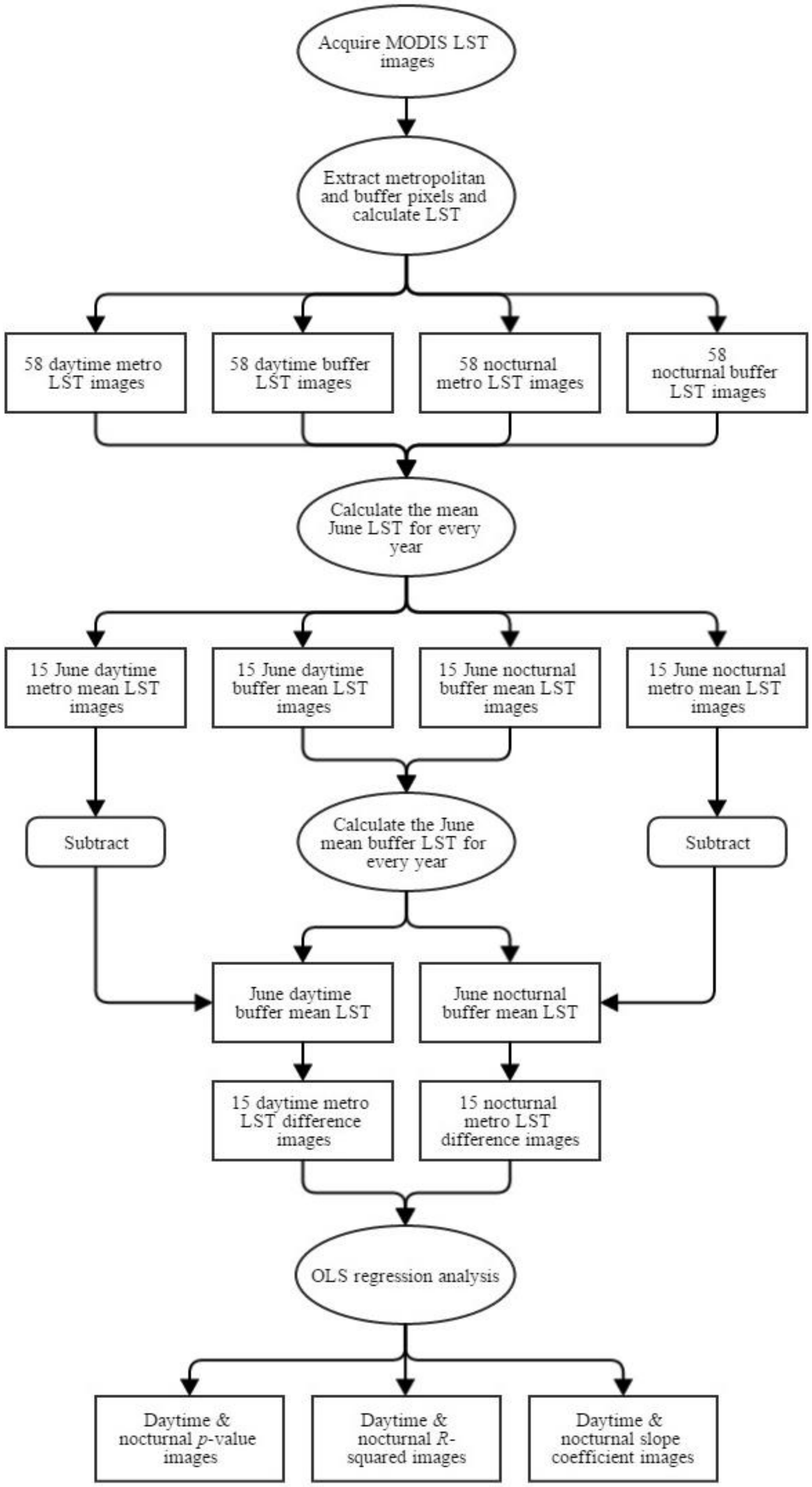

Figure 1.3 Image processing flowchart.

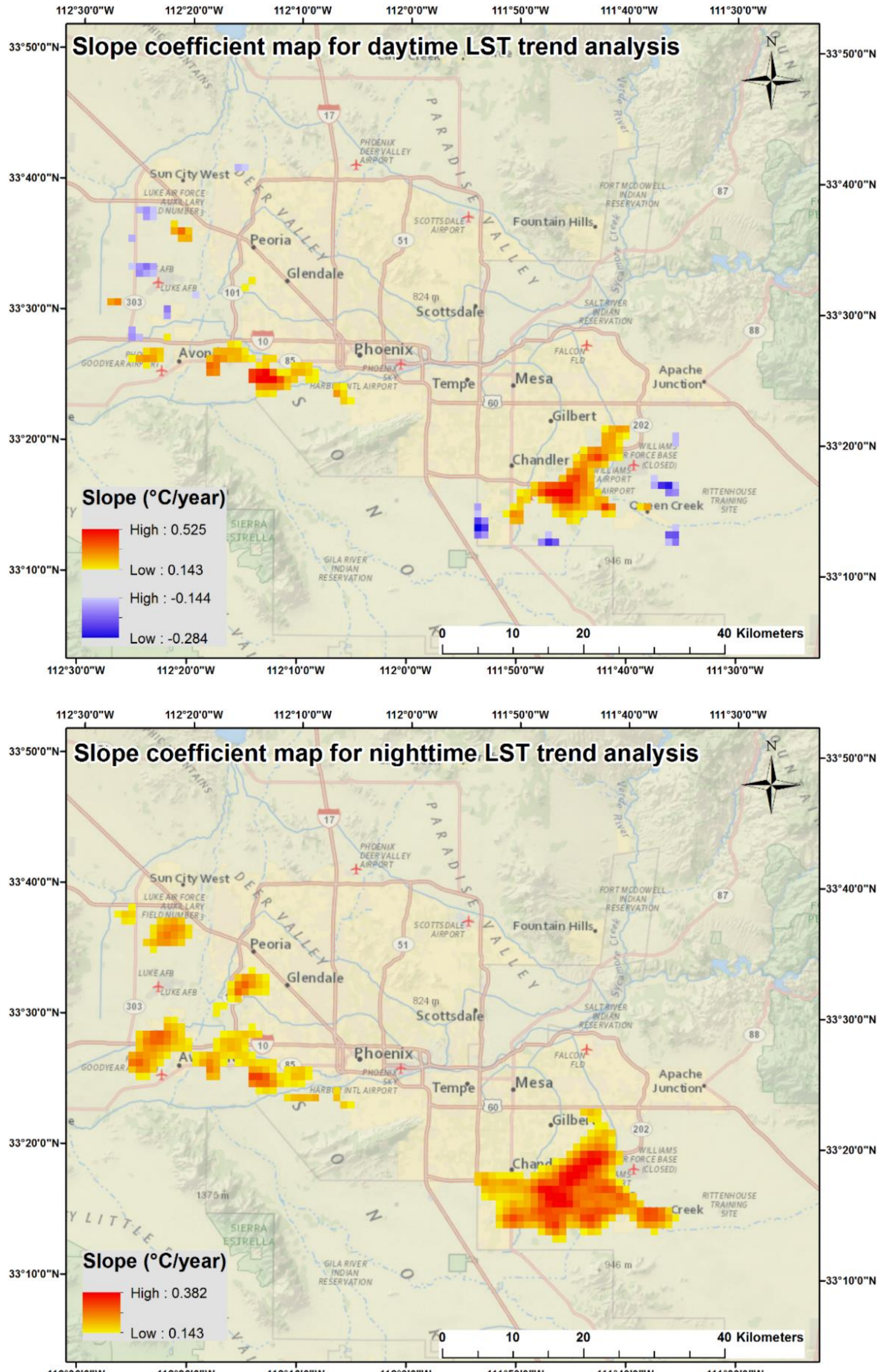

Figure 1.4 Slope coefficient maps for daytime and nighttime LST trend analysis.

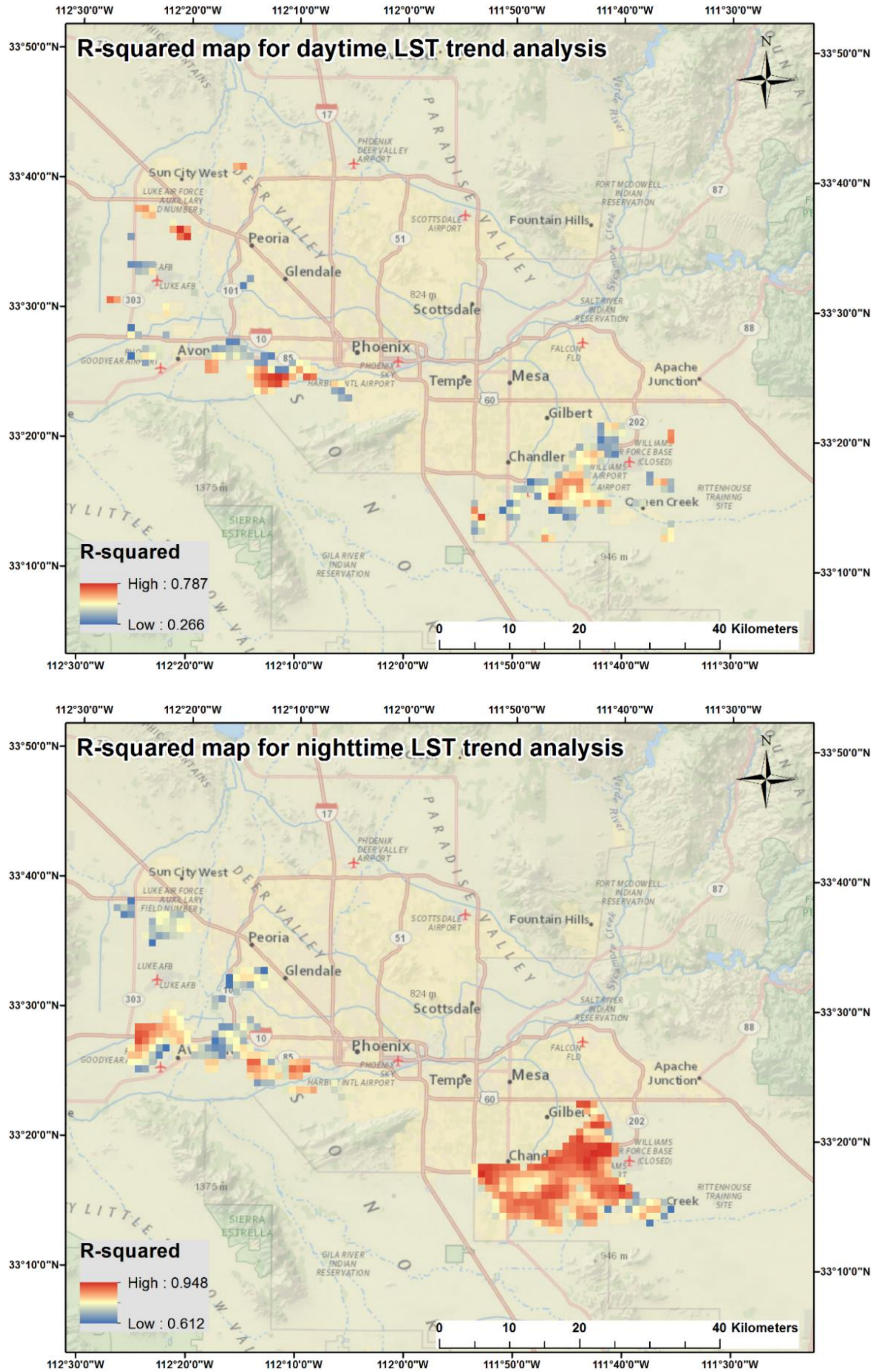

Figure 1.5 Daytime and nighttime *R*-squared value images.

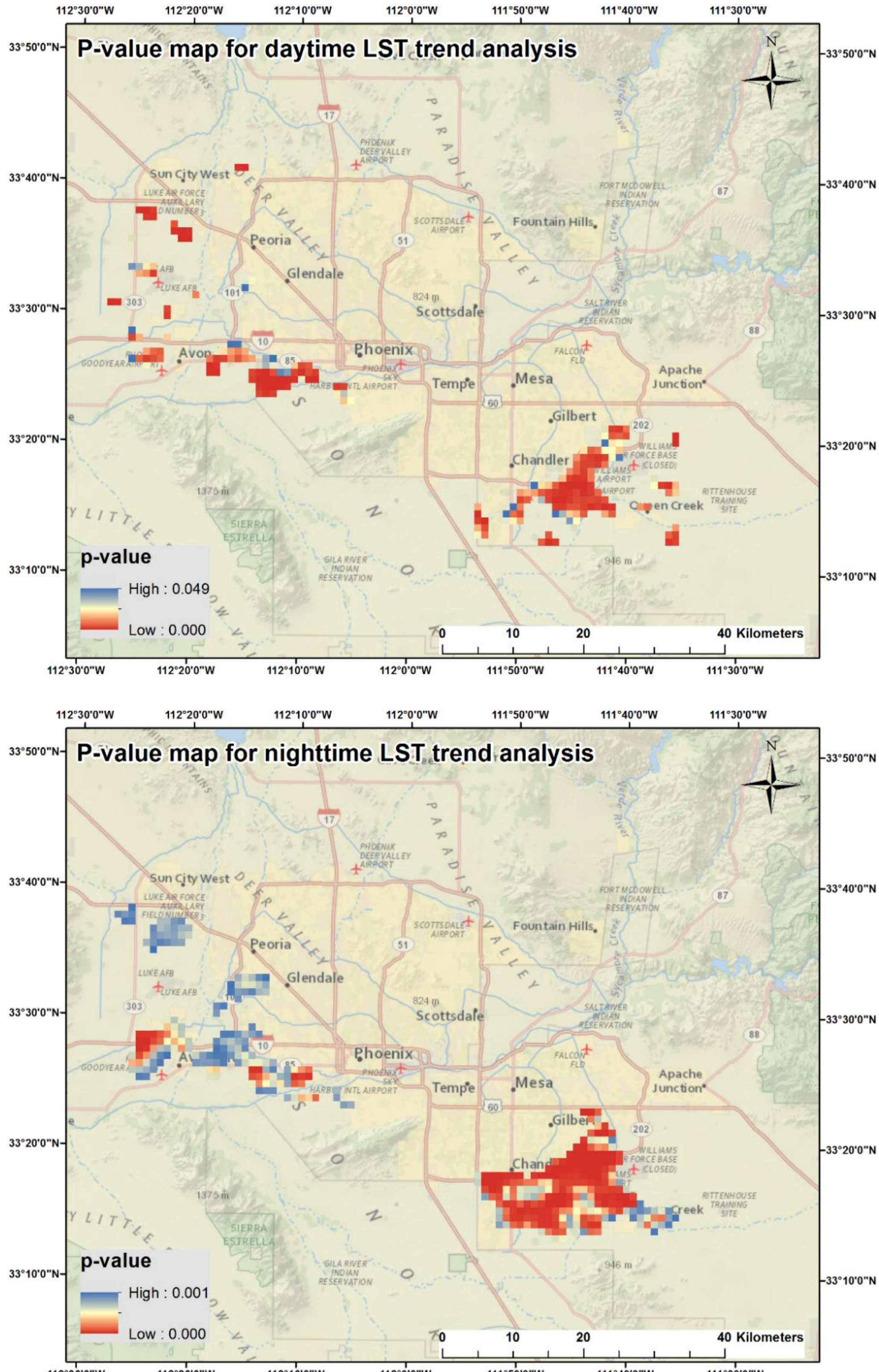

Figure 1.6 Daytime and nighttime *p*-value images.

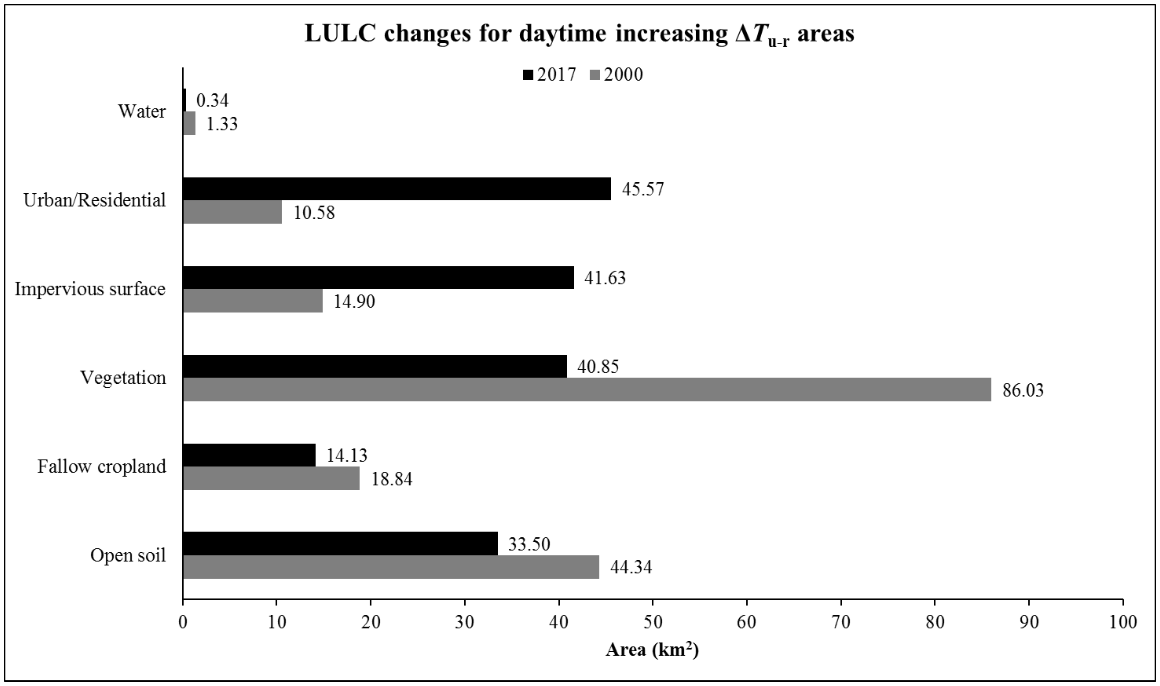

(a)

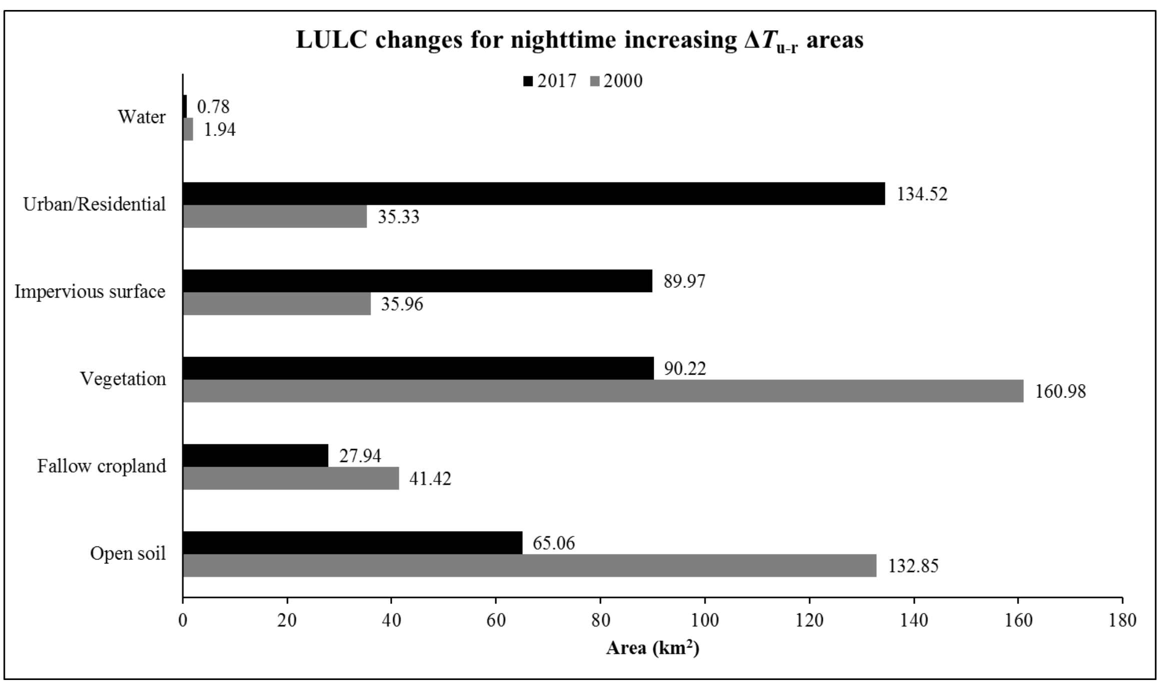

(b)

Figure 1.7 *Continued*.

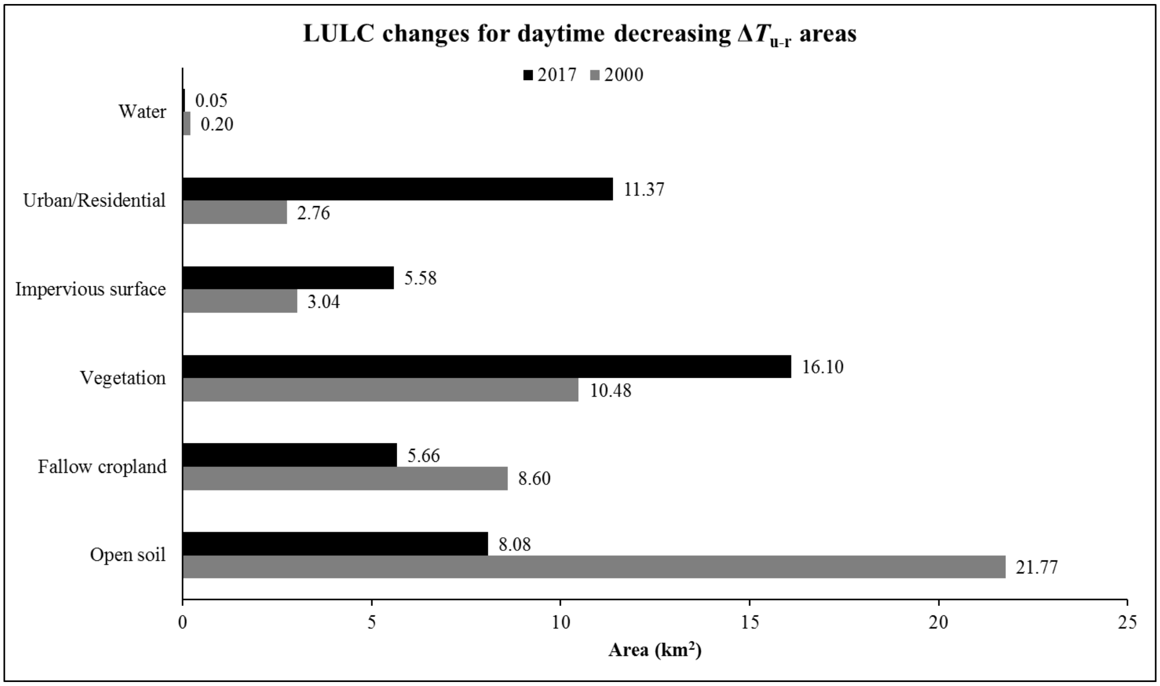

(c)

Figure 1.7 The comparison of total area for each LULC type between 2000 and 2014 for regions that have experienced significant $\Delta T_{u\text{-}r}$ changes. Please note that No significant decreasing $\Delta T_{u\text{-}r}$ has been observed for the nighttime.

Table 1.1 Image classification accuracy assessment

LULC types	2000 Landsat 5 TM image		2014 Landsat 8 OLI image	
	Producer's Accuracy	User's Accuracy	Producer's Accuracy	User's Accuracy
Open soil	79%	83%	77%	85%
Fallow cropland	79%	80%	84%	76%
Urban/Residential	83%	86%	79%	85%
Vegetation	100%	90%	98%	94%
Impervious surface	80%	85%	78%	81%
Water	97%	92%	97%	89%
Overall accuracy	86%		85%	
Kappa coefficient	0.83		0.82	

Table 1.2 Correlation analysis between slope coefficient values from LST trend analysis and LULC change for both daytime and nighttime.

	Open soil	Fallow cropland	Urban/ residential	Vegetation	Impervious surface	Water
Slope (daytime)	0.4287* (0.0000)	0.0564 (0.4016)	0.1136 (0.0905)	-0.6087* (0.0000)	0.3631* (0.0000)	0.0253 (0.7076)
Slope (nighttime)	0.1237* (0.0122)	-0.1463* (0.0030)	0.3009* (0.0000)	-0.4157* (0.0000)	0.3399* (0.0000)	0.0209 (0.6729)

Note: LULC change here means the area percentage difference between 2000 and 2014. See Section 3.3 for details. The *p*-values are in parentheses. The correlation coefficients that are statistically significant at the 0.05 level are marked by an asterisk (*).

DISCUSSION

The SUHI intensity in the Phoenix metropolitan area has increased dramatically in the past 15 years. The most significant changes occurred most often on the metropolitan outskirts, with little change observed in existing developed areas, such as downtown Phoenix, Tempe, and Mesa. Although LST can be very high in these developed areas, LST changes over time are insignificant because there were no obvious LULC changes.

Although the nighttime SUHI intensity for the entire Phoenix metropolitan area is slightly lower than that of the daytime (Figure 4), the total area that suffers increasing UHI effect is much larger at night. The LST increasing trend is much stronger (Figure 5) and more statistically significant (Figure 6) for the nighttime, resulting in the metropolitan Phoenix area's UHI effect becoming more and more prominent at night.

Urbanization in Phoenix has quickly converted geographic terrains from natural landscapes, such as grasslands, open soil, and undisturbed desert area, and cultivated vegetation such as croplands, to manmade engineered surfaces and infrastructure. The effect of built-up environment manifest itself by impacting turbulent transport radiative heat exchange and hydrological processes, especially in urban canopies (Wang et al., 2013). Schatz and Kucharik also demonstrated in their paper that the built-up environment was the primary driver of the spatial change in temperature patterns in the urban area (Schatz and Kucharik, 2014). They found that urban environments, together with their dark impervious surfaces and reduced vegetation cover, normally have large heat capacity and high thermal conductivity rates (Oke, 1982; Oke, 1995; Weng, 2001; Bouyer et a., 2009; Lu et al., 2012; Song and Wang, 2015). This not only causes less incoming solar radiant energy to be reflected, but also less of the energy to be converted to latent heat associated with evaporation and transpiration (Golden, 2004).

Manmade materials, especially dark impervious surfaces, absorb shortwave radiation and store heat during the daytime. They then release longwave radiation slowly at night, heating up the lower atmosphere (Oke, 1982; Mills, 1999; Bouyer, 2009). The correlation analysis results (Table 2) indicate that it is the percentage increase of impervious surfaces, rather than the urban/residential buildings, that have the highest and most significant positive correlation with the regression slope coefficients. This finding is consistent with some other studies (Yuan and Bauer, 2007; Myint et al., 2013). In addition, anthropogenic activities also have a great impact on urban climate by generating and releasing heat and water into the atmospheric boundary layer (Bohnenstengel et al., 2011; Pal et al., 2012; Lac et al., 2013), by way of fuel burning, air conditioning, automobiles, and machinery, that cannot be quickly dispersed (Golden, 2004). As rural landscapes are being continuously converted to built-up environments, larger rural areas suffers significant LST increase and UHI effect. All the aforementioned mechanisms explain why most significant increase of $\Delta T_{\text{u-r}}$ occurs on the city outskirts but not within the city's developed areas. It also explains why the $\Delta T_{\text{u-r}}$ increasing trend is much stronger and a much larger area of SUHI intensity has been observed for the nighttime rather than the daytime.

Vegetation evapotranspiration can lower LST by releasing more latent heat flux but less sensible heat flux from the surface to the atmosphere. Research has reported that normally lower LSTs are found in areas with higher vegetation cover (Yuan and Bauer, 2007), and increasing vegetation cover area is considered an effective mitigation strategy to reduce UHI effects (Rosenfeld et al., 1995; Ca et al., 1998; Ashie et al., 1999; Tong et al., 2005; Yu and Hien, 2006). In addition, controlled irrigation of green spaces in cities can help to reduce thermal stress and building energy consumption during hot seasons (Yang and Wang, 2015). Our correlation analysis shows that the increase of vegetation cover has the strongest and most significant negative relationship with the regression slope coefficients (Table 2), indicating that an increase of vegetation cover can lower LST in the urban area.

The reduction of green spaces (Figures 7a and 7b) in Phoenix has also caused significant increases of $\Delta T_{\text{u-r}}$ for both daytime and nighttime (Table 2). By 2017, more than half of the vegetated area has disappeared for the daytime scenario (Figure 7a), and about 44% of the vegetation cover has been converted for the nighttime scenario (Figure 7b). Conversely, for daytime decreasing $\Delta T_{\text{u-r}}$ areas, the vegetation cover area was increased by almost 60% although the urban/residential area and impervious surface area have also dramatically increased (Figure 7c).

The correlation analysis results (Table 2) also demonstrate that the absolute values of the correlation coefficients for the vegetation cover for both daytime and nighttime scenarios are higher than the urban/residential areas and impervious surfaces. This finding demonstrates that the cooling effect of increased vegetation cover is actually stronger than the heating effect due to urban development and expansion. This is consistent with a previous finding that anthropogenic heat has a smaller effect than albedo and vegetation cover (Taha, 1997). Therefore, the increased vegetation cover is the primary contribution to the decreased $\Delta T_{\text{u-r}}$. In addition, the cause of increased vegetation cover is the conversion from open soil, fallow cropland, and urban infrastructure because vegetation cover has significant negative correlations with all these LULC types (Table 2). As shown in the

2017 Landsat image, the most increased vegetated areas are irrigated croplands and golf courses. We therefore suggest that planting vegetation could effectively mitigate the UHI effects in a desert city like Phoenix for both daytime and nighttime.

Large water bodies have greater specific heat capacity and they have been found to provide potential cooling effect at daytime (Lo et al., 1997). Phoenix is a desert city so large open-air water body is very scarce. The lack of variation in open water surfaces, together with potential image classification error, means that there is no statistically significant relationship between the change of water body area and LST variation in this research.

CONCLUSION

Phoenix is a subtropical desert city that is also one of the warmest cities in the United States. Excessive heat in the urban area has been a major concern for decades, especially during the summer months. This heat compromises human health and comfort as well as causes water and energy consumption issues, and poor air quality. This research identified the regions in the Phoenix metropolitan area that have experienced the most significant changes of SUHI intensity from 2000 to 2017 using MODIS LST imagery. The relationship between LULC changes and LST variations has also been studied using classified LULC maps created from Landsat imagery.

For both daytime and nighttime, the regions that have experienced the most significant $\Delta T_{u\text{-}r}$ changes between 2000 and 2017 include the southeastern and western parts of the metropolitan area. Regions where $\Delta T_{u\text{-}r}$ has decreased are only observed for the daytime and are most often located on outskirts of metropolitan Phoenix. The increase of daytime $\Delta T_{u\text{-}r}$ is slightly higher than the nighttime. The areas that have experienced significant increases of SUHI intensity are, however, much larger at nighttime.

Urbanization is the primary cause for increased SUHI intensity during the study period. Despite the dramatic increase of urban/residential and impervious surface areas, some areas have decreasing $\Delta T_{u\text{-}r}$ during the daytime due to increased vegetation cover for those areas. This study found that the cooling effect of increased vegetation cover is stronger than the heating effect of urbanization for the Phoenix metropolitan area.

In conclusion, the UHI effect in the metropolitan Phoenix has been gradually exacerbated by the rapid development and expansion of the urban area since 2000. More sustainable landscape planning for future city development becomes more pressing, as Phoenix's rapid population and economic growth continues. Based on the results and findings from this research, we would recommend that increase in vegetation cover, with the trade-off between water and energy carefully studied, can be a potentially effective means to mitigate the UHI effect in those high SUHI intensity areas. It is an easy, low-cost, and feasible way to lower the UHI effect and conserve energy.

In addition, we suggest that urban planners, decision makers, and city managers formulate new policies and regulations that encourage residential, commercial, and industrial developers to include vegetation, such as trees, shrubs, and grass, when planning new construction. These policies should include setting certain percentages of vegetation cover or numbers of small trees with exact height and crown coverage or shrubs before structures are built. This would prevent the clearing of land for built-up areas that typically leaves no vegetation cover, resulting in large areas of exposed open soils, buildings, and impervious surfaces. The concentration of these manmade surfaces elevates LST dramatically over the long run. Keeping existing vegetation or adding vegetation during construction offsets the heat retained by these surfaces. This is especially true for desert cities. Thus, we believe that this is an emerging issue that policy makers and city planners need to pay attention to.

CHAPTER 2

EMPIRICAL MODELLING AND SPATIO-TEMPORAL PATTERNS OF URBAN EVAPOTRANSPIRATION FOR THE PHOENIX METROPOLITAN AREA, ARIZONA

INTRODUCTION

Conversion from natural terrain and agricultural land to built-up environment has taken place ubiquitously worldwide at an increasing rate to meet the ever-increasing demand of rapid growth of urban population (Seto *et al.* 2011). Associated with the use of construction and building materials, such as asphalt, concrete, bricks, etc., urbanization modifies surface energy balance and hydrological cycle, leading to significant impacts on local and regional hydroclimate (Owen *et al.* 1998; Kondoh and Nishiyama 2000; Zhang *et al.* 2009; Georgescu *et al.* 2012; Wang *et al*. 2013). Evapotranspiration (ET) is one of the major components of the hydrologic cycle, but the impacts of urbanization on ET vary largely with local climatic conditions. Liu *et al.* (2010) studied the relationship between different land use land cover (LULC) types and urban ET for a semi-arid city in Oklahoma, USA, and found that different LULC types have different ET rates in the urban area with the lowest ET found in highly developed areas. They also argued that the conversion from natural vegetated landscape and water body to built-up environment could significantly lower ET (Liu *et al.* 2010). On the other hand, Balling and Brazel (1987a) studied ET rates using Phoenix, Arizona, USA as the study area, and found that rapid urbanization had caused a significant increase of ET level under a subtropical desert climate.

In many circumstances, urban ET exceeds precipitation and is mainly sustained by the use of external water (Grimmond and Oke 1999), and urban vegetation receives a substantial amount of water from anthropogenic irrigation, especially in arid and semi-arid areas (Gober *et al*. 2009; Johnson and Belitz 2012). A previous study reported that irrigation of private gardens consumes about 16-34% of the total urban water supplied, let alone the water used for irrigating large open space such as public parks and golf courses (Mitchell *et al*. 2001). Field experiments also found that potential ET rate of irrigated urban lawn was about 1.3 times greater than that from a rural pasture (Oke 1979). This phenomenon is especially significant to desert cities because irrigated urban vegetation patches can help the city stay cooler than the surrounding dry desert region, which is known as the urban oasis effect (Oke 1979; Yang *et al*. 2015).

Although the impacts of LULC change on urban ET rate have long been a focal research area, most studies made use of temporally discrete ET data collected from local weather stations or flux towers, which only provide information for a limited spatial coverage surrounding the station. Predicting and mapping ET for the spatial continuum of the entire urban area remain challenging. A number of numerical methods have been developed for estimating urban ET during the past decade, which can be broadly categorized into two groups. The first group uses urban land surface models where ET is calculated using a bulk transfer formula (Best *et al.* 2011; Niu *et al.* 2011). This group of models is able to solve ET physically with a reasonable accuracy. However, it requires accurate estimates of input parameters related to urban geometry and thermal properties, which are not readily available from field collections and are very difficult to acquire. The second group is the empirical models that are developed from regression analysis using *in-situ* ET measurements (Granger and Hedstrom 2011; Morton 1983). Compared to the urban land surface models, empirical models are more site-specific, which may not be applicable to areas with different geographical and meteorological conditions. On the other hand, empirical models require significantly less input data and are usually more accurate at the local scale, as information of physical processes is implicitly contained in the measurements.

Remote sensing techniques offer great opportunities to acquire continuous Earth's surface observations without having direct physical contact with the surface. Many remote sensing based models have been developed and widely used to model and map ET at both regional and global scales, such as SEBAL (Bastiaanssen *et al.* 1998; Bastiaanssen *et al.* 2005), METRIC (Allen *et al*. 2007), ReSET (Elhaddad and Garcia 2008), and ALARM (Suleiman and Crago 2002) to name a few. All these models quantify the surface energy balance using remotely-sensed thermal data as an input that are associated with evaporation and transpiration processes to provide predicted ET maps. However, all these models also require the input of meteorological data to some degree, such as wind speed, humidity, solar radiation, and air temperature, which are very difficult to collect simultaneously with the acquisition of satellite images. Furthermore, meteorological data are usually collected from a limited number of local weather stations. An extrapolation technique is therefore required to predict and map ET for a larger geographic area which is sometimes not accurate for locations that are far away from weather stations. Some other studies developed models to estimate urban ET using remotely-sensed data through vegetation indices, such as the normalized difference vegetation index (NDVI) (Nouri *et al.* 2013;

Johnson and Belitz 2012). These models may be effectively applicable to a city with relatively high vegetation cover, but is not applicable to the Phoenix metropolitan area due to its unique desert environment.

One of the most widely used satellite remotely-sensed dataset is the MODerate-resolution Imaging Spectroradiometer (MODIS) data that provides daily observations for the entire surface of the Earth. Many MODIS land products have been produced at various spatial and temporal resolutions to meet different scientific demands. One of the most popular products is the MODIS global terrestrial ET product (MOD16) that provides regional and global observations for surface water and energy balances and soil moisture status (Mu *et al.* 2007; Mu *et al.* 2013). The predicted ET data from this product, however, are not available for urban areas because the model was not specifically developed for the urban land cover type. In addition, this dataset only covers the time period from 2000 to 2010 at 1 km spatial resolution. The short temporal coverage and relatively coarse spatial resolution make it unsatisfactory for urban ET studies. Therefore, a specific model is needed to predict urban ET using remotely-sensed data at a finer spatial resolution for a longer temporal coverage in order to study spatial and temporal changes of urban ET.

To fill the gap in literature, two objectives of this study are posed. The first objective is to establish an empirical model specifically for the Phoenix metropolis to predict urban ET using *in-situ* ET measurements and remotely-sensed data. The second objective is to discover specific areas that have experienced significant ET changes and the spatio-temporal patterns of urban ET change for the entire Phoenix metropolitan area from 2001 to 2015.

STUDY AREA

The Phoenix metropolitan area is located in the northeast part of the Sonoran Desert in the central Arizona, USA, and is the sixth largest U.S. city encompassing a total area of approximately 2,800 km^2 (Figure 1) with an estimated population of 4.4 million (U.S. Census Bureau 2013). It lies within an arid subtropical desert climate region with extremely hot summers but mild winters. Phoenix receives an average annual precipitation of 204 mm (8.04 in.) over the last 30 years (U.S. climate data 2014). Late spring and early summer are particularly dry periods, while the summer monsoon season normally occurs between early July and early September that can bring more than 30% of the total annual precipitation through intense thunderstorms (Balling and Brazel 1987b; Adams and Comrie 1997; Vivoni *et al.* 2008). The daily high temperature exceeds 37.8 °C (100 °F) for an average of 110 days every year that normally occurs from late May until early September. The highest temperature can reach more than 43.3 °C (110 °F) for an annual average of 18 days. The study area has diverse LULC types, including commercial, industrial, and residential areas, undisturbed desert, agriculture, grassland, and water bodies.

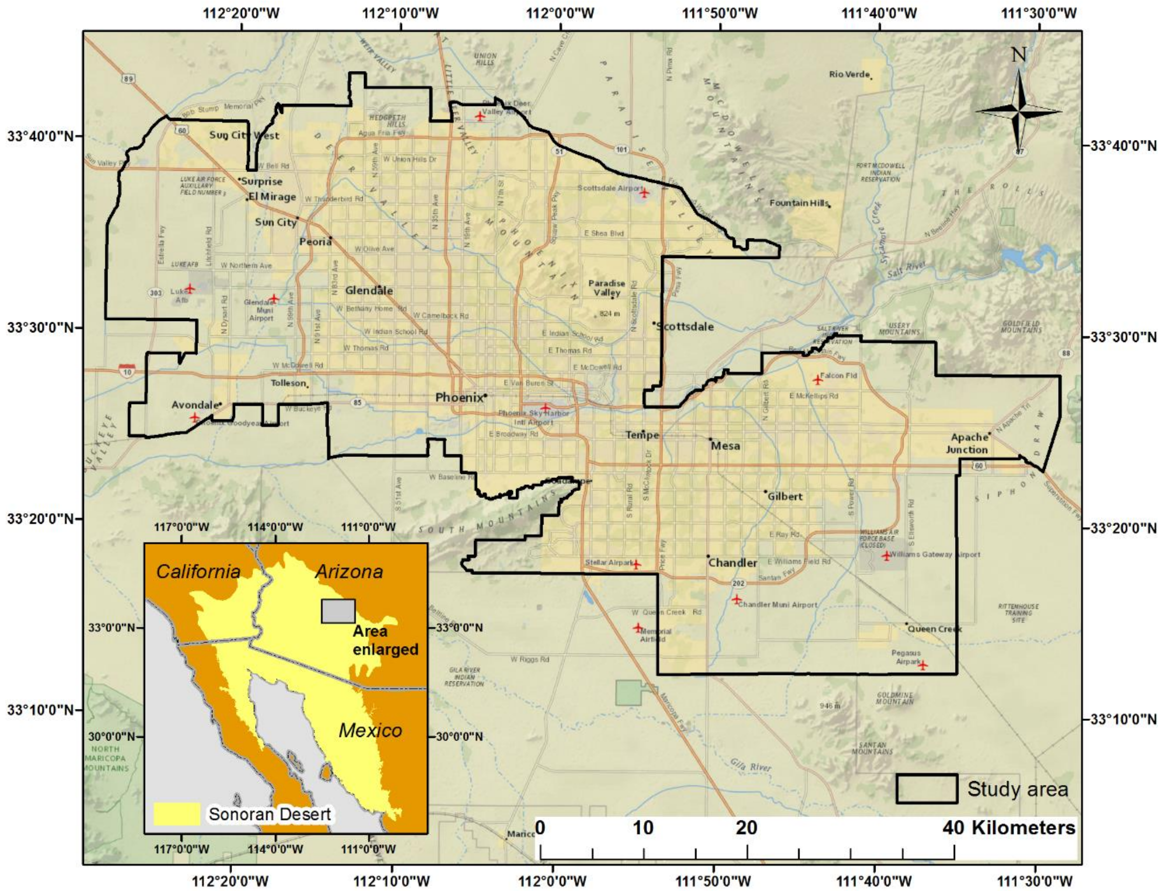

Figure 2.1 Map of study area: Phoenix metropolitan Area.

DATA AND METHODS

REMOTELY-SENSED DATA

This study uses three sets of readily available standard MODIS land products that are processed and distributed by NASA and USGS. These products have demonstrated high scientific quality and are being used to answer science questions in a variety of disciplines. The first MODIS land product contains the bidirectional reflectance distribution function and albedo (MCD43A3) that provides both directional hemispherical reflectance (black-sky albedo) and bihemispherical reflectance (white-sky albedo) images with a 500-m spatial resolution. The data accuracy is well less than 5% albedo at the majority of the validation sites (Wang *et al*. 2014). The production function of black-sky albedo is based on the assumption that the entire light source is directional, while the white-sky albedo is based on the assumption that the light source is diffuse. The actual albedo (blue-sky albedo) is an interpolation of these two as a function of the fraction of diffuse skylight using:

$$\alpha_{blue} = \alpha_{ws} \cdot f_{diff} + \alpha_{bs} \cdot (1 - f_{diff}) \tag{1}$$

where α_{blue}, α_{ws}, and α_{bs} are the blue-sky, white-sky, and black-sky albedo, respectively, and f_{diff} is the diffuse skylight ratio. This MODIS product is produced every 8 days with an acquisition duration of 16 days. For example, the first production period (Period 001) includes acquisition days from Day 1 to Day 16, and the second production period (Period 009) includes acquisition days from Day 9 to Day 24, and so on. It can be found that there is an 8-day overlap between every two consecutive production periods. Therefore, the last production period is Period 345 that includes acquisition days from Day 345 to Day 360. A total of 44 blue-sky albedo images are therefore acquired for every year.

The second MODIS product used is the temperature and emissivity (MOD11A1) product. This product provides daily land surface temperature (LST) with a spatial resolution of 1 km for both daytime and nighttime. The data validation study reported that the LST products were validated within 1K in the range of 263-322K and the atmospheric column water vapor range of 0.4-3.0cm (Wan *et al*. 2002). A mean daily LST dataset for Phoenix is generated by averaging daytime and nighttime LST images.

Another potentially relevant parameter is vegetation index for estimation urban ET. However, the MODIS vegetation indices do not include data for urban areas. It is therefore necessary to generate vegetation index datasets for the Phoenix metropolitan area on our own. The MODIS global surface reflectance (MOD09GA) product is collected daily at 500 m spatial resolution. It has been reported that 86.5% of the observation points for the red band (Terra Band 1) and 93.99% of the observation points for the near infrared (NIR) band (Terra Band 2) were within a relative error of ±(0.005+5%) (Vermote and Kotchenova, 2008). The NIR and red band reflectance images are used to calculate the NDVI using the formula below:

$$NDVI = \frac{\rho_{NIR} - \rho_{red}}{\rho_{NIR} + \rho_{red}} \tag{2}$$

where ρ_{NIR} is the reflectance of the near-infrared band, and ρ_{red} is the reflectance of the red band.

Using the same phased production method as the MODIS albedo datasets, 16-day mean LST and NDVI images are produced every 8 days with 16 days of acquisition from 2001 to 2015 for the entire Phoenix metropolitan area. This procedure generates 44 images for blue-sky albedo, mean LST, and NDVI for every year.

IN-SITU ET MEASUREMENTS

In-situ ET measurements were obtained from a flux tower deployed in a residential area located in western Phoenix (33.483847°N, 112.142609°W) through the Central Arizona-Phoenix Long-Term Ecological Research (CAP LTER) program funded by the National Science Foundation (NSF). This flux tower uses eddy-covariance methods to measure the exchanges (fluxes) of carbon dioxide (CO_2), water vapor, and energy between the terrestrial ecosystems and the overlying atmosphere within a footprint area of about 500 m in radius. The land cover/land use type around the flux tower mainly consists of low-rise, single-family residences of relatively small lot size (Chow and Brazel 2012). Garden hose for *ad-hoc* is mainly used for lawn watering, instead of automated watering systems (Chow *et al.* 2014). Swimming pools only cover less than 1% of the surface area, and most of them are left empty throughout the year (Chow *et al.* 2014).

Local scale urban surface energy balance data for the entire calendar year of 2012 and 2014 are available. The raw 10Hz flux data were collected and processed using the EDiRe software platform. The detailed data collection and processing procedures can be found in Chow *et al.* (2014). ET measurements were acquired, quality-controlled, and converted from W/m^2 to mm/day. The same phased production strategy used for MODIS data has also been applied to the ET measurements to calculate 16-day mean ET values.

The 2012 data are going to be used for establishing the empirical model, and the 2014 data are used for model verification.

MULTIPLE REGRESSION ANALYSIS

A 500-m-radius circle is created using the flux tower as the center in ArcGIS software. The circle feature is used to mask 2012 blue-sky albedo, LST, and NDVI images and to extract pixel values for the corresponding dates when ET data are available. The correlation matrix among these three variables is shown in Table 1. The low and insignificant correlation values indicate a small likelihood of multicollinearity problem.

An ordinary least squares (OLS) regression analysis is then performed using ET as the dependent variable, and albedo, LST, and NDVI as independent variables to establish a multiple regression model of the best fit. The model is formulated as:

$$ET = \beta_0 + \beta_1 \cdot albedo + \beta_2 \cdot LST + \beta_3 \cdot NDVI + \varepsilon \tag{3}$$

where β_1, β_2, and β_3 are the coefficients for albedo, LST, and NDVI respectively. β_0 is the intercept, and ε is the error term that assumes to be normally distributed with mean 0.

URBAN ET MAPPING AND TIME-SERIES TREND ANALYSIS

The multiple regression model established above is then applied to all the image pixels to make ET predictions for the entire Phoenix metropolitan area. The annual ET map is then created by adding all 44 predicted ET images for every year from 2001 to 2015. The 15-year mean annual ET values of every single pixel stack are treated as the dependent variable and analyzed against the year sequence (2001-2015) by OLS regression. The regression model is written as:

$$ET = a + b \cdot year + \varepsilon \tag{4}$$

where a is the intercept, b is the slope coefficient that carries a practical meaning of the mean annual ET change from 2001 to 2015, and ε is the error term. Only pixels that have statistically significant changes ($p \leq 0.05$) of ET over the study period are retained.

RESULTS

MULTIPLE REGRESSION MODEL

The blue-sky albedo, LST, and NDVI values extracted from the MODIS images are used to perform an OLS regression against the 2012 ET data to establish an empirical model for ET predictions. It was initially anticipated that NDVI could potentially be correlated to urban ET. However, it turned out that NDVI was not statistically significant at the 0.05 level. Adding NDVI does not help improve the goodness-of-fit of the model, it is therefore dropped. The detailed regression analysis results are reported in Table 2, and the estimated regression equation is written as:

$$ET = 0.171 - 2.258 \times albedo + 0.033 \times LST \tag{5}$$

The model adjusted R^2 value is 0.887, which means 88.7% of the total variance of measured

ET can be explained by the estimated regression equation, indicating that the model has a good fit of the data. The *p*-value of the *F*-statistic is smaller than 0.05, suggesting that the model is highly statistically significant. The *p*-values of the *t*-statistics for albedo and LST variables indicate that the coefficients are significantly different from zero, and both variables have statistically significant linear relationships with ET. The small variance inflation factor (VIF) value indicates no multicollinearity issue.

MODEL VERIFICATION

Using Formula (5) as the estimated regression equation and MODIS blue-sky albedo and LST image pixel values as variable inputs, 44 time-series predicted ET maps are then created for 2014. The predicted ET values are extracted from the image pixel where the flux tower is deployed, and then analyzed against the measured ET data for model verification using OLS regression. Figure 2 shows that the relationship between predicted and measured ET data is strong (R^2 = 0.9071) and statistically significant (p-value < 0.05), implying that the empirical model established is valid and can be used to predict urban ET for the Phoenix metropolitan area for other years.

PREDICTED ANNUAL ET MAPS AND TIME-SERIES TREND ANALYSIS RESULTS

Figure 3 shows annual urban ET maps of Phoenix from 2001 to 2015. The red pixels indicate areas of low annual ET, while blue pixels denote high ET areas. It can be found that low ET values have been consistently observed over the study period in suburban areas on the city outskirts, such as the southeast, northwest, and west parts of the metropolis. In contrast, high ET values are found in highly urbanized areas, such as the downtown and some high-density residential areas in northern Phoenix.

The results of time-series trend analysis are shown in Figure 4. Figures 4(a) and 4(b) are the slope coefficient and the coefficient of determination (R^2) maps, respectively, that show areas in the Phoenix metropolitan area where have experienced statistically significant (p-value ≤ 0.05) changes of ET during the study period. The slope coefficient represents the mean annual ET change from 2001 to 2015. The blue pixels in Figure 4(a) represent areas of increasing ET with positive slope coefficient values, while the red pixels denote areas of decreasing ET with negative slope coefficients. The total area of increasing ET is approximately 2050 km^2, which occupies more than 70% of the entire metropolitan area, while the total area of decreasing ET is only 19.5 km^2. The largest positive slope coefficient value is 5.35, representing the highest mean annual ET increase of 5.35 mm, while the largest negative slope coefficient is -5.10, representing a mean annual ET decrease of 5.1 mm. It can be found that the increasing magnitude of urban ET is overall much higher than the decreasing magnitude.

Areas of increasing ET overspread the entire city, but the highest increments are mainly found on the city outskirts such as the southeast (i.e. south of Chandler and Gilbert) and northwest (i.e. northwest of Sun City) parts of the metropolis. These areas also have relatively higher R^2 values (blue pixels in Figure 4b), indicating a much stronger increasing trend during the study period. The areas of decreasing ET can be mainly found in three regions that are downtown Phoenix, the residential areas to the west of Phoenix downtown, and southwestern Chandler. The ET decreasing trend is relatively low in these regions because of low R^2 values (red pixels in Figure 4b), although all the pixels are statistically significant at the 0.05 level.

The global Moran's *I* technique was used to assess the spatial autocorrelation and to discover if there is a statistically significant spatial pattern for those areas of increasing and decreasing ET. Table 3 shows that both increasing and decreasing ET areas exhibit a spatially-clustered pattern, and the low *p*-values tell that there is a very small likelihood that this clustered pattern could be the result of random chance.

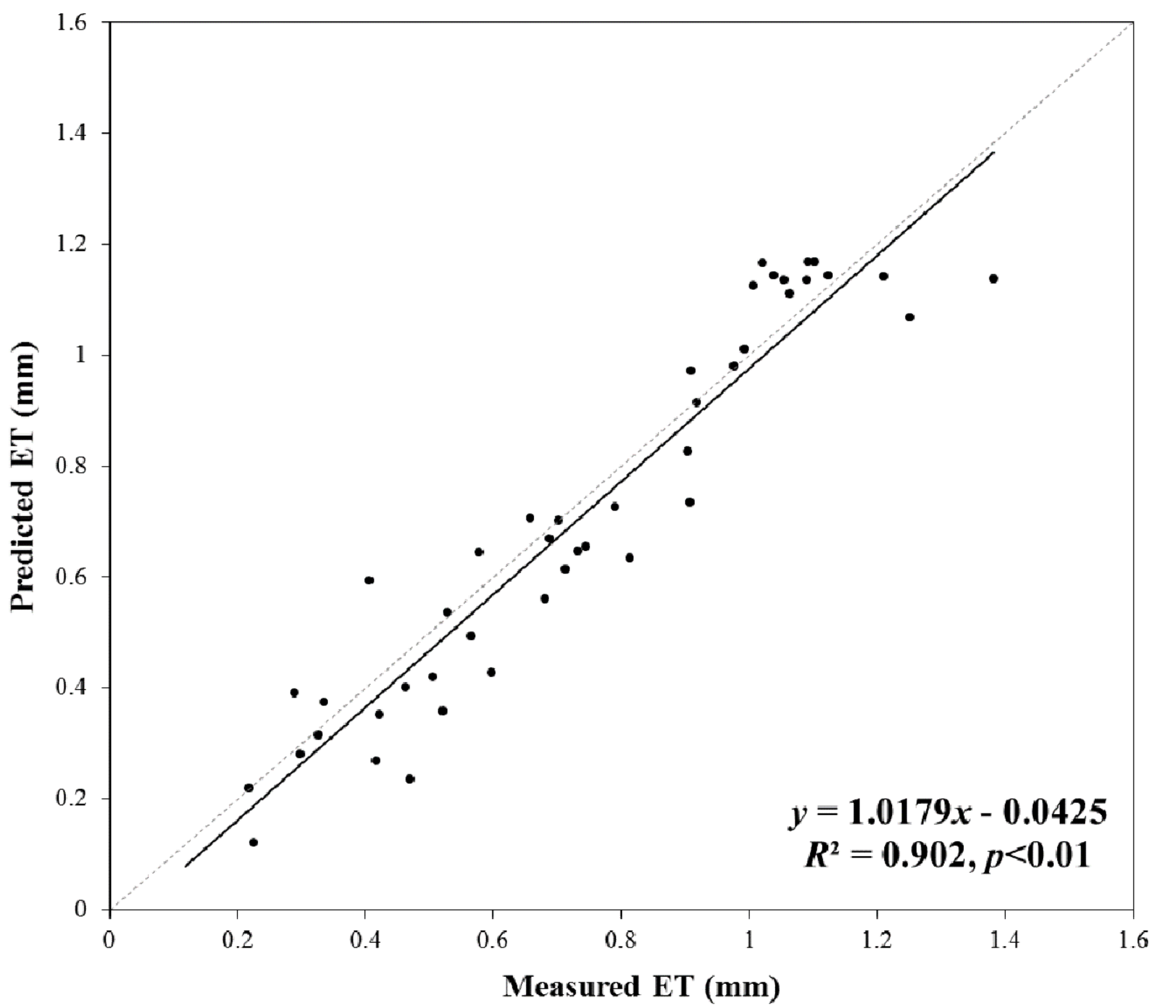

Figure 2.2 The relationship between modeled and measured urban ET for 2014.

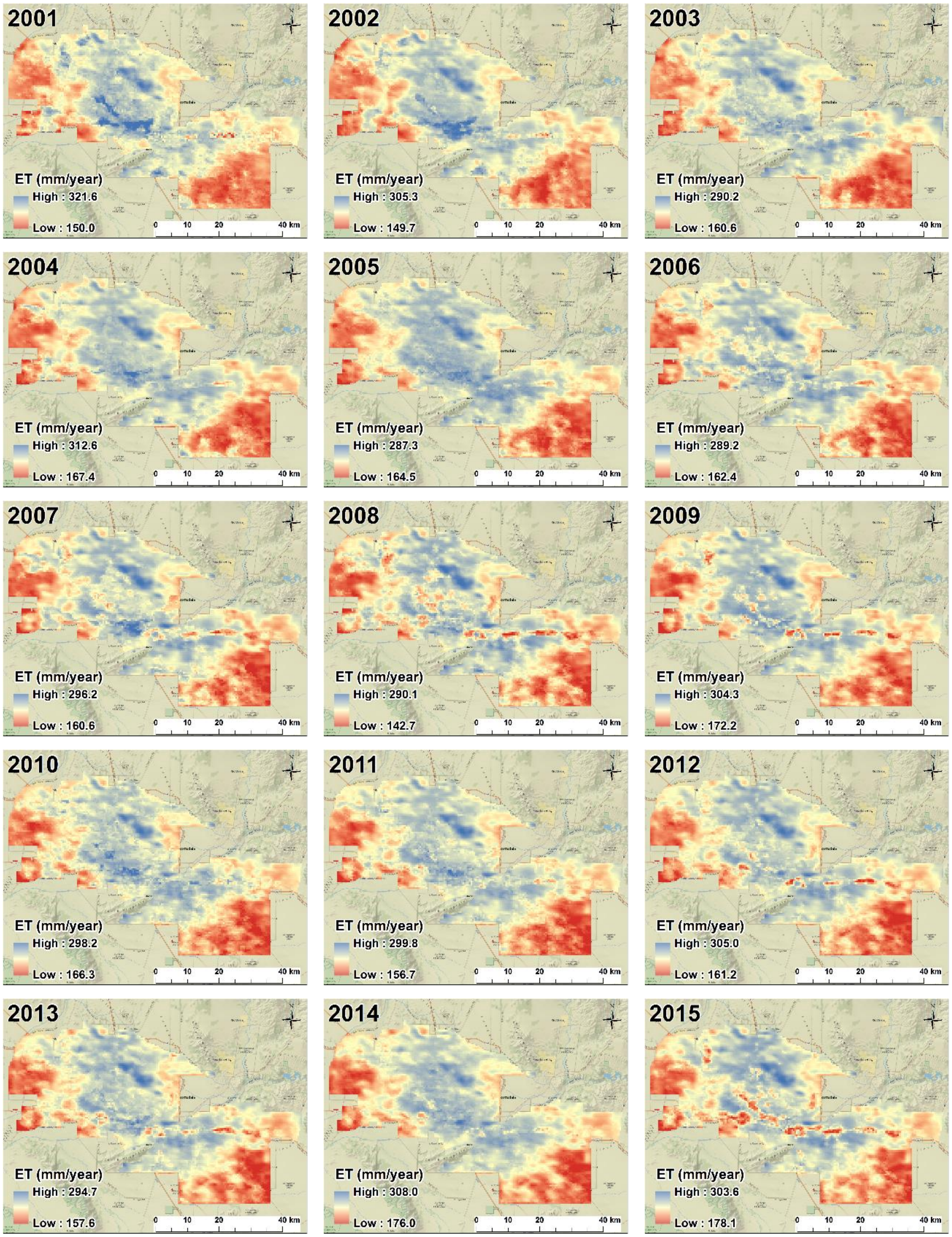

Figure 2.3 Predicted annual ET maps for the Phoenix metropolitan area from 2001 and 2015.

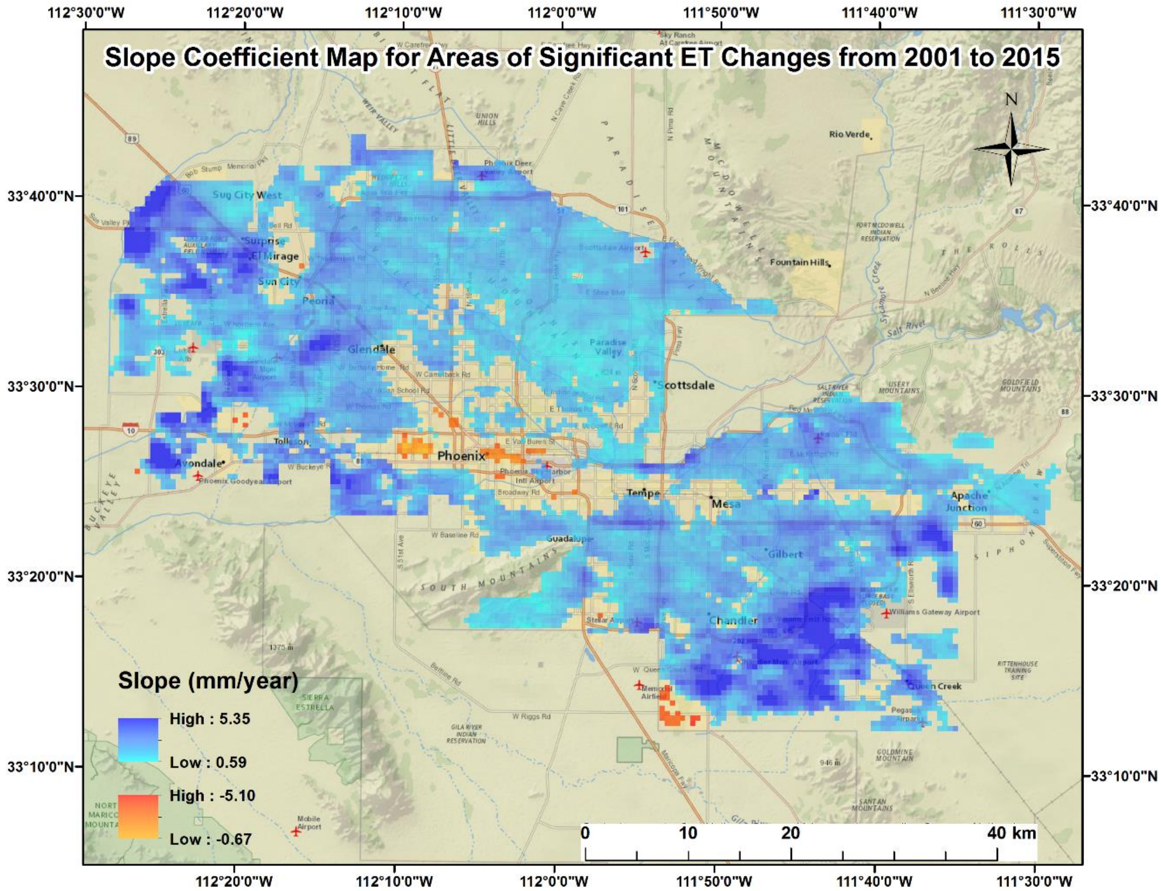

(a)

Figure 2.4 *Continued*.

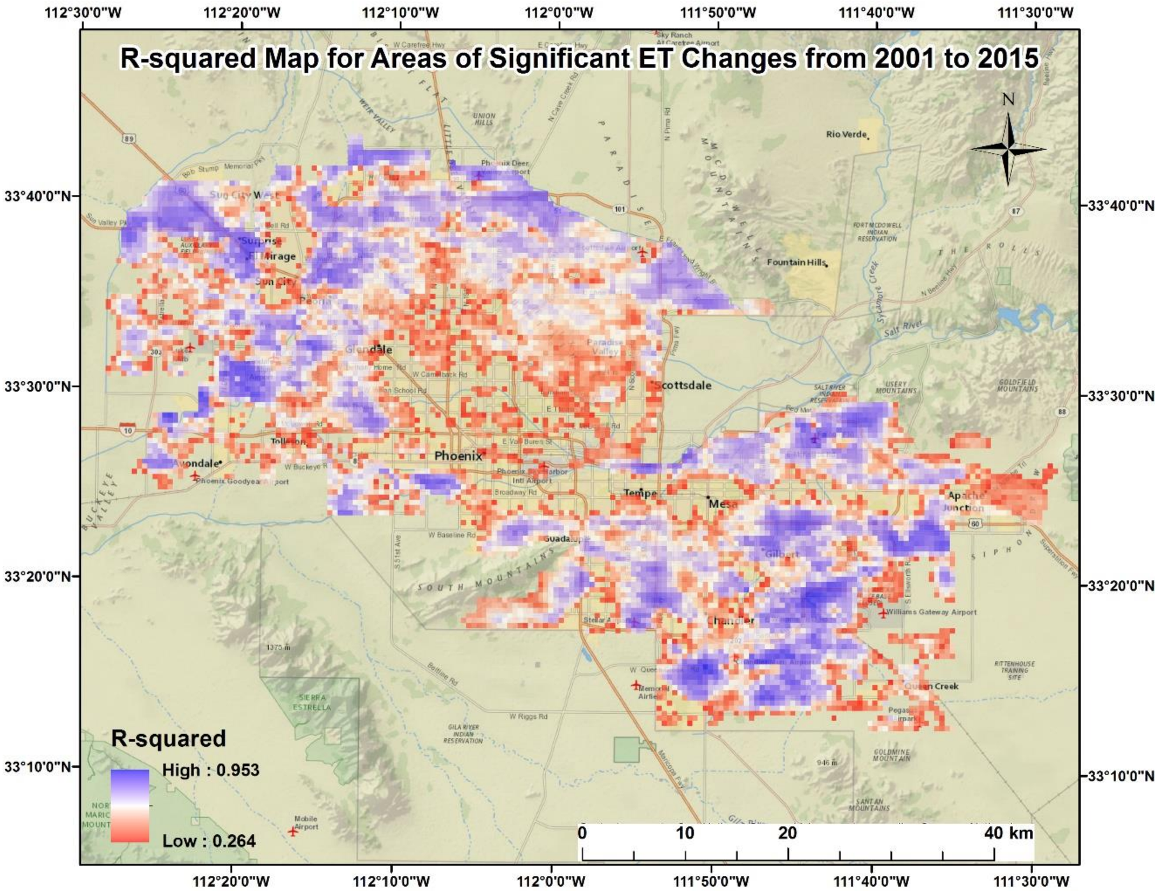

(b)

Figure 2.4 Time-series trend analysis results of predicted urban ET data for the Phoenix metropolitan area. (a) The slope coefficient map that shows the slope coefficient values derived from the OLS regression analysis, with blue pixels representing areas of increasingly higher ET and red pixels representing decreasing ET areas. The slope coefficient carries a practical meaning of mean annual ET change from 2001 to 2015. (b) The coefficient of determination (R^2) map that shows the goodness-of-fit of the OLS regression model for each pixel that has statistically significant changes of ET during the study period.

Table 2.1 Correlation matrix among blue-sky albedo, LST, and NDVI

Variable	Albedo	LST	NDVI
Albedo	1.0000		
LST	-0.0983 (0.5742)	1.0000	
NDVI	-0.3046 (0.0852)	-0.4110 (0.0642)	1.0000

Note: Values in parentheses are *p*-values.

Table 2.2 Multiple regression analysis results.

F-statistic	134.64
Prob. > F	0.000
R^2	0.894
Adjusted R^2	0.887
RMSE[1]	0.114

Variable	Coefficient	Standard error	t-statistic	p-value	95% confidence interval	
Albedo	-2.258	0.937	-2.41	0.022	-4.167	-0.350
LST	0.033	0.002	15.92	0.000	0.029	0.037
Constant	0.171	0.163	1.05	0.303	-0.162	0.504

[1] RMSE: Root mean square error

[2] VIF: Variance inflation factor

Table 2.3 Spatial autocorrelation analysis results for the areas of statistically significant ET changes from 2001 to 2015. Both increasing and decreasing ET areas show a significant clustered spatial pattern.

	Areas of increasing ET (positive slope coefficients)	Areas of decreasing ET (negative slope coefficients)
Moran's I index	0.7560	0.5865
Expected index	-0.0001	-0.0130
Variance	0.0000	0.0016
z-score	198.0650	15.0639
p-value	0.0000	0.0000
Spatial autocorrelation	Clustered	Clustered

DISCUSSION

In Formula (5) the parameter estimate for albedo is negative, while the estimated coefficient for LST is positive. It indicates that urban ET is negatively correlated with albedo but positively correlated to LST. It is because as the albedo of surface material increases, more incoming solar radiation would be reflected rather than absorbed. Less absorbed energy leads to the reduction in the energy available for vaporizing soil water content, therefore decreased ET. This finding is consistent with Jackson (1967), in which albedo was found to be negatively related to ET. Higher surface temperature in the urban area, on the contrary, enhances the surface vaporization process and therefore increases surface ET. Carlson and Buffum (1989) also found a strong positive relationship between remotely-sensed surface temperature and ET, and used this relationship, together with other meteorological variables, to calculate daily ET from the surface energy budget.

The insignificance of NDVI proves that vegetation cover is unnecessarily the major contribution to urban ET for a desert city, but it mainly comes from evaporation of soil water and outdoor water use, rather than transpiration from vegetation. It is not only because the vegetation cover rate is low in Phoenix, but also NDVI values lack a temporal variation throughout the year as the major vegetation type in this area is evergreen trees and shrubs. Although there are some small patches of grass and lawn, they are well maintained by outdoor irrigation system, so the moisture availability and biological functions are at a relatively constant level. NDVI of this area therefore does not have a large temporal variation.

Areas of increasing ET have been mainly found on the outskirts of the metropolitan area that are newly urbanized during the study period. Conversion from undisturbed desert and open soil to built-up area was the major LULC change type in these areas (Wang *et al*. 2016). Urbanization has introduced more outdoor water availability for a desert city through anthropogenic irrigation and pool construction, which would not only lead to the remarkable increase in ET over the outskirt areas but also create an urban oasis effect to cool down surface temperature (Oke 1979; Yang *et al*. 2015). This phenomenon is unique for a desert city and is contradictory to the existing research findings that ET would be significantly reduced due to urbanization and the rapid conversion from naturally vegetated landscape to built-up environment (Liu *et al.* 2010).

The areas that have experienced significant decreases of urban ET have been mainly found in the center of the metropolitan area, such as downtown Phoenix (red pixels in Figure 4a). It is because downtown Phoenix had been highly urbanized before 2001, and the surface had been completely covered by impervious and other anthropogenic materials. Increased urbanization during the study period has resulted in more constructions and more use of anthropogenic materials, which would therefore result in decreased ET. In addition, downtown Phoenix is mainly composed of compact high-rise buildings with little vegetation cover. It is unlike residential and recreational land uses that have higher percent vegetation cover and more outdoor water use. Urbanization would therefore cause decreased ET in central Phoenix metropolitan area. The highly significant cluster pattern of ET changes (Table 3) demonstrates that urbanization activities in Phoenix are also spatially clustered.

The time-series urban ET changes show similar spatial distribution patterns as LST changes for Phoenix described in Wang *et al.* (2016). It has been found that the most significant changes of the urban heat island (UHI) intensity took place on the city outskirts for both daytime and nighttime, and the highest UHI intensity was found at the southeast corner of the Phoenix metropolitan area due to rapid urban expansion. Our results show that the southeast Phoenix areas also experienced the highest increase of ET. The co-existence and co-evolution of ET and UHI intensity in this area are intriguing, but this seems contradictory to the generally accepted perception that reduced evaporative cooling contributes considerably to the formation of the UHI effect. In fact, the positive relationship between the ET increase and UHI intensity is reasonable and unique for desert cities. Self-supporting native vegetation in the desert has a small evapotranspiration capacity to prevent moisture lost to intensive temperatures. On the other hand, urban vegetation can have a much larger evapotranspiration capacity, as moisture supply is secured by anthropogenic irrigations. Under this circumstance, although vegetative fraction is reduced in the process of urbanization, ET arise from the same area actually increases. Furthermore, higher temperature associated with urbanized areas enhances potential ET of sparse urban vegetation through the oasis effect. Therefore, urbanization activities under an arid desert environment can actually lead to increases in regional ET.

CONCLUSIONS

This study explores the statistical relationship between urban ET measurements and MODIS data, and examines the spatial-temporal patterns of urban ET change from 2001 to 2015 for the Phoenix metropolitan area. An empirical model was first established to predict urban ET using blue-sky albedo and LST datasets as explanatory variables that were derived from MODIS products. The model was then applied to the entire Phoenix metropolitan area to create predicted annual ET maps. A time-series trend analysis was also performed to discover urban areas that have experienced statistically significant changes of ET during the study period.

Unexpectedly, NDVI is not statistically significant to model urban ET for Phoenix. Phoenix is a city with an arid subtropical desert climate, where vegetation cover rate is low and NDVI lacks a large temporal variation. The urban surface moisture availability is mainly controlled by anthropogenic irrigation, especially in residential areas. Both surface albedo and LST, rather than the vegetation cover, play significant roles in determining the magnitude of urban ET.

Rapid urbanization in Phoenix has caused extensive LULC changes from agriculture, naturally vegetated landscape, and desert to built-up environment, such as high-density residential areas and impervious surfaces. Urban expansion has been mainly found on the outskirts of the metropolis during the study period. The time-series trend analysis indicates that urban ET has increased substantially in southeast and northwest parts of the metropolis, which correspond to newly urbanized areas during the study period. Although changes in urban ET have been well studied for the Phoenix metropolitan area, this research has its own limitation. The ET prediction model developed in this study was based on ET measurements from a local residential area. Thus, the model may not be fully applicable to all the other LULC types, such as industries, and croplands. More *in-situ* ET measurements over various LULC types in the built-up areas are required to more accurately model urban ET.

CHAPTER 3

PREDICTING AND UNDERSTANDING URBAN OUTDOOR WATER USE IN A DESERT CITY — A CASE STUDY OF THE PHOENIX METROPOLITAN AREA, ARIZONA

INTRODUCTION

Water resource is a key component of sustainability to a desert city such as Phoenix, Arizona. The mean annual precipitation over the past 30 years was 204 mm (U.S. Climate Data, 2017), which is far less than the national average of 767 mm (NOAA, 2016). Phoenix water supply mainly comes from rivers and underground aquifers (Guhathakurta and Gober, 2007). Extensive water supply projects and large ground water reserves have been built, including canals that bring water from the Colorado River, and the Salt and Verde projects that collect runoff into reservoirs. In the past two decades, urban expansion has increased outdoor water usage as more urban landscapes require irrigation (Kaplan et al., 2014). Currently, the increased usage for urban activities is supported by the water previously allocated to agricultural land on which the new urban area was built. Further growth may threaten the sustainability of water supply sources, especially groundwater (Gober et al., 2011).

Although water is naturally scarce in the desert, the City of Phoenix ranks among the highest in the U.S. cities in water demand and water use. Many previous studies were mainly focused on the residential sector of urban water use because it accounts for approximately 67% of the total urban water supply (Domene et al., 2005; Balling and Gober, 2007; Guhathakurta and Gober, 2007; Haley et al., 2007; Endter-Wada et al., 2008; Mini et al., 2014). Balling and Gober (2007) investigated how residential water use in Phoenix was influenced by climate variables. Guhathakurta and Gober (2007) examined the urban heat island (UHI) effects on single-family residences' water use. Guhathakurta and Gober (2010) studied the feedback relationships between residential water use and vegetation intensity, diurnal temperature variation, and characteristics of the built environment. Wentz and Gober (2007) investigated the determinants of single-family water use in Phoenix using municipal water records and census data.

Consumptive water use refers to surface water that is evaporated and transpired from soils, vegetation, water bodies, and other types of land cover features, which is collectively called evapotranspiration (ET). Water consumption estimation is normally made through actual evapotranspiration (ET_a), which is an important component of the water cycle. It has been estimated that about 70% of precipitation returns to the atmosphere through ET_a in the United States (Carr et al., 1990). It is therefore of specific interest for users and water resource managers in accurately determining consumptive water use in the urban area, especially when considering about the effect of population growth and regional climate change on urban water demand and supply (Vörösmarty et al., 2000). For example, Kaplan et al. (2014) used modeled ET_a to compared seasonal outdoor water use (OWU) between a dry and a wet year, and to compared OWU among different urban land use/land cover (LULC) types.

Many studies have made great contributions to our understanding of urban water use, especially for the residential area. However, the total urban OWU besides residential water in the Phoenix metropolitan area (PMA) was neglected. The spatio-temporal pattern of urban OWU and its relationship with LULC types, built environment, vegetation species, and socio-demographic variables is still unknown.

Research on residential water use found different socio-economic variables that were potentially affecting residents' water use behavior. These factors include income, awareness of water conservation and household size (Gregory and Di Leo, 2003), block size, housing price, lifestyle (Syme et al., 2004), types of water using appliances, rainfall, consumer price index and location (Renwick and Archibald, 1998), and so on. Even these studies looked at the impact of the same factors, the influence of these factors was found to vary widely among different cities. In addition, although some econometric models (Renwick and Archibald, 1998; Renwick and Green, 2000) and social models (Syme et al., 1990-1991; Corral-Verdugo et al., 2002; Syme et al., 2004) were developed, these models were specifically designed to study residential water use only. Very few studies have paid attention to the entire metropolitan area that has many different LULC types in order to understand the effect of socio-demographic factors on OWU for a desert city.

In order to fill these gaps in literature, this study is designed to answer three research questions. First, what is the spatio-temporal pattern of urban OWU in the Phoenix metropolitan area within a year? Second, are there statistically significant differences of urban OWU among different LULC types, and what is the statistically relationship between annual OWU and different urban LULC types? Third, what are the socio-demographic factors that have potential influence on urban OWU? This study is going to address all these questions using remotely-sensed satellite imagery and census data using PMA as the study area.

STUDY AREA

The case study is focused on the Phoenix Metropolitan Area (PMA) in the State of Arizona, USA (Figure 1). PMA has a total population of about 4.66 million in 2016 (U.S. Census Bureau, 2017), making it the 12th largest metropolitan area in the United States by population. PMA has a subtropical semi-arid desert climate (Köppen climate classification: BWh) that is characterized by long, hot summers, and short, mild winters. July is the hottest month with an average high temperature of 41.2 °C (U.S. Climate Data, 2017). Winter months feature mean daily high temperatures above 13°C and low temperatures rarely below 4°C (U.S. Climate Data, 2017). The mean annual precipitation over the past 30 years was 204 mm (U.S. Climate Data, 2017). The North American Monsoon that normally takes place between mid-June to early September brings the largest amount of rainfall within a year (Wang et al., 2018). The highest mean daily precipitation occurs in July and August with monthly averages of over 23 mm (Balling and Brazel, 1987; Vivoni et al., 2008). PMA is a desert oasis city with abundant green spaces that include orchards, trees, shrubs and grass. Water is naturally scarce in this region due to its semi-arid desert climate, but population has been steadily increasing since the 1990s. It is therefore of great importance to study OWU in PMA for water use efficiency and water conservation for the purpose of sustainable development.

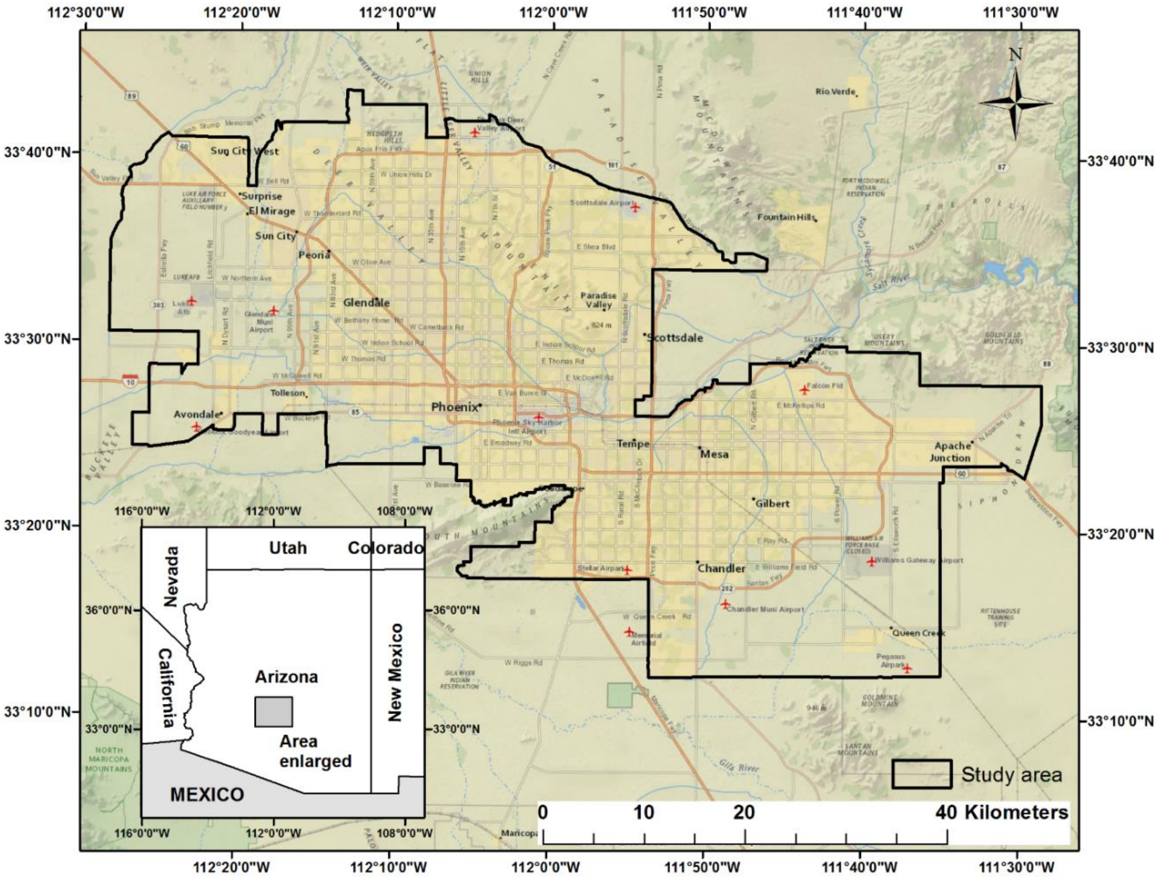

Figure 3.1 Map of study area: Phoenix metropolitan area.

DATA AND METHODS

MODELING AND PREDICTING OWU

OWU in PMA was predicted using ET_a as a proxy, and ET_a was modeled using time-series Landsat 5 Thematic Mapper (TM) images acquired throughout the year of 2010 and a surface energy balance model named METRIC (Mapping Evapotranspiration at high spatial Resolution with Internalized Calibration) (Allen et al., 2007a; Allen et al., 2007b). Surface energy balance model is an essential approach for heat flux and evaporation estimation in applied meteorology and hydrology. More specifically, the METRIC model computes the latent heat flux as the residue of the surface energy balance, which can be written as:

$$LE = R_n - G - H \tag{1}$$

where R_n is the net incoming radiation, G is the ground heat flux, H is the sensible heat flux, and LE is the latent heat flux. The METRIC model also combines surface albedo, land surface temperature (LST) and vegetation index derived from multispectral satellite imagery. These variables are used to estimate spatial variability in aerodynamic roughness of the landscape. Moreover, the METRIC model utilizes meteorological measurements to capture impacts of regional advection and changing wind and humidity conditions (Fleck, 2013; IPCC, 2014). This study uses daily and hourly weather data collected from the Maricopa County weather stations in the Arizona Meteorological Network (AZMET, 2018). The METRIC model has better performance and more attractive features for retrieving ET_a over heterogeneous urban areas than other types of models because: (1) it uses an internal calibration approach based on the selection of a cold pixel (well-watered or flooded area) and a hot pixel (bare soil) from each image so the requirement of atmospheric correction of short-wave and thermal band images is reduced; (2) the METRIC model includes terrain information to calculate solar and thermal radiation; and (3) the model uses the reference ET fraction (ET_rF) to interpolate relative ET between the dates of acquired satellite images. ET_rF is calculated as the ratio of ET_a of an image pixel to its reference ET (ET_r) value at the location of a weather station.

There were 22 cloud-free Landsat 5 TM images available for PMA in 2010. Modeled ET_a maps were created using these images, and the gaps between each two images were filled using a polynomial curve-fitting method for every single image pixel. This procedure creates 365 layers of daily ET_a of 30 m spatial resolution for the PMA in 2010. Monthly and annual ET_a maps were also created by aggregating corresponding daily ET_a maps.

The METRIC approach has demonstrated ET_a accuracies of 15%, 10% and 5% for daily, monthly, and seasonal timescales (USDA-NASS, 2004; Plaza et al. 2009; Shao and Lunetta, 2012; USDA, 2010). The METRIC model has been successfully applied to Landsat and MODIS images to predict ET at various spatial scales (Trezza, 2002; Bastiaanssen et al., 2005; Hendrickx and Hong, 2005; Allen et al., 2007a; Allen et al., 2007b; Zheng et al., 2015). The modeled ET can effectively represent the ET_a for both urban and non-urban areas with or without irrigation (Allen et al., 2007b).

THE EFFECTS OF URBAN LULC ON OWU

A very high resolution (1 m) LULC map for the PMA created using 2010

National Agriculture Imagery Program (NAIP) Imagery is publicly available through the Central Arizona-Phoenix Long-Term Ecological Research (CAP-LTER) website (CAP-LTER, 2015). The original map has 13 classes with an overall accuracy of 91.9% (CAP-LTER, 2015). Detailed classification methods and metadata can also be found on the CAP-LTER website.

A neighborhood residential area subset of 10×10 km in the east part of PMA was used to study the statistical relationship between land cover types and annual OWU. The subset region was then resampled to 30 m resolution by calculating the area percentage of six major land cover types within a 30×30 m moving window that include open soil (*S*), grass (*G*), tree and shrub (*TS*), orchard (*O*), impervious surface (*IS*), and swimming pool (*SP*). A multivariate regression analysis was then performed using annual OWU as the dependent variable and the area percentage of six land cover types as independent variables. The regression model is formulated as:

$$OWU = \beta_0 + \beta_1 \times S\% + \beta_2 \times G\% + \beta_3 \times TS\% + \beta_4 \times O\% + \beta_5 \times IS\% + \beta_6 \times SP\% + \varepsilon \qquad (2)$$

where OWU is annual OWU, and β_0 is the intercept constant. $\beta_{1\text{-}6}$ are the coefficients for the area percentage values of open soil (*S%*), grass (*G%*), tree and shrub (*TS%*), orchard (*O%*), impervious surface (*IS%*), and swimming pool (*SP%*), respectively.

In order to study the effect of different urban land use types on OWU, twenty sampling plots of 5-by-5 pixel (150×150 m) will be randomly selected to extract monthly and annual OWU values for six major urban land use types that are park, business/commercial, industrial, mesic residential, xeric residential, and oasis residential using very high spatial resolution satellite imagery acquired in 2010 in Google Earth software. Monthly mean and annul OWU values were extracted and calculated for each land use type and then plotted against the monthly sequence.

A paired sample *t*-test was then used to examine if there is a statistically significant difference in monthly mean OWU values between each two urban land use types. The paired sample *t*-test has two competing hypotheses. The null hypothesis (H_0) assumes that the true mean difference in monthly mean OWU between two urban land use types is zero. Conversely, the alternative hypothesis (H_a) assumes that the true mean difference in monthly mean OWU between two urban land use types is not equal to zero. This study is also interested in finding out which land use type consumes higher monthly OWU compared with the others if H_0 is rejected and H_a is accepted. A two-tailed *t*-test was therefore used. More specifically, H_a was split into two separate alternative hypotheses. The first alternative hypothesis (H_{a1}) states that the true mean difference between two land use types is smaller than zero. The second alternative hypothesis (H_{a2}) assumes that the true mean difference between two land use types is greater than zero.

THE RELATIONSHIP BETWEEN SOCIO-DEMOGRAPHIC FACTORS AND OWU

Socio-demographic variables that have potential influence on urban OWU were selected and calculated at census track scale using 2010 American Community Survey (ACS) single year estimates data set downloaded from the U.S. Census Bureau website (U.S. Census Bureau, 2011). Variables under investigation include median age (Age_m), percentage of population that has a Bachelor's degree or higher ($BA\%$), number of houses ($\#H$), average household size (HS_a), percentage of family houses ($FH\%$), median household income ($income_m$), house occupancy rate (*OCCUP*%), percentage of houses lived by owners (*owner*%), percentage of houses lived by renters (*renter*%), and median housing value (HV_m). Mean annual OWU values were calculated for each census track region in PMA, and analyzed against all the socio-demographic variables using Pearson's correlation analysis.

RESULTS

MODEL VALIDATION AND PREDICTED OWU

Figure 2 shows the relationship between modeled annual ET_a values and actual annual water usage data acquired from 49 parks in PMA as described in Kaplan et al. (2014). Park water use was collected in cubic meter (m^3), while ET_a was modeled in millimeter (mm), and because both data sets are not normally distributed, a natural log (Ln) transformation was therefore applied. The relationship is positive and highly significant with an R^2 equals 0.93 (p-value < 0.01) (Figure 2), which demonstrates that the natural log transferred ET_a values can be used to explain about 93% of the total variation in log transferred annual water use values for 49 park locations in PMA. The estimated slope coefficient value is slightly higher than 1 (β_1=1.044), which means METRIC-modeled ET_a values are in agreement with actual OWU statistically, and therefore the regression model can be used to predict actual OWU for PMA.

The regression model in Figure 2 was then used to convert annual ET_a to annual OWU using this regression model, which is shown in Figure 3. Blue areas show higher OWU values, which are mainly found in agricultural areas on the outskirt of the city and in most residential areas. Low OWU areas are coded with red color, which are found in the desert and open soils. The highest annual OWU is 198.3 million m^3, while the lowest is 0 in PMA.

THE RELATIONSHIP BETWEEN OWU AND LAND COVER TYPES

Figures 4 shows the relationship between annual ET_a and the area proportion of each land cover type in PMA, and Table 1 shows the corresponding Pearson's correlation coefficient values. All the correlation coefficients are statistically significant at the 0.05 level. Note that all the vegetation land cover types that include orchard, grass, trees and shrubs have a strong positive relationship with ET_a, while impervious surface, open soil and swimming pool all show a negative relationship. The orchard land cover type has the strongest positive relationship, which means that increasing orchard area proportion would significantly increase OWU in PMA. The strongest negative relationship is found for impervious surface. Therefore, increasing the proportion of impervious surface area would decrease ET_a and OWU in PMA.

Table 2 shows the multivariate regression analysis result between annual ET_a and area proportion of six land cover types. The *F*-statistic and its *p*-value indicate that the model overall is highly statistically significant with an R^2 value of 0.3646, which means that this model can be used to explain about 36.5% of the total variation in annual OWU. All the variable coefficient values are significant at 99% confidence level, except the swimming pool that is significant at the 0.05 level. Note that all the coefficient values are positive, which means all the six major land cover types all together makes positive contributions to the total OWU in PMA. The highest coefficient value is found for orchard, followed by tree/shrub. This result is in agreement with the Pearson's correlation analysis result in Table 1. Generally, the contribution of annual OWU from each land cover type can be ranked as:

$$\text{Orchard} > \text{Tree/Shrub} > \text{Grass} > \text{Open Soil} > \text{Impervious surface} \qquad (3)$$

THE RELATIONSHIP BETWEEN OWU AND URBAN LAND USE TYPES

Figure 5 is a line graph showing the temporal trend of monthly mean OWU in 2010. In general, all the urban land use types exhibit similar trend within a year. OWU started rising rapidly in March, reached its peak in June, and then declined to the lowest level in December.

Table 3 shows paired sample *t*-test result between each two urban land use types. The difference of true mean between Group 1 and Group 2 ($mean_{group1}$-$mean_{group2}$) was tested, and H_0 was either accepted or rejected based on the *p*-value. If *t*-statistic < 0 and *p*-value ≤ 0.05, there is a statistically significant difference in monthly mean OWU between two land use types, and the difference is small than zero ($mean_{group1} < mean_{group2}$). Conversely, if *t*-statistic > 0 and *p*-value ≤ 0.05, the difference in monthly mean OWU between two groups is greater than zero ($mean_{group1} > mean_{group2}$). If *p*-value > 0.05, H_0 is not rejected and there is no significant difference in monthly mean OWU between two land use types.

From Table 3 and Figure 5 it can be discovered that parks consumed the highest OWU than any other land use types in 2010, and the difference is highly significant. Business/commercial and xeric residential areas both consumed much lower OWU, but the difference between business/commercial and xeric residential is not significant (*p*-value = 0.4276). Industry has higher OWU than oasis and xeric residential, but lower than mesic residential and parks. Mesic residential has greater monthly OWU than oasis and xeric residential types, but the difference between oasis and xeric is not significant at the 0.05 level (*p*-value = 0.0788). Generally, based on the paired sample *t*-test result, the ranking of monthly mean and annual total OWU can be mathematically expressed as:

$$\text{Park} > \text{Mesic residential} > \text{Industry} > \text{Oasis residential} > \text{Xeric residential} = \text{Business/Commercial} \tag{4}$$

Annual, monthly mean, monthly highest, and monthly lowest OWU for each urban land use type were calculated and listed in Table 4. It is found that annual, monthly mean, and monthly highest OWU all follow the same order as shown in Equation (4). Parks consumed the highest amount of annual OWU of 73.60 million m^3 and a monthly mean of 5.50 million m^3. Business/commercial sector only consumed 33.48 million m^3 in 2010 with a monthly mean of 2.50 million m^3, which is the lowest. The monthly highest OWU was consistently found in June for all land use types, while the monthly lowest was found in December or November (oasis residential).

THE RELATIONSHIP BETWEEN OWU AND SOCIO-DEMOGRAPHIC VARIABLES

Table 5 shows Pearson’s correlation coefficient values between annual OWU and selected socio-demographic variables at the census-track level. Variables that have a statistically significant relationship with annual OWU include percentage of population that has a Bachelor's degree or higher (*BA*%), percentage of family houses (*FH*%), median household income ($income_m$), house occupancy rate (*OCCUP*%), percentage of houses lived by owners (*owner*%), percentage of houses lived by renters (*renter*%), and median housing value (HV_m). Most variables show a statistically significant positive relationship with annual OWU, except *BA*% and *renter*%. More specifically, if a census track region in PMA has a higher percentage of family houses, a higher house occupancy rate, a higher percentage of houses lived by owners, a higher median household income, and a higher median housing value, the annual OWU would be higher. Conversely, OWU would be lower if a census track region has higher educational attainment or higher percentage of houses lived by renters. Median age, number of houses, and average household size do not show a significant relationship with annual OWU in PMA.

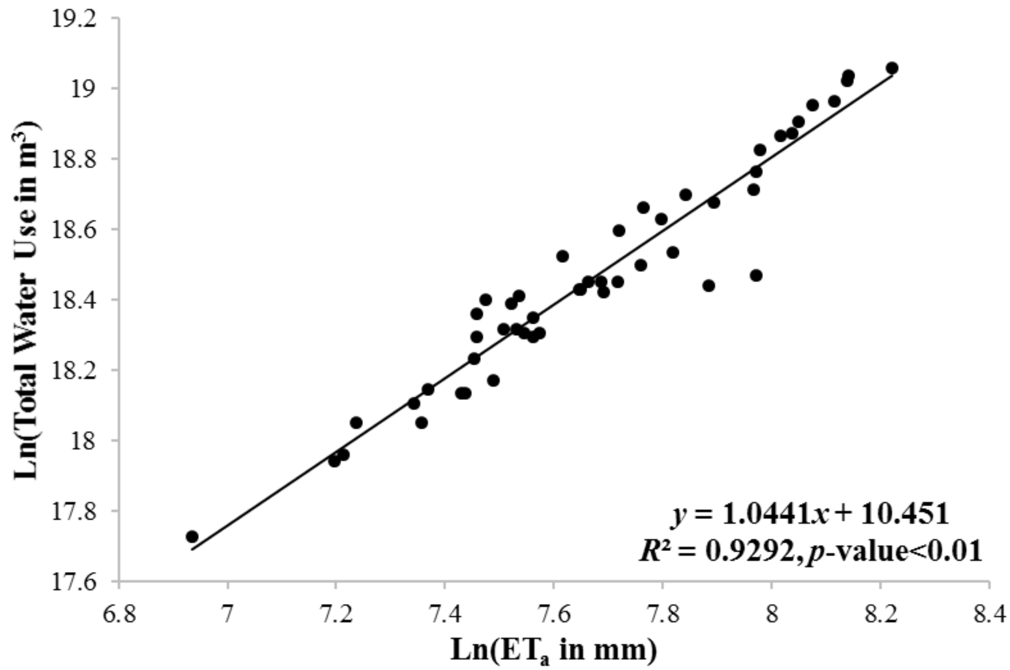

Figure 3.2 The relationship between modeled annual ET_a values and actual annual total water use for 49 parks in the PMA.

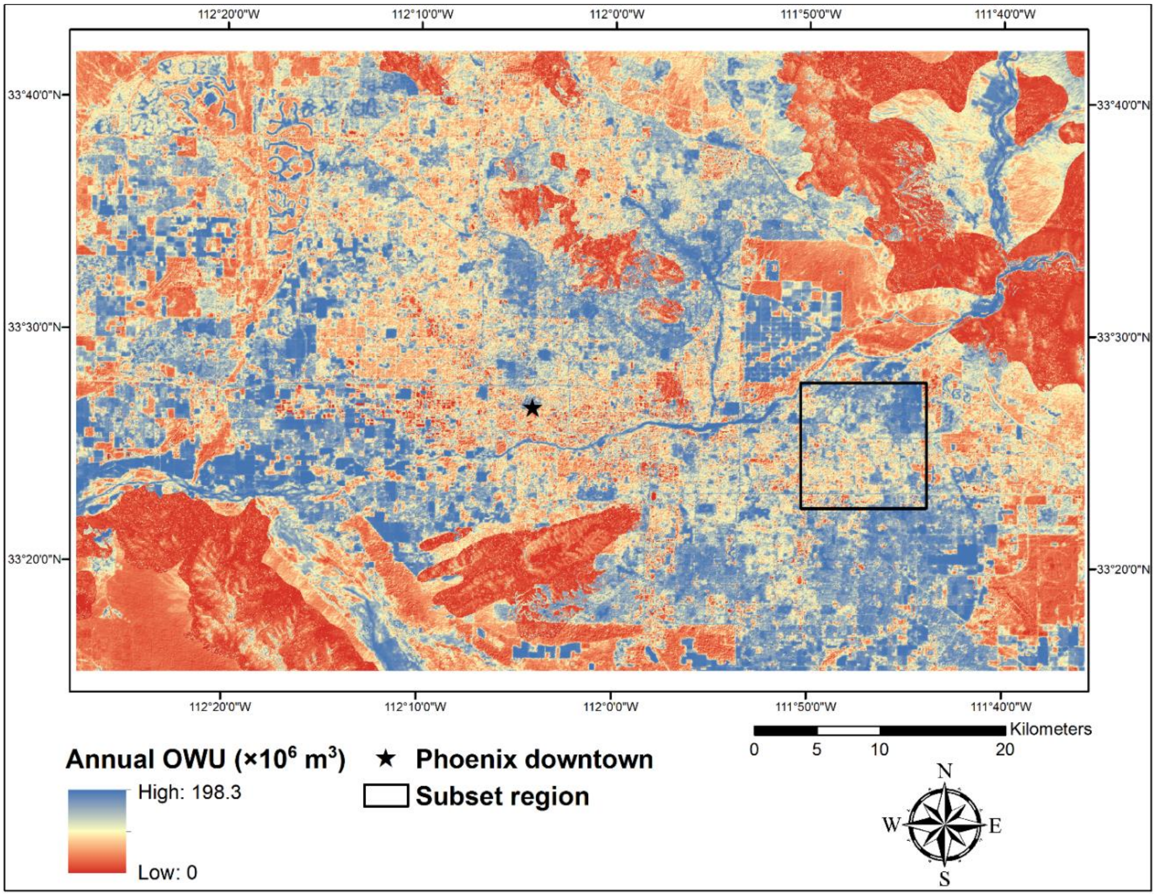

Figure 3.3 Predicted annual OWU map for the PMA.

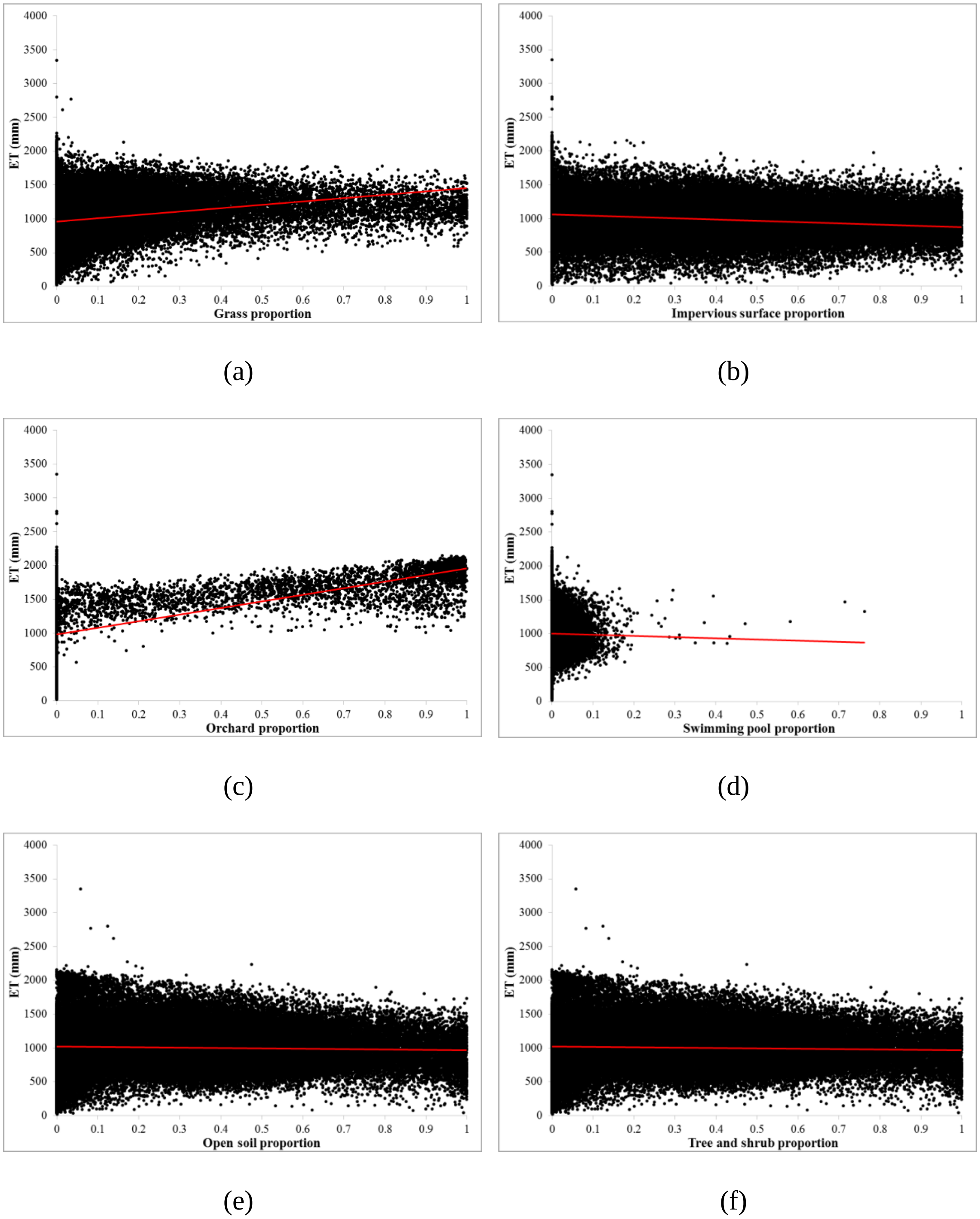

Figure 3.4 The relationship between annual ET_a values and the area proportion of each land cover type.

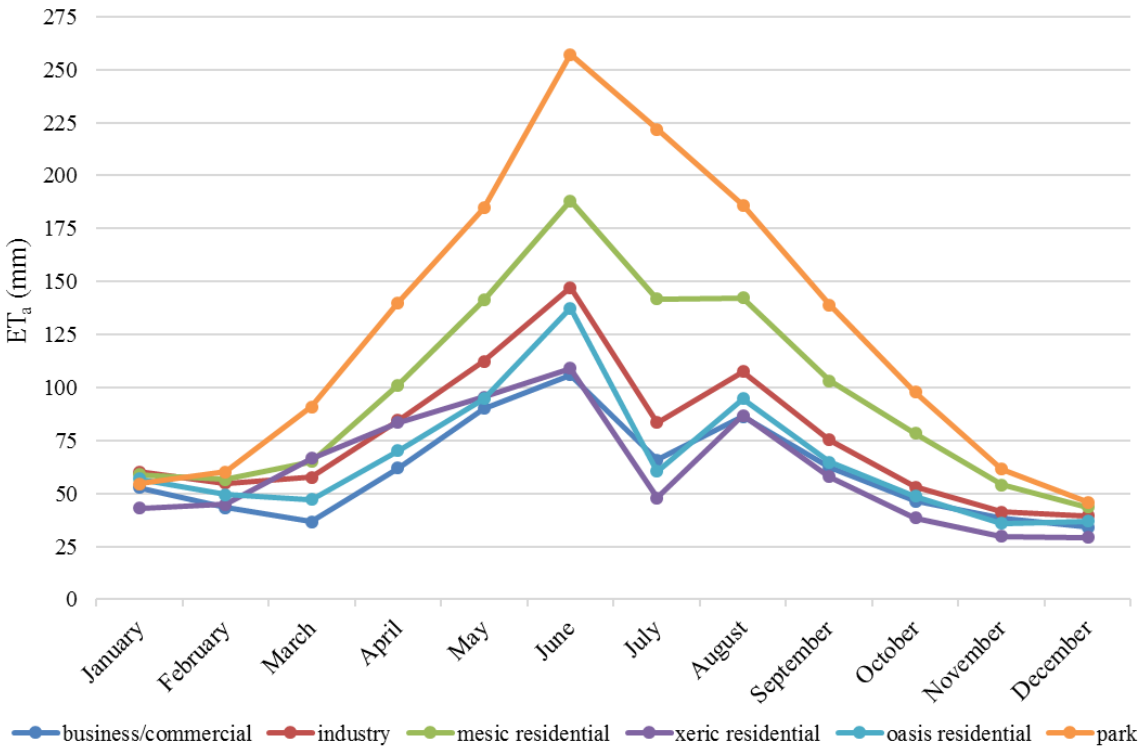

Figure 3.5 Monthly mean OWU of six major urban land use types.

Table 3.1 Pearson's correlation coefficients between annual ET_a and area proportion of each land cover type. Values in parentheses are p values.

Variables	ET_a
Grass%	0.2443 (0.0000)
Impervious%	-0.1892 (0.0000)
Orchard%	0.4275 (0.0000)
Pool%	-0.009 (0.0035)
Soil%	-0.0417 (0.0000)
Tree/Shrub%	0.2744 (0.0000)

Table 3.2 Multivariate regression result.

Number of observations	*F-statistic*	*p*-value	R^2	Adjusted R^2	RMSE
106077	10143.69	0.0000	0.3646	0.3646	228.52

Variable	Coefficient	Standard Error	*t*	*p*-value	VIF
Grass%	615.8181	5.8404	105.44	0.0000	1.37
Impervious%	233.2577	4.0833	57.12	0.0000	2.83
Orchard%	1286.099	6.3338	203.05	0.0000	1.29
Pool%	86.46567	50.1559	1.72	0.0850	1.05
Soil%	256.6437	4.5599	56.28	0.0000	2.22
Tree/Shrub%	891.5812	6.9697	127.92	0.0000	1.42
constant	678.3374	3.2619	207.96	0.0000	-

Table 3.3 Paired sample *t*-test (two tailed) result. Values in parentheses are *p* values.

Variables		Group 1				
		Business/ commercial	Industry	Mesic residential	Oasis residential	Xeric residential
Group 2	Industry	-5.2319 (0.0001)*	-	-	-	-
	Mesic residential	-5.1710 (0.0002)*	-4.1469 (0.0008)*	-	-	-
	Oasis residential	-2.3240 (0.0201)*	5.5075 (0.0001)#	4.7133 (0.0003)#	-	-
	Xeric residential	-0.1869 (0.4276)	4.1184 (0.0009)#	4.4320 (0.0005)#	1.5164 (0.0788)	-
	Park	-4.5737 (0.0004)*	-4.1082 (0.0009)*	-3.9674 (0.0011)*	-4.3658 (0.0006)*	-4.3722 (0.0006)*

* H_{a1}: The difference between the true mean of Group 1 and Group 2 is smaller than zero.

\# H_{a2}: The difference between the true mean of Group 1 and Group 2 is greater than zero.

Table 3.4 Annual total, monthly mean, monthly highest and lowest OWU for urban land use types. (unit: $\times 10^6$ m^3)

	Annual total	Monthly mean	Monthly highest	Monthly lowest	Variance (unitless)
Business/Commercial	33.48	2.50	4.50	1.38	542.35
Industry	42.85	3.20	6.35	1.61	1,056.77
Mesic residential	55.48	4.14	8.19	1.78	2,137.87
Xeric residential	33.90	2.53	4.64	1.18	721.56
Oasis residential	37.04	2.77	5.90	1.46	867.23
Park	73.60	5.50	11.36	1.88	5,068.44

Table 3.5 Pearson's correlation coefficients between annual OWU and socio-economic variables. Variables are median age (Age_m), percentage of population that has a Bachelor's degree or higher (*BA*%), number of houses (#*H*), average household size (HS_a), percentage of family houses (*FH*%), median household income ($income_m$), house occupancy rate (*OCCUP*%), percentage of houses lived by owners (*owner*%), percentage of houses lived by renters (*renter*%), and median housing value (HV_m). Values in parentheses are p values. Results that are statistically significant at 0.05 level are marked with an asterisk (*).

Variables	Age_m	*BA*%	#*H*	HS_a	*FH*%
OWU	0.210 (0.070)	-0.663 (0.000)*	0.035 (0.328)	-0.056 (0.116)	0.563 (0.000)*
	$income_m$	*OCCUP*%	*owner*%	*renter*%	HV_m
	0.745 (0.000)*	0.394 (0.012)*	0.588 (0.000)*	-0.322 (0.008)*	0.620 (0.000)*

DISCUSSION

The strong correlation observed between modeled ET_a and actual OWU data collected from parks (Figure 2) demonstrate that the METRIC model can be effectively used to predict ET_a for urban OWU estimation for a heterogeneous urban environment in a semi-arid desert climate. However, the slope coefficient in the regression model in Figure 2 is slightly higher than 1 (β=1.0441), which means the model overestimates OWU. The reason of overestimation is that this study used actual annual OWU from 49 parks in PMA. As shown in Figure 5, Table 3, and Table 4, park is the land use type that consumed the largest amount of OWU in PMA. Many parks are mostly covered by turf grass with a small coverage of impervious surfaces (e.g. sidewalk, pedestrian trail, and parking lot), and grass itself has a very strong positive relationship with ET_a (Tables 1 & 2). In addition, parks in PMA are routinely irrigated using flood irrigation that consumes much more water beyond the actual needs of turf grass. Using actual OWU data from parks for model building would therefore overestimate OWU for other land use types. However, parks are the only one public data source for predicting annual OWU in PMA, and no other data sources are currently available.

Other studies also reported a strong positive relationship between modeled ET_a and OWU. Kaplan and Myint (2012) compared modeled ET_a from Landsat 5 imagery and agricultural water use data in four agricultural districts in the Phoenix Active Management Area (AMA), and found an R^2 value as high as 0.93. Kaplan et al. (2014) also used Landsat 5 images and a hybrid model combining SEBAL and RESET models named S-ReSET (Kaplan and Myint, 2012) to predict ET_a for different land use types in PMA, and found a strong relationship with actual OWU with an R^2 of 0.77. Mayer et al. (1999) studied 14 cities in the U.S. and found an R^2 value of 0.59 between net ET and mean annual household water use using data collected from households. It can be concluded that the METRIC model outperforms the S-ReSET model and household sample data, and has produced the most satisfactory result for predicting OWU for PMA. Torres-Rua et al. (2016) also claimed that the METRIC model has better performance for predicting ET_a for arid desert areas where water availability is restricted.

All the vegetation land cover types that include orchard, tree/shrub, and grass have statistically significant positive correlation with annual OWU, which is mainly due to frequent anthropogenic irrigation. Liu et al. (2010) studied the effect of urban LULC types on ET_a, and found that forests, shrublands, and grass have much higher ET_a values than developed areas in urban settings. The ranking was reported as: forest > grass > shrubland > developed area. Additionally, Zhang et al. (2001) studied 250 catchments worldwide and reported that, even in the dry seasons, forests generally sustain much higher ET than shrubs, croplands and grasslands due to the ability to uptake soil moisture from greater depth (Hadjimitsis et al., 2008; Rwasoka et al., 2011). Our results are generally in accordance with their findings even though PMA does not have large, contiguous area of natural forests, but orchard can be regarded as a patch of cultivated woody area in the city. Liu et al. (2010) reported that shrublands have lower ET than grass in a semi-arid climate region in central Oklahoma, but our study suggests that individual trees and shrubs have higher ET_a values than grass, which is mainly due to a relative smaller proportion of grass coverage but a much higher area percentage of shrubs in a desert environment.

Impervious surfaces, swimming pools and open soils are found to be negatively correlated with ET_a (Figure 4 and Table 1). This finding is contradictory to that suggested by Guhathakurta and Gober (2010), in which impervious surfaces and large lots containing pools both contribute to increased residential water use. The reason is that our study used remotely sensed data to predict OWU for the entire PMA region and examined the effect of different urban LULC types on OWU as a whole, not only for residential areas or for residential water use. However, it is noted that the relationship between pool area and ET_a is less significant than other land cover types (p-value > 0.05), and the slope coefficient value of pool in the regression model is also insignificant. This is because the area proportion of swimming pool (mostly < 20%) is much smaller than all other land cover types (Figure 4d), and the data do not follow a normal distribution. It violates the multivariate normality assumption in a linear regression analysis.

Kaplan et al. (2014) found that cultivated grass has much higher water consumption than other land use types regardless of climatic conditions. Our study results also prove that parks, which are mainly covered by cultivated turf grass and vegetation, have the highest OWU among all the urban land use types throughout the year (Figure 5 and Table 4). It is because cultivated vegetation under municipal management in PMA has to keep constant soil moisture level through routine anthropogenic irrigation in order to maintain physiologically active in a desert environment. Even though parks have the largest OWU, the variance is also the highest (Table 4), which demonstrates ET of cultivated vegetation in parks is most sensitive to seasonal conditions in a semi-arid desert climate.

Previous studies reported that residential water use account for about 67% of the total water supply in PMA (Guhathakurta and Gober, 2007; Balling and Gober, 2007; Balling et al., 2007), but these studies did not report indoor and outdoor residential water use separately. Our study shows that three residential land use types all together consumed

126.42 million m^3 OWU in 2010, which was about 46% of the total OWU in PMA. It proves that residential water was mainly used for outdoor landscape irrigation, which is more than twice as much as indoor use. Residential area is the largest sector of outdoor water consumption in the urban area of PMA, even though agricultural use remains the largest sector in the entire Phoenix Active Management Area (AMA) (ADWR, 2017). It is therefore evident that residential area has the largest potential for water conservation in PMA. Mesic residential OWU is the highest among three residential types, and its variance is also the highest (Table 4). This result follows Balling and Gober (2007) and Balling et al. (2007) who reported greater change in OWU for neighborhoods with a high portion of mesic landscaping. Xeric residential consumed the least amount of outdoor water and had the smallest variance. Similar results were also found in Kaplan et al. (2014), Balling and Gober (2007), Balling et al. (2007), and Balling and Cubaque (2009).

Although water demand more or less keeps pace with population growth and urban expansion, total water use has actually declined in PMA. Population in PMA has been growing steadily since the early 1990s, but the total water use in 2014 was even less than that in early 1990s (City of Phoenix, 2014). As water has become more sufficiently planed, managed, and used, per capita use has therefore significantly declined. In order to support the growing population in the southwestern U.S., water policymakers have been trying to identify ways to reduce OWU. Many studies have discovered that a unique residential landscaping design that integrates mesic, xeric, oasis, and native types of yardscape can effectively reduce OWU and sustainably conserve water resource for residential areas in a desert city (Larsen and Harlan, 2006; Martin et al., 2007; Martin, 2008; Yabiku et al., 2008; Larson et al., 2009; Volo et al., 2014; Volo et al., 2015).

It is also interesting to note that there is an obvious dip in OWU in July for almost all the urban land use types except parks (Figure 5). July is normally the time for the North American monsoon that has a pronounced increase in thunderstorms and rainfall over large areas of the southwestern United States, and the PMA is under its influence. ET and total OWU should be the highest in July but it turned out to be one of the lowest months in 2010. One possible explanation is that 2010 is one of the driest years for the PMA, and the month of July only received 0.22-inch rainfall total, which was far below the 20-year average of 1.06 inches. The other explanation is that people might intentionally turn off the irrigation and watering systems because people tend to understand the monsoon would bring a lot of precipitation so less irrigation is needed. In order to fully understand the dip in July, more years need to be examined in the future.

Renwick and Archibald (1998)'s econometrics model suggested that some household characteristics, such as housing density, household size, house location and number of faucets play an important role in determining residential water use. The effect of housing density on water use was also observed in Barcelona, Spain where low density housing had a much higher water use (Domene and Sauri, 2006). Our study has made a great contribution to uncover the relationship between socio-demographic variables and OWU for the entire PMA, not only for residential areas. It is noted that besides household characteristics, residents' educational attainment (variable *BA*% in Table 5) also has a significant influence on OWU, which has been neglected by most studies. Census track regions of population with a higher educational attainment tend to use less water because people are more educated and better aware of the value of water (Jorgensen et al. 2009), which is essential to water conservation for a desert city like Phoenix. Unlike what was reported by other studies (e.g. Renwick and Archibald, 1998; Jorgensen et al. 2009), average household size and the number of houses did not play a significant role in affecting OWU in PMA. On the other hand, percentage of family houses, house occupancy rate, and percentage of houses lived by owners all have significant positive relationship with OWU. A specific econometrics model or social model should be established for desert cities to study OWU using socio-demographic variables, but this is beyond the aims and scope of this current study.

CONCLUSIONS

This research has examined the empirical relationship between modeled ET_a and actual OWU, the relationship between urban LULC types and total OWU, and the effect of socio-demographic variables on OWU using PMA as the study area in 2010. Remotely sensed imagery and the METRIC model has provided great advantage to effectively model ET_a and to study OWU for a contiguous area in the heterogeneous urban environment in a semi-arid desert climate region.

Results have suggested that parks and mesic residential land use types consumed the largest amount of annual OWU, while business/commercial and xeric residential areas used the least amount. In general, all the urban land use types followed the same temporal trend in 2010, reached its peak in June, and then declined to the lowest level in December. OWU shows significant positive relationship with all the vegetation land cover types. Orchard made the greatest contribution, while impervious surface had the strongest negative relationship with annual OWU.

Socio-demographic variables that have potential positive influence on OWU include percentage of family houses, house occupancy rate, percentage of houses lived by owners, median household income, and median housing value. Conversely, if a census track region has higher educational attainment or higher percentage of houses lived by renters, annual OWU would be lower.

This is the first comprehensive study that models, predicts, maps, and analyzes OWU for the entire PMA and examines its relationship with urban LULC types and socio-demographic variables. This study has a great potential to be used as a guidance for urban planners and city managers to formulate better water use policies or to develop new policies to conserve water resource for the sustainable development of a desert city.

CONCLUSIONS

This dissertation has studied the long-term effects of urbanization on urban climate and the spatio-temporal dynamics of urban climate in terms the UHI effect, urban ET, and outdoor water use, using the Phoenix metropolitan area (PMA), Arizona as the study area.

The first chapter identified regions in PMA that have experienced significant changes of SUHI intensity from 2000 to 2017 using MODIS LST imagery. The relationship between LULC changes and LST variations was also studied using classified LULC maps created from Landsat imagery. In conclusion, the UHI effect in PMA has been gradually exacerbated by the rapid development and expansion of the urban area since 2000. Urbanization is the primary cause for increased SUHI intensity during the study period. Despite the dramatic increase of urban/residential and impervious surface areas, some areas have decreasing $\Delta T_{\text{u-r}}$ during the daytime due to increased vegetation cover for those areas. This study found that the cooling effect of increased vegetation cover is stronger than the heating effect of urbanization for the Phoenix metropolitan area.

The second chapter explored the empirical relationship between urban ET measurements from a flux tower and remotely sensed MODIS data, and examined the spatial-temporal patterns of urban ET change from 2001 to 2015 for the Phoenix metropolitan area. An empirical model was established to predict urban ET using blue-sky albedo and LST datasets as explanatory variables that were derived from MODIS products. The model was then applied to the entire Phoenix metropolitan area to create predicted annual ET maps. A time-series trend analysis was also performed to discover urban areas that have experienced statistically significant changes of ET during the study period. The time-series trend analysis indicated that urban ET increased substantially in southeast and northwest parts of PMA, which correspond to newly urbanized areas during the study period.

The third chapter examined the relationship between modeled ET_a and actual OWU, the relationship between urban LULC types and total OWU, and the effect of socio-demographic variables on OWU for PMA in 2010. Remotely sensed imagery and the METRIC model has provided great advantage to effectively model ET_a and to study OWU for a contiguous area in the heterogeneous urban environment in a semi-arid desert climate region. Results showed that parks and mesic residential land use types consumed the largest amount of annual OWU, while business/commercial and xeric residential areas used the least amount. OWU had positive relationship with all the vegetation land cover types. Socio-demographic variables that have potential influence on OWU include percentage of family houses, house occupancy rate, percentage of houses lived by owners, median household income, and median housing value, educational attainment, and percentage of houses lived by renters.

This dissertation is one of the systematic studies to examine long-term spatio-temporal dynamics of urban climate change for the PMA using remote sensing data and geospatial analysis. PMA is a subtropical desert city that is also one of the warmest cities in the United States. Excessive heat in the urban area has been a major concern for decades, especially during the summer months. This heat compromises human health and comfort, as well as causes water and energy consumption issues, and poor air quality. This dissertation research has identified regions in PMA that have experienced the most significant changes of SUHI intensity from 2000 to 2017. Research findings and results can be used: 1) to provide constructive suggestions to urban planners, decision-makers, and city manager to formulate new policies and regulations when planning new constructions for a desert city; 2) to provide constructive suggestions regarding the mitigation strategy of the UHI and a research guideline of SUHI intensity for other desert cities around the world.

This dissertation would also make significant contributions to our knowledge of urban ET and OWU in the PMA from four perspectives. First, this will be the first study to map urban ET and OWU distributions for the entire PMA. The spatio-temporal pattern of ET and OWU will help better understand where and how OWU is distributed. Second, the relationship between ET/OWU and LULC types will explain how built environment, urban cultivation, and natural vegetation interact with each other and influence outdoor water differently. Third, this study will explain how social environment and background influence people behaviors on OWU. Fourth, results and findings will help urban planners and managers adjust existing water policies or formulate new policies for a smarter design of urban environment in order to better conserve water, to achieve sustainable water use, and to ensure water security.

This dissertation also has its own limitations. For the first chapter, it discovered that Phoenix downtown area has no significant LST change during the study period. However, many studies reported that central Phoenix area is one of the hottest spots in the PMA. Even though there was no obvious LULCC taking place, the urban morphology and structure have been constantly changing and the City of Phoenix is planning to grow its urban forest and green infrastructure to provide more shade canopy. One of the future research is to continue monitoring LST in central Phoenix area to examine how urban form changes influences LST in the long run.

The second chapter used ET data from a flux tower located in a residential area in western Phoenix to build the empirical model for the PMA. The model may not be scientifically sound and technically applicable to all other different areas in the PMA or other cities. More *in situ* ET measurements over various LULC types are required for a more accurate prediction of urban ET. Some future work may include using ET data collected from a mobile flux tower to further verify the empirical model and to predict ET for different LULC types.

The third chapter evaluated socio-demographic variables that have potential influences on urban OWU, and interestingly educational attainment was found to be negatively correlated with OWU but household median income was positively correlated. It is necessary to follow up on this finding and to discover how exactly these variables play a role in influencing people's behavior of water use. In addition, the obvious dip of OWU and ET in July in 2010 needs further exploration. More years need to be examined to find out if the pattern would be consistent in dry years.

REFERENCES

INTRODUCTION AND LITERATURE REVIEW

Adams, D. K., & A. C. Comrie. (1997). The North American Monsoon. *Bulletin of the American Meteorological Society,* 78: 2197–2213.

Allen, R.G., Tasumi, M., & Trezza, R. (2007a). Satellite-based energy balance for mapping evapotranspiration with internalized calibration (METRIC) – Model. *Journal of irrigation and drainage engineering,* 133(4), 380-394.

Allen, R.G., Tasumi, M., Morse, A., Trezza, R., Wright, J.L., Bastiaanssen, W., Kramber, W., Lorite, I., & Robison, C.W. (2007b). Satellite-based energy balance for mapping evapotranspiration with internalized calibration (METRIC) – Applications. *Journal of irrigation and drainage engineering,* 133(4), 395-406.

Anderson, C. A., & E. R. Vivoni. (2016). Impact of land surface states within the flux footprint on daytime land-atmosphere coupling in two semiarid ecosystems of the Southwestern U.S. *Water Resources Research,* 52, 4785–4800.

Arnfield, A. J. (2003). Two decades of urban climate research: a review of turbulence, exchanges of energy and water, and the urban heat island. *International Journal of Climatology,* 23, 1-26.

Balling, R. C., Jr., & Brazil, S. W. (1987a). Time and space characteristics of the Phoenix urban heat island. *Journal of Arizona-Nevada Academy of Science,* 21, 75–81.

Balling, R., & S. W. Brazel. (1987b). The Impact of Rapid Urbanization on Pan Evaporation in Phoenix, Arizona. *International Journal of Climatology,* 7, 593–597.

Balling, R. C., & S. W. Brazel. (1987c). Recent Changes in Phoenix, Arizona Summertime Diurnal Precipitation Patterns. *Theoretical and Applied Climatology,* 38, 50–54.

Balling, R.C. & Gober, P. (2007). Climate variability and residential water use in the City of Phoenix, Arizona. *Journal of Applied Meteorology and Climatology, 46*(7), 1130-1137.

Bastiaanssen, W. G. M., M. Menenti, R. A. Feddes, & A. A. M. Holtslag. (1998). A Remote Sensing Surface Energy Balance Algorithm for Land (SEBAL): Part 1. Formulation. *Journal of Hydrology,* 212-213, 198–212.

Bastiaanssen, W. G. M., Noordman, E. J. M., Pelgrum, H., Davids, G., Thoreson, B. P., & Allen, R. G. (2005). SEBAL model with remotely sensed data to improve water-resources management under actual field conditions. *Journal of Irrigation and Drainage*

Engineering, 131(1), 85-93.

Best, M. J., M. Pryor, D. B. Clark, G. G. Rooney, R. Essery, C. B. Ménard, J. M. Edwards, et al. (2011). The Joint UK Land Environment Simulator (JULES), Model Description-Part 1: Energy and Water Fluxes. *Geoscientific Model Development*, 4(3), 677–699.

Boegh, E., R. N. Poulsen, M. Butts, P. Abrahamsen, E. Dellwik, S. Hansen, C. B. Hasager, A. Ibrom, J.-K. Loerup, K. Pilegaard, H. Soegaard. (2009). Remote sensing based evapotranspiration and runoff modeling of agricultural, forest and urban flux sites in Denmark: From field to macro-scale. *Journal of Hydrology*, 377(3–4), 300–316.

Brazel, A., Gober, P., Lee, S.-J., Grossman-Clarke, S., Zehnder, J., Hedquist, B., & Comparri, E. (2007). Determinants of changes in the regional urban heat island in metropolitan Phoenix (Arizona, USA) between 1990 and 2004. *Climate Research*, 33, 171–182.

Buyantuyev, A, & Wu, J. (2010). Urban heat islands and landscape heterogeneity: linking spatiotemporal variations in surface temperatures to land-cover and socioeconomic patterns. *Landscape Ecology,* 25, 17-33.

Chen, X.-L., Zhao, H.-M., Li, P.-X., & Yin, Z.-Y. (2006). Remote sensing image-based analysis of the relationship between urban heat island and land use/cover changes. *Remote Sensing of Environment*, 104, 133–146.

Chow, W. T. L., & A. J. Brazel. (2012). Assessing Xeriscaping as a Sustainable Heat Island Mitigation Approach for a Desert City. *Building and Environment*, 47, 170–181.

Chow, W. T., T. J. Volo, E. R. Vivoni, G. D. Jenerette, & B. L. Ruddell. (2014). Seasonal Dynamics of a Suburban Energy Balance in Phoenix, Arizona. *International Journal of Climatology*, 34 (15), 3863–3880.

Clarke, J.F. (1972). Some effects of the urban structure on heat mortality. *Environmental Research,* 5, 93-104.

Coomes, P. (2010). *North America Residential Water Usage Trends Since 1992*. Water Research Foundation, Denver, Colorado, ISBN: 160573070X.

Dietzel, C, Herold, M, Hemphill, J. J., & Clarke, K. C. (2005). Spatio-temporal dynamics in California's Central Valley: Empirical links to urban theory. *International Journal of Geographical Information Science,* 19, 175-195.

Elhaddad, A., & L. A. Garcia. (2008). Surface Energy Balance-Based Model for Estimating Evapotranspiration Taking into Account Spatial Variability in Weather. *Journal of Irrigation and Drainage Engineering*, 134, 681–689.

Georgescu, M., A. Mahalov, & M. Moustaoui. (2012). Seasonal Hydroclimatic Impacts of Sun Corridor Expansion. *Environmental Research Letters,* 7(3), 034026.

Gober, P., Brazil, A., Quay, R., Myint, S., Grossman-Clarke, S., Miller, A., & Rossi, S. (2009). Using watered landscape to manipulate urban heat island effects: How much water will it take to cool Phoenix? *Journal of the American Planning Association,* 76, 109–121.

Granger, R. J., & N. Hedstrom. (2011). Modelling Hourly Rates of Evaporation from Small Lakes. *Hydrology and Earth System Sciences,* 15(1), 267–277.

Grimmond, C. S. B., & T. R. Oke. (1999). Evapotranspiration Rates in Urban Areas. In *Impacts of Urban Growth on Surface Water and Groundwater Quality: Proceedings of IUGG 99 Symposium HS5,* edited by J. Bryan Ellis, 235–243. Birmingham: IAHS Publications.

Grimmond, C.S.B., C. Souch, & M.D. Hubble. (1996). Influence of tree cover on summer-time surface energy balance fluxes, San Gabriel Valley, Los Angeles. *Climate Research,* 6, 45–57.

Guhathakurta, S. & Gober, P. (2007). The impact of the Phoenix urban heat island on residential water use. *Journal of the American Planning Association, 73*(3), 317-329.

Guhathakurta, S. & Gober, P. (2010). Residential land use, the urban heat island, and water use in Phoenix: A path analysis. *Journal of Planning Education and Research, 30*(1), 40-51.

Hart, Q. J., M. Brugnach, B. Temesgen, C. Rueda, S. L. Ustin, & K. Frame. (2009). Daily reference evapotranspiration for California using satellite imagery and weather station measurement interpolation. *Civil Engineering and Environmental Systems,* 26(1), 19–33.

Howard, L. (1833). Climate of London Deduced from Meteorological Observations (3rd edtion). London: Harver & Darton.

Imhoff, M.L., Zhang, P., Wolfe, R.E., & Bounoua, L. (2010). Remote sensing of the urban heat island effect across biomes in the continental USA. *Remote Sensing of Environment,* 114, 504–513.

Jauregui, E. (1997), Heat island development in Mexico City. *Atmospheric Environment*, 31, 3821-3831.

Jo, J.H., Carlson, J.D., Golden, J.S., & Bryan, H. (2010). An integrated empirical and modeling methodology for analyzing solar reflective roof technologies on commercial buildings. *Building and Environment,* 45, 453–460.

Johnson, T. D., & K. Belitz. (2012). A Remote Sensing Approach for Estimating the

Location and Rate of Urban Irrigation in Semi-Arid Climates. *Journal of Hydrology*, 414-415, 86–98.

Kaplan, S., Myint, S.W., Fan, C., & Brazel, A.J. (2014). Quantifying outdoor water consumption of urban land use/land cover: Sensitivity to drought. *Environmental Management*, *53*(4), 855-864.

Kato, S., & Yamaguchi, Y. (2005). Analysis of urban heat-island effect using ASTER and ETM+ data: Separation of anthropogenic heat discharge and natural heat radiation from sensible heat flux. *Remote Sensing of Environment*, 99, 44–54.

Kondoh, A., & Nishiyama, J. (2000). Changes in Hydrological Cycle Due to Urbanization in the Suburb of Tokyo Metropolitan Area, Japan. *Advances in Space Research,* 26, 1173–1176.

Lee, T.-W., Lee, J. Y., & Wang, Z.-H. (2012). Scaling of the urban heat island intensity using time-dependent energy balance. *Urban Climate,* 2, 16–24.

Liu, W., Y. Hong, S. I. Khan, M. Huang, B. Vieux, S. Caliskan, & T. Grout. (2010). Actual Evapotranspiration Estimation for Different Land Use and Land Cover in Urban Regions Using Landsat 5 Data. *Journal of Applied Remote Sensing,* 4(1), 041873.

Liu, L., & Zhang, Y. (2011). Urban heat island analysis using the Landsat TM data and ASTER data: A case study in Hong Kong. *Remote Sensing*, 3, 1535–1552.

Mitchell, V. G., R. G. Mein, & T. A. McMahon. (2001). Modelling the Urban Water Cycle. *Environmental Modelling & Software,* 16(7), 615–629.

Morton, F. I. (1983). Operational Estimates of Lake Evaporation. *Journal of Hydrology,* 66(1–4), 77–100.

Mu, Q., F. A. Heinsch, M. Zhao, & S. W. Running. (2007). Development of a Global Evapotranspiration Algorithm Based on MODIS and Global Meteorology Data. *Remote Sensing of Environment,* 111, 519–536.

Mu, Q., M. Zhao, & S. W. Running. (2013). *Algorithm Theoretical Basis Document: MODIS Global Terrestrial Evapotranspiration (ET) Product (NASA MOD16A2/A3) Collection 5.*

Missoula, MT: NASA Headquarters. Numerical Terradynamic Simulation Group, University of Montana.

Myint, S.W., Wentz, E.A., Brazel, A.J., & Quattrochi, D.A. (2013). The impact of distinct anthropogenic and vegetation features on urban warming. *Landscape Ecology,* 28, 959–978.

National Oceanic and Atmospheric Administration (NOAA). (2016). *National Overview of Annual 2016*. Available at https://www.ncdc.noaa.gov/sotc/national/201613#over

Nichol, J.E., Fung, W.Y., Lam, K., & Wong, M.S. (2009). Urban head island diagnosis using ASTER satellite images and "in situ" air temperature. *Atmospheric Research*, 94, 276–284.

Niu, G.-Y., Z.-L. Yang, K. E. Mitchell, F. Chen, M. B. Ek, M. Barlage, A. Kumar, & et al. (2011). The Community Noah Land Surface Model with Multiparameterization Options (Noah-Mp): 1. Model Description and Evaluation with Local-Scale Measurements. *Journal of Geophysical Research: Atmospheres (1984–2012),* 116(D12).

Nouri, H., S. Anderson, S. Beecham, & D. Bruce. (2013a). *Estimation of Urban Evapotranspiration through Vegetation Indices Using WorldView 2 Satellite Remote Sensing Images.* EFITAWCCA- CIGR Conference "Sustainable Agriculture through ICT Innovation", Turin, Italy, June 24–27.

Nouri, H., S. Beecham, F. Kazemi, & A. M. Hassanli. (2013b). A review of ET measurement techniques for estimating the water requirements of urban landscape vegetation. *Urban Water Journal,* 10(4), 247–259.

Offerle, B., C. S. B. Grimmond, K. Fortuniak, & W. Pawlak. (2006). Intraurban differences of surface energy fluxes in a Central European City. *Journal of Applied Meteorology and Climatology,* 45(1), 125–136.

Oke, T. R. (1979). Advectively-Assisted Evapotranspiration from Irrigated Urban Vegetation. *Boundary-Layer Meteorology*, 17 (2): 167–173.

Oke, T.R. (1982). The energetic basis of the urban heat island. *Quarterly Journal of the Royal Meteorological Society*, 108, 1-24.

Oke, T.R. (1995). The heat island of the urban boundary layer: Characteristics, causes and effects. In *Wind Climate in Cities*. Cermak, J.E., Davenport, A.G., Plate, E.J., Viegas, D.X., Eds., Kluwer Academic: Dordrecht, the Netherlands, pp. 81–107.

Oke, T.R. (2002). *Boundary layer climates*: Routledge.

Onishi, A., Cao, X., Ito, T., Shi, F., & Imura, H. (2010). Evaluating the potential for urban heat-island mitigation by greening parking lots. *Urban Forestry & Urban Greening*, 9, 323-332.

Owen, T. W., Carlson, T. N., & Gillies, R. R. (1998). An Assessment of Satellite Remotely-Sensed Land Cover Parameters in Quantitatively Describing the Climatic Effect of Urbanization. *International Journal of Remote Sensing,* 19, 1663–1681.

Pataki, D. E., C. G. Boone, & T. S. Hogue. (2011a). Socio-ecohydrology and the urban water challenge. *Ecohydrology,* 347, 341–347.

Pataki, D. E., H. R. McCarthy, E. Litvak, & S. Pincetl. (2011b). Transpiration of urban forests in the Los Angeles metropolitan area. *Ecological Applications,* 21(3), 661–677.

Peters, E. B., R. V. Hiller, & J. P. McFadden. (2011). Seasonal contributions of vegetation types to suburban evapotranspiration. *Journal of Geophysical Research,* 116, G01003.

Pittenger, D. R., & D. A. Shaw. (2007). *Review of research on water needs of landscape plants, in Symposium on Efficient Water Use in the Urban Landscape,* New Mexico State University, Las Cruces, NM.

Pittenger, D. R., & D. A. Shaw. (2010). Estimating water needs of urban landscapes, in Annual Conference of the American Society for Horticultural Science, Supplement to HortScience 45(8), S95, Palm Desert, California. Available at http://hortsci.ashspublications.org/content/suppl/2010/08/16/45.8.DC1/HortScienceVol45-8supplement.pdf

Rizwan, A.M., Dennis, L.Y.C., & Liu, C. (2008). A review on the generation, determination and mitigation of Urban Heat Island. *Journal of Environmental Sciences,* 20, 120-128.

Rossi, F., Pisello, A.L., Nicolini, A., Filipponi, M., & Palombo, M. (2014). Analysis of retro-reflective surfaces for urban heat island mitigation: A new analytical model. *Applied Energy,* 114, 621–631.

Santamouris, M., Synnefa, A., & Karlessi, T. (2011). Using advanced cool materials in the urban built environment to mitigate heat islands and improve thermal comfort conditions. *Solar Energy,* 85, 3085–3102.

Seto, K. C., Fragkias, M., Güneralp, B., & Reilly, M. K. (2011). A Meta-Analysis of Global Urban Land Expansion. *PloS One,* 6(8), e23777.

Shields, C. A., & C. L. Tague. (2012). Assessing the role of parameter and input uncertainty in ecohydrologic modeling: Implications for a semi-arid and urbanizing coastal California catchment. *Ecosystems,* 15, 775–791.

Steward, I.D., & Oke, T.R. (2012). Local climate zones for urban temperature studies. *Bulletin of the American Meteorological Society,* 93, 1879–1900.

Suleiman, A. A., & R. D. Crago. (2002). Analytical Land Atmosphere Radiometer Model. *Journal of Applied Meteorology,* 41, 177–187.

Sun, H., K. Kopp, & R. Kjelgren. (2012). Water-efficient urban landscapes: Integrating different water use categorizations and plant types. *HortScience,* 47(2), 254–263.

U.S. Census Bureau. (2016). *Annual Estimates of the Resident Population: April 1, 2010 to July 1, 2016.* Available online at: https://factfinder.census.gov/faces/tableservices/jsf/pages/productview.xhtml?src=bkmk

U.S. Climate Data. (2014). *Phoenix Weather Averages*. Available online at: http://www.usclimatedata.com/climate/phoenix/arizona/united-states/usaz0166

U.S. Geological Survey. (2014). *Trends in Water Use in the United States, 1950 – 2005*. U.S. Geological Survey, Reston, Virginia. Available online at: https://water.usgs.gov/watuse/wutrends.html

Uemoto, K.L., Sato, N.M.N., & John, V.M. (2010). Estimating thermal performance of cool colored paints. *Energy and Buildings*, 42, 17–22.

Vermote, E. F., & S. Kotchenova. (2008). Atmospheric Correction for the Monitoring of Land Surfaces. *Journal of Geophysical Research: Atmospheres*, 113 (D23).

Vivoni, E. R., H. A. Moreno, G. Mascaro, J. C. Rodriguez, C. J. Watts, J. Garatuza-Payan, & R. L. Scott. (2008). Observed Relation between Evapotranspiration and Soil Moisture in the North American Monsoon Region. *Geophysical Research Letters*, 35, L22403.

Voogt, J. A., & Oke, T. R. (2003). Thermal remote sensing of urban climates. *Remote Sensing of Environment*, 86, 370-384.

Wang, Z., C. B. Schaaf, A. H. Strahler, M. J. Chopping, M. O. Román, Y. Shuai, C. E. Woodcock, D. Y. Hollinger, & D. R. Fitzjarrald. (2014). Evaluation of MODIS Albedo Product (MCD43A) over Grassland, Agriculture and Forest Surface Types during Dormant and Snow-Covered Periods. *Remote Sensing of Environment*, 140, 60–77.

Wang, Z.-H., E. Bou-Zeid, & J. A. Smith. (2013). A Coupled Energy Transport and Hydrological Model for Urban Canopies Evaluated Using A Wireless Sensor Network. *Quarterly Journal of the Royal Meteorological Society*, 139, 1643–1657.

Wentz, E.A. & Gober, P. (2007). Determinants of small-area water consumption for the city of Phoenix, Arizona. *Water Resources Management, 21*(11), 1849-1863.

Whitman, S., Good, G., Donoghue, E. R., Benbow, N., Shou, W. & Mou, S. (1997). Mortality in Chicago attributed to the July 1995 heat wave. *American Journal of Public Health*, 87, 1515-1518.

Yang, J., Wang, Z.-H., & Kaloush, K. E. (2015). Environmental impacts on reflective materials: Is high albedo a “silver bullet” for mitigating urban heat island? *Renewable & Sustainable Energy Reviews*, 47, 830–843.

Yang, J., Z.-H. Wang, F. Chen, S. Miao, M. Tewari, J. A. Voogt, & S. Myint. (2015b). Enhancing Hydrologic Modelling in the Coupled Weather Research and Forecasting-Urban Modelling System. *Boundary-Layer Meteorology*, 155(1), 87–109.

Yuan, F., & Bauer, M. E. (2007). Comparison of impervious surface area and normalized difference vegetation index as indicators of surface urban heat island effects in Landsat imagery. *Remote Sensing of Environment*, 106, 375–386.

Zhang, C. L., Chen, F., Miao, S. G., Li, Q. C., Xia, X. A., & Xuan, C. Y. (2009). Impacts of Urban Expansion and Future Green Planting on Summer Precipitation in the Beijing Metropolitan Area. *Journal of Geophysical Research: Atmospheres* (1984–2012), 114: D02116.

Zheng, B., Myint, S.W., & Fan, C. (2014). Spatial configuration of anthropogenic land cover impacts on urban warming. *Landscape and Urban Planning*, 130, 104–111.

CHAPTER 1

Akbari, H., Pomerantz, M., & Taha, H. (2001). Cool surfaces and shade trees to reduce energy use and improve air quality in urban areas. *Solar Energy*, 70(3), 295-310.

Ashie, Y., Thanh, V.C., & Asaeda, T. (1999). Building canopy model for the analysis of urban climate. *Journal of Wind Engineering and Industrial Aerodynamics*, 81, 237-248.

Balling, R.C. Jr. & Brazil, S.W. (1987). Time and space characteristics of the Phoenix urban heat island. *Journal of the Arizona-Nevada Academy of Science*, 21, 75-81.

Bohnenstengel, S.I., Evans, S., Clark, P.A., & Belcher, S.E. (2011) Simulations of the Landon urban heat island. *Quarterly Journal of the Royal Meteorological Society*, 137, 1625-1640.

Bouyer, J., Musy, M., Huang, Y., & Athamena, K. (2009, June). Mitigating urban heat island effect by urban design: forms and materials. In *Proceedings of the 5th urban research symposium, cities and climate change: responding to an urgent agenda, Marseille* (pp. 28-30).

Brazel, A., Gober, P., Lee, S. J., Grossman-Clarke, S., Zehnder, J., Hedquist, B., & Comparri, E. (2007). Determinants of changes in the regional urban heat island in metropolitan Phoenix (Arizona, USA) between 1990 and 2004. *Climate Research*, 33(2), 171-182.

Brazel, A. J., Selover, N., Vose, R., & Heisler, G. (2000). Tale of two climates – Baltimore and Phoenix urban LTER sites. *Climate Research*, 15, 123-135.

Ca, V. T., Asaeda, T., & Abu, E. M. (1998). Reductions in air-conditioning energy caused by a nearby park. *Energy and Buildings*, 29, 83-92.

Chen, X. L., Zhao, H. M., Li, P. X., & Yin, Z. Y. (2006). Remote sensing image-based analysis of the relationship between urban heat island and land use/cover changes. *Remote Sensing of Environment*, 104(2), 133-146.

Cheval, S., & Dumitrescu, A. (2009). The July urban heat island of Bucharest as derived from MODIS images. *Theoretical and Applied Climatology*, 96(1-2), 145-153.

Filleul, L., Cassadou, S., Médina, S., Fabres, P., Lefranc, A., Eilstein, D., et al. (2006). The relation between temperature, ozone, and mortality in nine French cities during the heat wave of 2003. *Environmental Health Perspectives*, 114(9), 1344.

Gober, P., Brazel, A., Quay, R., Myint, S., Grossman-Clarke, S., Miller, A., & Rossi, S. (2009). Using watered landscapes to manipulate urban heat island effects: how much water will it take to cool Phoenix? *Journal of the American Planning Association*, 76(1), 109-121.

Golden, J.S. (2004). The built environment induced urban heat island effect in rapidly urbanizing arid regions – A sustainable urban engineering complexity. *Environmental Sciences*, 1(4), 321-349.

Guhathakurta, S. & Gober, P. (2007). The impact of the Phoenix urban heat island on residential water use. *Journal of the American Planning Association*, 73(3), 317-329.

Hansen, J., Ruedy, R., Glascoe, J., & Sato, M. (1999). GISS analysis of surface temperature change. *Journal of Geophysical Research: Atmospheres*, 104(D24), 30997-31022.

Imhoff, M. L., Zhang, P., Wolfe, R. E., & Bounoua, L. (2010). Remote sensing of the urban heat island effect across biomes in the continental USA. *Remote Sensing of Environment*, 114, 504-513.

Jo, J. H., Carlson, J. D., Golden, J. S., & Bryan, H. (2010). An integrated empirical and modeling methodology for analyzing solar reflective roof technologies on commercial buildings. *Building and Environment*, 45(2), 453-460.

Kato, S., & Yamaguchi, Y. (2005). Analysis of urban heat-island effect using ASTER and ETM+ Data: Separation of anthropogenic heat discharge and natural heat radiation from sensible heat flux. *Remote Sensing of Environment*, 99(1-2), 44-54.

Kolokotroni, M., Ren, X., Davies, M., & Mavrogianni, A. (2012). London's urban heat island: Impact on current and future energy consumption in office buildings. *Energy and Buildings*, 47, 302-311.

Lac, C., Donnelly, R. P., Masson, V., Pal, S., Riette, S., Donier, S., & et al. (2013). CO_2 dispersion modelling over Paris region within the CO_2-MEGAPARIS project. *Atmospheric*

Chemistry & Physics, 13(9).

Lee, T.-W., Lee, J.Y., &Wang, Z.H. (2012). Scaling of the urban heat island intensity using time-dependent energy balance. *Urban Climate*, 2, 16-24.

Liu, L., & Zhang, Y. (2011). Urban heat island analysis using the Landsat TM data and ASTER data: A case study in Hong Kong. *Remote Sensing*, 3(7), 1535-1552.

Lo, C. P., Quattrochi, D. A., & Luvall, J. C. (1997). Application of high-resolution thermal infrared remote sensing and GIS to assess the urban heat island effect. *International Journal of Remote Sensing*, 18(2), 287-304.

Lu, J., Li, C., Yu, C., Jin, M., & Dong, S. (2012). Regression analysis of the relationship between urban heat island effect and urban canopy characteristics in a mountainous city, Chongqing. *Indoor and Built Environment*, 21(6), 821-836.

Mills, G. (1999, November). Urban climatology and urban design. In *Proceedings of the 15th ICB & ICUC*. Sydney, Australia.

Myint, S.W., Wentz, E.A., Brazel, A.J., & Quattrochi, D.A. (2013). The impact of distinct anthropogenic and vegetation features on urban warming. *Landscape Ecology*, 28(5), 959-978.

Nichol, J. E., Fung, W. Y., Lam, K. S., & Wong, M. S. (2009). Urban heat island diagnosis using ASTER satellite images and 'in situ' air temperature. *Atmospheric Research*, 94(2), 276-284.

Oke, T.R. (1982). The energetic basis of the urban heat island. *Quarterly Journal of the Royal Meteorological Society*, 108(455), 1-24.

Oke, T.R. (1995). The heat island of the urban boundary layer: Characteristics, causes and effects. *Wind Climate in Cities*, 277, 81-107.

Pal, S., Xueref-Remy, I., Ammoura, L., Chazette, P., Gibert, F., Royer, P., & et al. (2012). Spatio-temporal variability of the atmospheric boundary layer depth over the Paris agglomeration: An assessment of the impact of the urban heat island intensity. *Atmospheric Environment*, 63, 261-275.

Peng, S., Piao, S., Ciais, P., Friedlingstein, P., Ottle, C., Bréon, F.M., & et al. (2011). Surface urban heat island across 419 global big cities. *Environmental Science & Technology*, 46(2), 696-703.

Rajasekar, U., & Weng, Q. (2009). Urban heat island monitoring and analysis using a non-parametric model: A case study of Indianapolis. *ISPRS Journal of Photogrammetry and Remote Sensing*, 64(1), 86-96.

Rosenfeld, A.H., Akbari, H., Bretz, S., Fishman, B.L., Kurn, D.M., Sailor, D., & Taha, H. (1995). Mitigation of urban heat islands: Materials, utility programs, updates. *Energy and Buildings*, 22, 255-265.

Rossi, F., Pisello, A. L., Nicolini, A., Filipponi, M., & Palombo, M. (2014). Analysis of retro-reflective surfaces for urban heat island mitigation: A new analytical model. *Applied Energy*, 114, 621-631.

Santamouris, M., Synnefa, A., & Karlessi, T. (2011). Using advanced cool materials in the urban built environment to mitigate heat islands and improve thermal comfort conditions. *Solar Energy*, 85(12), 3085-3102.

Schatz, J., & Kucharik, C.J. (2014). Seasonality of the urban heat island effect in Madison, Wisconsin. *American Meteorological Society*, 53(10), 2371-2386.

Schwarz, N., Lautenbach, S., & Seppelt, R. (2011). Exploring indicators for quantifying surface urban heat islands of European cities with MODIS land surface temperatures. *Remote Sensing of Environment*, 115(12), 3175-3186.

Song, J., & Wang, Z.-H. (2015). Interfacing the urban land-atmosphere system through coupled urban canopy and atmospheric models. *Boundary-Layer Meteorology*, 154(3), 427-448.

Steward, I.D., & Oke, T.R. (2012). Local climate zones for urban temperature studies. *Bulletin of the American Meteorological Society*, 93, 1879-1900.

Taha, H. (1997). Urban climates and heat islands: Albedo, evapotranspiration, and anthropogenic heat. *Energy and Buildings*, 25, 99-103.

Taha, H., Douglas, S., & Haney, J. (1994). The UAM sensitivity analysis: the August 26-28 1987 oxidant episode. In *Analysis of Energy Efficiency and Air Quality in the South Coast Air Basin – Phase II*, Taha, H. et al. (Ed.). Lawrence Berkeley Laboratory Report LBL-35728, Berkeley, CA, Chapter 1.

Taha, H., Kalkstein, L. S., Sheridan, S. C., & Wong, E. (2004, August). The potential of urban environmental control in alleviatine heat-wave health effects in five US regions. In *Proceedings, 16th Conference on Biometeorology and Aerobiology, American Meteorological Society*.

Tomlinson, C. J., Chapman, L., Thornes, J. E., & Baker, C. J. (2012). Derivation of Birmingham's summer surface urban heat island from MODIS satellite images. *International Journal of Climatology*, 32(2), 214-224.

Tong, H., Walton, A., Sang, J., & Chan, J. C. L. (2005). Numerical simulation of the urban boundary layer over the complex terrain of Hong Kong. *Atmospheric Environment*, 39, 3549-3563.

Tran, H., Uchihama, D., Ochi, S., & Yasuoka, Y. (2006). Assessment with satellite data of the urban heat island effects in Asian mega cities. *International journal of applied Earth observation and Geoinformation*, 8(1), 34-48.

Uemoto, K. L., Sato, N. M., & John, V. M. (2010). Estimating thermal performance of cool colored paints. *Energy and Buildings*, 42(1), 17-22.

U.S. Census Bureau. (2016). Available online:
http://www.census.gov/popest/data/metro/totals/2013/index.html

U.S. Climate Data. 2016. Available online:
http://www.usclimatedata.com/climate/phoenix/arizona/united-states/usaz0166

Wang, Z. H., Bou‐Zeid, E., & Smith, J. A. (2013). A coupled energy transport and hydrological model for urban canopies evaluated using a wireless sensor network. *Quarterly Journal of the Royal Meteorological Society*, 139(675), 1643-1657.

Weng, Q. (2001). A remote sensing GIS evaluation of urban expansion and its impact on surface temperature in the Zhujiang Delta, China. *International Journal of Remote Sensing*, 22, 1999-2014.

Yang, J., & Wang, Z. H. (2015). Optimizing urban irrigation schemes for the trade-off between energy and water consumption. *Energy and Buildings*, 107, 335-344.

Yang, J., Wang, Z. H., & Kaloush, K. E. (2015). Environmental impacts of reflective materials: Is high albedo a 'silver bullet' for mitigating urban heat island? *Renewable and Sustainable Energy Reviews*, 47, 830-843.

Yu, C., & Hien, W.N. (2006). Thermal benefits of city parks. *Energy and Buildings*, 38(2), 105-120.

Yuan, F., & Bauer, M.E. (2007). Comparison of impervious surface area and normalized difference vegetation index as indicators of surface urban heat island effects in Landsat imagery. *Remote Sensing of Environment*, 106, 375-386.

Zheng, B., Myint, S.W., & Fan, C. (2014). Spatial configuration of anthropogenic land cover impacts on urban warming. *Landscape and Urban Planning*, 130, 104-111.

CHAPTER 2

Adams, D. K., & A. C. Comrie. (1997). The North American Monsoon. *Bulletin of the American Meteorological Society,* 78, 2197-2213.

Allen, R. G., M. Tasumi, A. Morse, R. Trezza, W. Kramber, & I. Lorite. (2007). Satellite-

Based Energy Balance for Mapping Evapotranspiration with Internalized Calibration (METRIC) -Applications. *Journal of Irrigation and Drainage Engineering*, 133, 395-406.

Balling, R., & S. W. Brazel. (1987a). The impact of rapid urbanization on pan evaporation in Phoenix, Arizona. *International Journal of Climatology*, 7, 593-597.

Balling, R. C., & S. W. Brazel. (1987b). Recent changes in Phoenix, Arizona summertime diurnal precipitation patterns. *Theoretical and Applied Climatology*, 38, 50-54.

Bastiaanssen, W. G. M., M. Menenti, R. A. Feddes, & A. A. M. Holtslag. (1998). A Remote Sensing Surface Energy Balance Algorithm for Land (SEBAL): Part 1. Formulation. *Journal of Hydrology*, 212-213, 198-212.

Bastiaanssen, W. G. M., E. J. M. Noordman, H. Pelgrum, G. Davids, B. P. Thoreson, & R. G. Allen. (2005). SEBAL Model with Remotely Sensed Data to Improve Water-Resources Management under Actual Field Conditions. *Journal of Irrigation and Drainage Engineering, ASCE*, 131, 85-93.

Best, M.J., M. Pryor, D. B. Clark, G. G. Rooney, R. Essery, C. B. Ménard, & R. J. Harding. (2011). The Joint UK Land Environment Simulator (JULES), model description-Part 1: energy and water fluxes. *Geoscientific Model Development*, 4(3), 677-699.

Carlson, T. N., & M. J. Buffum. (1989). On estimating total evapotranspiration from remote surface temperature measurements. *Remote Sensing of Environment*, 29, 197-207.

Chow, W. T. L., & A. J. Brazel. (2012). Assessing xeriscaping as a sustainable heat island mitigation approach for a desert city. *Building and Environment*, 47, 170-181.

Chow, W. T., T. J. Volo, E. R. Vivoni, G. D. Jenerette, & B. L. Ruddell. (2014). Seasonal dynamics of a suburban energy balance in Phoenix, Arizona. *International Journal of Climatology*, 4(15), 3863-3880.

Elhaddad, A., & L. A. Garcia. (2008). Surface energy balance-based model for estimating evapotranspiration taking into account spatial variability in weather. *Journal of Irrigation and Drainage Engineering*, 134, 681-689.

Georgescu, M., A. Mahalov, & M. Moustaoui. (2012). Seasonal hydroclimatic impacts of Sun Corridor expansion. *Environmental Research Letters*, 7(3), 034026.

Gober, P., A. Brazel, R. Quay, S. Myint, S. Grossman-Clarke, A. Miller, & S. Rossi. (2009). Using watered landscapes to manipulate urban heat island effects: how much water will it take to cool Phoenix? *Journal of the American Planning Association*, 76(1), 109-121.

Granger, R. J., & N. Hedstrom. (2011). Modelling hourly rates of evaporation from small lakes. *Hydrology and Earth System Sciences*, 15(1), 267-277.

Grimmond, C. S. B., & T. R. Oke. (1999). Evapotranspiration rates in urban areas. In: *Impacts of Urban Growth on Surface Water and Groundwater Quality, International Association of Hydrological Sciences*, 259, 235-243.

Jackson, R. J. (1967). The effect of slope, aspect and albedo on potential evapotranspiration from hill-slopes and catchments. *Journal of Hydrology (New Zealand),* 6, 60-69.

Johnson, T. D., & K. Belitz. (2012). A remote sensing approach for estimating the location and rate of urban irrigation in semi-arid climates. *Journal of Hydrology,* 414, 86-98.

Kondoh, A., & J. Nishiyama. (2000). Changes in hydrological cycle due to urbanization in the suburb of Tokyo Metropolitan area, Japan. *Advances in Space Research,* 26, 1173-1176.

Liu, W., Y. Hong, S. I. Khan, M. Huang, B. Vieux, S. Caliskan, & T. Grout. (2010). Actual evapotranspiration estimation for different land use and land cover in urban regions using Landsat 5 data. *Journal of Applied Remote Sensing,* 4(1), 041873.

Mitchell, V. G., R. G. Mein, & T. A. McMahon. (2001). Modelling the urban water cycle. *Environmental Modelling & Software,* 16(7), 615-629.

Morton, F. I. (1983). Operational estimates of lake evaporation. *Journal of Hydrology,* 66(1), 77-100.

Mu, Q., F. A. Heinsch, M. Zhao, & S. W. Running. (2007). Development of a global evapotranspiration algorithm based on MODIS and global meteorology data. *Remote Sensing of Environment,* 111, 519–536.

Mu, Q., M. Zhao, & S. W. Running. (2013). *Algorithm Theoretical Basis Document: MODIS Global Terrestrial Evapotranspiration (ET) Product (NASA MOD16A2/A3) Collection 5.* NASA Headquarters. Numerical Terradynamic Simulation Group, University of Montana, Missoula, MT, USA, 20 November 2013.

Niu, G. Y., Z. -L. Yang, K. E. Mitchell, F. Chen, M. B. Ek, M. Barlage, A. Kumar, K. Manning, D. Niyogi, E. Rosero, M. Tewari, & Y. Xia. (2011). The community Noah land surface model with multiparameterization options (Noah - MP): 1. Model description and evaluation with local - scale measurements. *Journal of Geophysical Research: Atmospheres* (1984–2012), 116(D12).

Nouri, H., S. Anderson, S. Beecham, & D. Bruce. (2013). Estimation of Urban Evapotranspiration through Vegetation Indices Using WorldView 2 Satellite Remote Sensing Images. In: *EFITA-WCCA-CIGR Conference "Sustainable Agriculture through ICT Innovation"*, Turin, Italy, 24-27 June, 2013.

Oke, T.R. (1979). Advectively-assisted evapotranspiration from irrigated urban vegetation. *Boundary-layer meteorology*, 17(2), 167-173.

Owen, T. W., T. N. Carlson, & R. R. Gillies. (1998). An assessment of satellite remotely-sensed land cover parameters in quantitatively describing the climatic effect of urbanization. *International Journal of Remote Sensing*, 19, 1663-1681.

Seto, K. C., M. Fragkias, B. Güneralp, & M. K. Reilly. (2011). A meta-analysis of global urban land expansion. *PloS One*, 6(8), e23777.

Suleiman, A. A., & R. D. Crago. (2002). Analytical land atmosphere radiometer model. *Journal of Applied Meteorology*, 41, 177-187.

U.S. Census Bureau. (2013). *Population estimates*. Retrieved May 10, 2016 from http://www.census.gov/popest/data/metro/totals/2013/index.html

U.S. Climate Data. (2014). *Phoenix weather averages*. Retrieved May 10, 2016 from http://www.usclimatedata.com/climate/phoenix/arizona/united-states/usaz0166

Vermote, E. F. & Kotchenova, S. (2008). Atmospheric correction for the monitoring of land surfaces. *Journal of Geophysical Research: Atmospheres*, 113(D23).

Vivoni, E. R., H. A. Moreno, G. Mascaro, J. C. Rodriguez, C. J, Watts, J. Garatuza-Payan, & R. L. Scott. (2008). Observed relation between evapotranspiration and soil moisture in the North American monsoon region. *Geophysical Research Letters*, 35, L22403.

Wan, Z., Y. Zhang, Q. Zhang, & Z.-L. Li. (2002). Validation of the land-surface temperature products retrieved from Terra Moderate Resolution Imaging Spectroradiometer data. *Remote Sensing of Environment*, 83, 163-180.

Wang, C., S. W. Myint, Z. -H. Wang, & J. Song. (2016). Spatio-temporal modeling of the urban heat island in the Phoenix metropolitan area: Land use change implications. *Remote Sensing*, 8(3), 185.

Wang Z. -H., E. Bou-Zeid, & J. A. Smith. (2013). A coupled energy transport and hydrological model for urban canopies with evaluation using a wireless sensor network. *Quarterly Journal of the Royal Meteorological Society*, 139, 1643-1657.

Wang, Z., C. B. Schaaf, A. H. Strahler, M. J. Chopping, M. O. Román, Y. Shuai, C. E. Woodcock, D. Y. Hollinger, & D. R. Fitzjarrald. (2014). Evaluation of MODIS albedo product (MCD43A) over grassland, agriculture and forest surface types during dormant and snow-covered periods. *Remote Sensing of Environment*, 140, 60-77.

Yang, J., Z. -H. Wang, F. Chen, S. Miao, M. Tewari, J. A. Voogt, & S. Myint. (2015). Enhancing Hydrologic Modelling in the Coupled Weather Research and Forecasting-Urban Modelling System. *Boundary-Layer Meteorology*, 155(1), 87-109.

Zhang, C. L., F. Chen, S. G. Miao, Q. C. Li, X. A. Xia, & C. Y. Xuan. (2009). Impacts of urban expansion and future green planting on summer precipitation in the Beijing metropolitan area. *Journal of Geophysical Research: Atmospheres* (1984–2012), 114, D02116.

CHAPTER 3

Allen, R.G., Tasumi, M., & Trezza, R. (2007a). Satellite-based energy balance for mapping evapotranspiration with internalized calibration (METRIC) – Model. *Journal of irrigation and drainage engineering*, 133(4), 380-394.

Allen, R.G., Tasumi, M., Morse, A., Trezza, R., Wright, J.L., Bastiaanssen, W., Kramber, W., Lorite, I., & Robison, C.W. (2007b). Satellite-based energy balance for mapping evapotranspiration with internalized calibration (METRIC) – Applications. *Journal of irrigation and drainage engineering*, 133(4), 395-406.

Arizona Department of Water Resources (ADWR). (2017). *Arizona's water supplies and water demands*. Available online at: http://www.azwater.gov/AzDWR/PublicInformationOfficer/documents/supplydemand.pdf

Balling Jr., R.C., & Brazel, S.W. (1987). Time and space characteristics of the Phoenix urban heat island. *Journal of the Arizona-Nevada Academy of Science*, 75-81.

Balling Jr., R.C., & Cubaque, C. (2009). Estimating future residential water consumption in Phoenix, Arizona based on simulated changes in climate. *Physical Geography*, 30, 308-323.

Balling Jr., R.C., & Gober, P. (2007). Climate variability and residential water use in the City of Phoenix, Arizona. *Journal of Applied Meteorology and Climatology*, 46(7), 1130-1137.

Balling Jr., R.C., Gober, P., & Jones, N. (2008). Sensitivity of residential water consumption to variations in climate: An intraurban analysis of Phoenix, Arizona. *Water Resources Research*, 44(10).

Bastiaanssen, W.G.M., Noordman, E.J.M., Pelgrum, H., Davids, G., Thoreson, B.P., &

Allen, R.G. (2005). SEBAL model with remotely sensed data to improve water-resources management under actual field conditions. *Journal of Irrigation and Drainage Engineering*, 131(1), 85-93.

Carr, J.E., Chase, E.B., Paulson, R.W., & Moody, D.W. (1990). *National water summary 1987 - Hydrologic events and water supply and use* (Vol. 2350). United States Government Printing Office.

Central Arizona-Phoenix Long-Term Ecological Research (CAP-LTER). (2015). *CAP LTER land cover classification using 2010 National Agriculture Imagery Program (NAIP) Imagery*. Available online at: https://sustainability.asu.edu/caplter/data/data-catalog/view/knb-lter-cap.623.1/

City of Phoenix. 2014. *Historical population & water use: Growing population, changing demand*. Available online at: https://www.phoenix.gov/waterservices/resourcesconservation/yourwater/historicaluse

Corral-Verdugo, V., Frias-Armenta, M., Perez-Urias, F., Orduna-Cabrera, V., & Espinoza-Gallego, N. (2002). Residential water consumption, motivation for conserving water and the continuing tragedy of the commons. *Environmental Management*, 30, 527–535.

Domene, E., & Saurí, D. (2006). Urbanisation and water consumption: influencing factors in the metropolitan region of Barcelona. *Urban Studies*, 43(9), 1605–1623.

Domene, E., Saurí, D., & Parés, M. (2005). Urbanization and sustainable resource use: The case of garden watering in the metropolitan region of Barcelona. *Urban Geography*, 26(6), 520–535.

Endter-Wada, J., Kurtzman, J., Keenan, S.P., Kjelgren, R.K., & Neale, C.M. (2008). Situational waste in landscape watering: Residential and business water use in an urban Utah community. *JAWRA Journal of the American Water Resources Association*, 44(4), 902–920.

Fleck, B. (2013). *Factors Affecting Agricultural Water Use and Sourcing in Irrigation Districts of Central Arizona*. Thesis, University of Arizona, Tucson, Arizona.

Gober, P., Wentz, E.A., Lant, T., Tschudi, M.K., & Kirkwood, C.W. (2011). WaterSim: a simulation model for urban water planning in Phoenix, Arizona, USA. *Environment and Planning B: Planning and Design*, 38(2), 197-215.

Gregory, G.D., & Leo, M.D. (2003). Repeated behavior and environmental psychology: The role of personal involvement and habit formation in explaining water consumption. *Journal of Applied Social Psychology*, 33(6), 1261-1296.

Guhathakurta, S., & Gober, P. (2007). The impact of the Phoenix urban heat island on residential water use. *Journal of the American Planning Association,* 73(3), 317-329.

Guhathakurta, S., & Gober, P. (2010). Residential land use, the urban heat island, and water use in Phoenix: A path analysis. *Journal of Planning Education and Research*, 30(1), 40-51.

Hadjimitsis, D.G., Papadavid, G., Themistokleous, K., Kounoudes, A., & Toulios, L. (2008, October). Estimating irrigation demand using satellite remote sensing: a case study of Paphos District area in Cyprus. In *Remote Sensing for Agriculture, Ecosystems, and Hydrology X* (Vol. 7104, p. 71040I). International Society for Optics and Photonics.

Haley, M.B., Dukes, M.D., & Miller, G.L. (2007). Residential irrigation water use in Central Florida. *Journal of Irrigation and Drainage Engineering*, 133(5), 427–434.

Hendrickx, J.M., & Hong, S.H. (2005, May). Mapping sensible and latent heat fluxes in arid areas using optical imagery. In *Targets and Backgrounds XI: Characterization and Representation* (Vol. 5811, pp. 138-147). International Society for Optics and Photonics.

Intergovernmental Panel on Climate Change (IPCC). (2014). *Climate Change 2014: Synthesis Report. Contribution of Working Groups I, II and III to the Fifth Assessment Report of the Intergovernmental Panel on Climate Change*. Pachauri, R.K., & Meyer, L.A. (Eds.). Geneva, Switzerland.

Jorgensen, B., Graymore, M., & O'Toole, K. (2009). Household water use behavior: An integrated model. *Journal of Environmental Management*, 91: 227-236.

Kaplan, S., & Myint, S. (2012). Estimating irrigated agricultural water use through Landsat TM and a simplified surface energy balance modeling in the semi-arid environments of Arizona. *Photogrammetry Engineering and Remote Sensing*, 78, 849-859.

Kaplan, S., Myint, S.W., Fan, C., & Brazel, A.J. (2014). Quantifying outdoor water consumption of urban land use/land cover: Sensitivity to drought. *Environmental Management*, 53(4), 855-864.

Larsen, L., & Harlan, S.L. (2006). Desert dreamscapes: residential landscape preference and behavior. *Landscape and urban planning*, *78*(1-2), 85-100.

Larson, K.L., Casagrande, D., Harlan, S.L., & Yabiku, S.T. (2009). Residents' yard choices and rationales in a desert city: social priorities, ecological impacts, and decision tradeoffs. *Environmental Management*, 44(5), 921.

Liu, W., Hong, Y., Khan, S.I., Huang, M., Vieux, B., Caliskan, S., & Grout, T. (2010). Actual evapotranspiration estimation for different land use and land cover in urban regions using Landsat 5 data. *Journal of Applied Remote Sensing*, 4, 041873.

Martin, C.A. (2008). Landscape sustainability in a Sonoran Desert city. *Cities and the Environment (CATE)*, 1(2), 5.

Martin, C.A., Busse, K., & Yabiku, S.T. (2007). North Desert Village: The effect of landscape manipulation on microclimate and its relation to human landscape preferences. *Hortscience*, 42(4):853.

Mayer, P.W., DeOreo, W.B., Opitz, E.M., Kiefer, J.C., Davis, W.Y., Dziegielewski, B., & Nelson, J.O. (1999). Residential end uses of water. *American Water Works Association Research Foundation and American Water Works Association Report*. Denver, Colorado.

Mini, C., Hogue, T.S., & Pincetl, S. (2014). Estimation of residential outdoor water use in Los Angeles, California. *Landscape and Urban Planning*, 127, 124-135.

National Oceanic and Atmospheric Administration (NOAA). 2016. *National Overview of Annual 2016*. Available online at https://www.ncdc.noaa.gov/sotc/national/201613#over

Plaza, A., Benediktsson, J.A., Boardman, J.W., Brazile, J., Bruzzone, L., Camps-Valls, G., & et al. (2009). Recent advances in techniques for hyperspectral image processing. *Remote Sensing of Environment*, 113, S110-S122.

Renwick, M.E., & Archibald, S.O. (1998). Demand side management policies for residential water use: who bears the conservation burden? *Land Economics*, 74, 343–360.

Renwick, M.E., & Green, R.D. (2000). Do residential water demand side management policies measure up? An analysis of eight California water agencies. *Journal of Environmental Economics and Management*, 40, 37–55.

Rwasoka, D.T., Gumindoga, W., & Gwenzi, J. (2011). Estimation of actual evapotranspiration using the Surface Energy Balance System (SEBS) algorithm in the Upper Manyame catchment in Zimbabwe. *Physics and Chemistry of the Earth, Parts A/B/C*, 36(14-15), 736-746.

Shao, Y., & Lunetta, R.S. (2012). Comparison of support vector machine, neural network, and CART algorithms for the land-cover classification using limited training data points. *ISPRS Journal of Photogrammetry and Remote Sensing*, 70, 78-87.

Syme, G.J., Seligman, C., & Thomas, J.F. (1990-1991). Predicting water consumption from homeowners' attitudes. *Journal of Environmental Systems*, 20(2), 157-168.

Syme, G.J., Shao, Q., Po, M., Campbell, E. (2004). Predicting and understanding home garden water use. *Landscape and Urban Planning*, 68, 121-128.

The Arizona Meteorological Network (AZMET). (2018). *AZMET Weather Data*. Available online at: https://cals.arizona.edu/azmet/az-data.htm

Torres-Rua, A.F., Ticlavilca, A.M., Bachour, R., & McKee, M. (2016). Estimation of surface soil moisture in irrigated lands by assimilation of Landsat vegetation indices, surface energy balance products, and relevance vector machines. *Water*, 8(4), 167.

Trezza, R. (2002). *Evapotranspiration using a satellite-based surface energy balance with standardized ground control*. Dissertation, Utah State University, Logan, Utah.

U.S. Climate Data. (2017). Available online at: http://www.usclimatedata.com/

U.S. Census Bureau. (2017). *American Community Survey 1-Year Estimates*. Available online at: https://www.census.gov/programs-surveys/acs/technical-documentation/table-and-geography-changes/2016/1-year.html

U.S. Census Bureau. (2011). *American Community Survey (ACS) Public Use Microdata Sample (PUMS) Data*. Available online at: https://www.census.gov/programs-surveys/acs/data/pums.html

U.S. Department of Agriculture (USDA). (2010). *2007 Census of Agriculture: Farm and Ranch Irrigation Survey (2008)*, Volume 3, Special Studies, Part 1. Available online at: https://www.agcensus.usda.gov/Publications/2007/Online_Highlights/Farm_and_Ranch_Irrigation_Survey/fris08.pdf

Vivoni, E.R., Moreno, H.A., Mascaro, G., Rodriguez, J.C., Watts, C.J., Garatuza-Payan, J., & Scott, R.L. (2008). Observed relation between evapotranspiration and soil moisture in the North American monsoon region. *Geophysical Research Letters*, 35(22).

Volo, T.J., Vivoni, E.R., Martin, C.A., Earl, S., & Ruddell, B.L. (2014). Modelling soil moisture, water partitioning, and plant water stress under irrigated conditions in desert urban areas. *Ecohydrology*, 7(5), 1297-1313.

Volo, T.J., Vivoni, E.R., & Ruddell, B.L. (2015). An ecohydrological approach to conserving urban water through optimized landscape irrigation schedules. *Landscape and Urban Planning*, 133, 127-132.

Vörösmarty, C.J., Green, P., Salisbury, J., & Lammers, R.B. (2000). Global water resources: vulnerability from climate change and population growth. *Science*, 289(5477), 284-288.

Wang, C., Middel, A., Myint, S.W., Brazel, A.J., Kaplan, S., & Lukasczyk, J. (2018). Assessing Local Climate Zones in Arid Cities: The Case of Phoenix, Arizona and Las Vegas, Nevada. *ISPRS Journal of Photogrammetry and Remote Sensing*, 141(2018): 59-71.

Wentz, E.A., & Gober, P. (2007). Determinants of small-area water consumption for the city of Phoenix, Arizona. *Water Resources Management*, 21(11), 1849-1863.

Yabiku, S.T., Casagrande, D.G., & Farley-Metzger, E. (2008). Preferences for landscape choice in a southwestern desert city. *Environment and Behavior*, 40(3), 382-400.

Zhang, L., Dawes, W. R., & Walker, G.R. (2001). Response of mean annual evapotranspiration to vegetation changes at catchment scale. *Water Resources Research*, 37(3), 701-708.

Zheng, B., Myint, S.W., Thenkabail, P.S., & Aggarwal, R.M. (2015). A support vector machine to identify irrigated crop types using time-series Landsat NDVI data. *International Journal of Applied Earth Observation and Geoinformation*, 34, 103-112.